AWARD NUMBER: W81XWH-07-1-0525

TITLE: CD8 T Cells and Immunoediting of Breast Cancer

PRINCIPAL INVESTIGATOR: Keith L. Knutson

CONTRACTING ORGANIZATION: Mayo Clinic
Rochester, MN 55906

REPORT DATE: August 2008

TYPE OF REPORT: Annual

PREPARED FOR: U.S. Army Medical Research and Materiel Command
Fort Detrick, Maryland 21702-5012

REPORT DOCUMENTATION PAGE

Form Approved
OMB No. 0704-0188

1. REPORT DATE	2. REPORT TYPE	3. DATES COVERED
1 August 2008	Annual	1 Aug 2007 – 31 Jul 2008

4. TITLE AND SUBTITLE

CD8 T Cells and Immunoediting of Breast Cancer

5a. CONTRACT NUMBER

5b. GRANT NUMBER
W81XWH-07-1-0525

5c. PROGRAM ELEMENT NUMBER

6. AUTHOR(S)

Keith L. Knutson

E-Mail: knutson.keith@mayo.edu

5d. PROJECT NUMBER

5e. TASK NUMBER

5f. WORK UNIT NUMBER

7. PERFORMING ORGANIZATION NAME(S) AND ADDRESS(ES)

Mayo Clinic
Rochester, MN 55906

8. PERFORMING ORGANIZATION REPORT NUMBER

9. SPONSORING / MONITORING AGENCY NAME(S) AND ADDRESS(ES)
U.S. Army Medical Research and Materiel Command
Fort Detrick, Maryland 21702-5012

10. SPONSOR/MONITOR'S ACRONYM(S)

11. SPONSOR/MONITOR'S REPORT NUMBER(S)

12. DISTRIBUTION / AVAILABILITY STATEMENT
Approved for Public Release; Distribution Unlimited

13. SUPPLEMENTARY NOTES

14. ABSTRACT
T-cells populate breast tumors early in the course of disease and are amongst the most abundant immune effectors in early and advanced lesions. The typical paradigm suggests that T-cells are associated with an improved outcome. Infiltration of CD8 T-cells into the breast cancers often portends a poorer outcome suggesting they have a negative impact. One potential mechanism by which CD8 T-cells may act is by induction of epithelial to mesenchymal transition (EMT). In cancer, EMT is used aberrantly and is involved in invasion and metastasis. It has been suggested that tumor antigen-specific CD8 T-cells are the drivers of EMT. The goal of the study is to further define the interactions between CD8 T-cells and breast cancer. It was found that CD8 T cells may be able to directly immunoedit tumor cells through the induction of EMT. This ability of CD8 T-cells may be shared by NK cells. The resulting immunoedited tumor cells have a reduced inflammatory signature and produce immunosuppressive substances, that latter of which may act in an autocrine fashion to modulate tumor functions in addition to their immunosuppressive actions. These findings provide an explanation how an immune response in breast cancers may drive disease progression rather than regression.

15. SUBJECT TERMS
Epithelial-to Mesenchymal Transition, Immunosuppression, Breast Cancer, Immune System

16. SECURITY CLASSIFICATION OF:			17. LIMITATION OF ABSTRACT	18. NUMBER OF PAGES	19a. NAME OF RESPONSIBLE PERSON
a. REPORT	b. ABSTRACT	c. THIS PAGE			USAMRMC
U	U	U	UU	47	19b. TELEPHONE NUMBER *(include area code)*

Table of Contents

INTRODUCTION:

T cells populate breast tumors very early in the course of disease and are amongst the most abundant immune effectors in early and advanced lesions. The typical paradigm suggests that T cells are associated with an improved outcome. Such findings have not been conclusively extended to breast cancer. Infiltration of CD8 T cells into the breast cancer microenvironment often portends a poorer outcome suggesting they have a negative impact (1, 2). One potential mechanism by which CD8 T cells may act is by induction of epithelial to mesenchymal transition (EMT). In cancer, EMT is used aberrantly and is involved in invasion and metastasis by allowing epithelial tumor cells to change adhesive properties along with the activation of proteolysis and motility. In prior work, it has been suggested that tumor antigen-specific CD8 T cells are the drivers of EMT (3). The goal of the proposed study is to further define the interactions between CD8 T cells and breast cancer.

BODY:

The **Specific Aims** of this project were:

Specific Aim 1: To determine if CD8 T cells directly cause breast tumor cells to undergo epithelial to mesenchymal transition. *In vitro* studies will be done assessing the mechanism by which CD8 T cells mediate EMT. *In vivo* and *in vitro* studies will be done to assess whether other immune cells cooperate with CD8 T cells to induce EMT.

Specific Aim 2: To determine if breast tumors cells, induced by CD8 T cells to undergo EMT, demonstrate increased immunosuppression compared to native epithelial breast cancer cells. Our goal in this aim is to determine if breast cancer cells that have undergone EMT produce immunosuppressive cytokines and inhibitory cell surface receptors.

The results are described below as related to the **Statement of Work**.

Task 1: To determine if CD8 T cells directly cause breast tumor cells to undergo epithelial to mesenchymal transition (EMT).

Preliminary work at the time of award of this grant suggested that CD8 T cells were involved in induction of EMT. Data generated using funds from this grant were included in a publication in *Cancer Research* in April 2009 authored by Santisteban et al. (4). In brief, it was shown in that report that CD8 T cells caused the generation of neu-negative tumor variants using EMT. The most important finding described in that manuscript was that the immunoedited variants possessed qualities of breast cancer stem cells. See attached manuscript for additional details. Experimental results contained within that manuscript that are pertinent to this report are discussed below in additional details.

Task 1A: Deplete various immune subsets (e.g. CD4 T cells, macrophages, B cells or NK cells) and define the role of each in mediating EMT *in vivo* in a mouse model of human breast cancer.

- *Experiment 1: To determine whether CD8 T cell depletion in vivo abrogates immunoediting of neu+ breast cancer cells.*

In this experiment, neu+ breast cancer cells were implanted into FBV/n mice in which the neu antigen is a strong tumor rejection antigen. As was previously shown in Knutson et al. (5), implantation of these tumors into FVB/n mice results in the outgrowth of neu-negative (neu-) antigen-loss variants. In some groups of mice, CD4 or CD8 T cells were depleted prior to injection with monoclonal antibodies. As shown in **Figure 1A of Santisteban** (4) deletion of CD8 T cells prevented resulted in complete tumor rejection without the outgrowth of neu-negative variants that had undergone EMT. Conversely, depletion of CD4 T cells resulted in rapid outgrowth of neu+ epithelial tumor cells. These results confirm preliminary studies and show that CD4 T cells are required for tumor rejection and CD8 T cells are required for generation of immunoedited mesenchymal

tumor variants.

- *Experiment 2: To determine whether CD8 T cells are required for the growth of neu- immunoedited cells.*

One explanation of the results obtained in Experiment 1 above in the CD8 T cell depleted mice is that CD8 T cells are required for the growth of the mesenchymal tumor cells. Whether this was true was tested by injecting mesenchymal variants into FVB/n mice depleted of CD8 T cells and which had rejected an initial challenge with neu+ tumor cells. As shown in **Figure 1B of Santisteban et al.**, when these mice were challenged with mesenchymal variants, tumor grew out readily showing that CD8 T cells are not just simply required for growth, which supports the contention that CD8 T cells actually generate loss variants. This conclusion is supported by an *in vitro* experiment (shown in **Santisteban Figure 1C**) which shows that media conditioned with CD8 T cells does not supported enhanced *in vitro* growth of mesenchymal tumor cells.

- *Experiment 3: To determine if natural killer cells are necessary for the generation of immunoedited neu- tumor cells in vivo.*

One hypothesis established in the proposal was that natural killer (NK) or tumor or macrophages participate along with CD8 T cells in immunoediting. To test this, NK cells were depleted using an anti-NK antibody prior to tumor challenge using the same methods described in Santisteban et al. (4). Control mice received an isotype control antibody. Depletion was verified using flow cytometric analysis (not shown) and mice were then challenged with neu+ tumor cells. Tumor growth was then monitored. In contrast to prior experiments, the emergence of neu- variants in the control mice was not observed. Ongoing troubleshooting experiments indicate that the mice being used are distinct from the mice used in the past.

To circumvent the mouse problem, a second model system was developed to ascertain a role for NK cells in the generation of neu-antigen loss variants. In prior studies, our group observed that neu-antigen loss variants can develop in mice treated with a neu-specific antibody (6). Three cell lines were generated from these variant tumor cells and examined for evidence of EMT and breast cancer stem cell properties. First, RNA was purified from the cells as well as from the parental neu+ cell line MMC. The RNA was examined using PCR evaluating for E-Cadherin (an epithelial marker), N-Cadherin (a mesenchymal marker) and GAPDH (housekeeping gene). The methodology is identical to that used in Santisteban et al. (4) **Figure 1** of this document shows that the neu- cell lines generated have undergone EMT as demonstrated by the downregulation of E-cadherin and upregulation of N-cadherin. Next, the cell lines were examined for the $CD24^{lo\text{-}int}/CD44^{hi}$ breast cancer stem cell phenotype as we have previously described (4). **Figure 2** shows that the majority of cells in the cultures are $CD24^{lo\text{-}int}/CD44^{hi}$ which is consistent with a breast cancer stem cell phenotype. Lastly, tumorigenicity studies also showed that the neu- tumor cells are highly tumorigenic being able to form tumors in neu-transgenic mice in doses as low as 100 cells **(Figure 3)**. The parental neu+ cells only form tumors in doses above 1 million (4). Based on these three findings, it was concluded that this model system is adequate for evaluating a role of other non-CD8 immune effectors in EMT induction.

To determine a role for NK cells in driving relapse of mice with neu- negative tumors following treatment with anti-neu antibody, mice were depleted of NK cell prior to tumor challenge and antibody therapy. Complete methodology of anti-neu antibody treatments can be found in Knutson et al. (6). As shown in **Figure 4** and consistent with prior work (6), treatment of NK replete mice with anti-neu resulted in prevention of tumor take which was ultimately followed by relapse in about 80% of mice. NK depletion however reduced the relapse rate such that only 20% of mice developed tumors. The results were obtained in two experiments and suggest that NK cells are important in driving relapse with mesenchymal tumor cells. *In vitro* analysis, as described below is underway to evaluate for potential mechanism of action.

Task 1B: Conduct *in vitro* studies co-culturing immune effectors with epithelial tumor cells and then assessing for the induction of EMT and its mechanism.

- *Experiment 1: To determine if CD8 T cells can drive induction of neu- CD24$^{lo/int}$ tumor cells in vitro.*

In order to address the question as to whether CD8 T cells are solely responsible for driving the generation of immunoedited mesenchymal cells, an *in vitro* assay system was established in which tumor antigen-primed CD8 T cells are co-cultured with neu+ epithelial tumor cells. Several experiments have been done and the general results suggest some capability of CD8 T cells to directly immunoedit neu+ tumor cells. The results of these studies are summarized in Santisteban et al. (4). For example, as shown in **Figure 1D** of Santisteban et al., CD8 T cells primed against tumor antigen drive production of neu- CD24$^{lo/int}$ variants which is suppressed by irradiation which is known to blunt T cell activation. In contrast to primed CD8 T cells, naïve CD8 T cells do not have the same effect, demonstrating specificity (not shown). Ongoing experiments are being done to determine if immunoediting resulted in the induction of EMT and whether T cell receptor activation is required for immunoediting. Preliminary experiments (not shown) suggest that TCR engagement is not required suggesting that other molecules associated with activated CD8 T cells are required. In conclusion, our results suggest that CD8 T cells may be able to immunoedit tumor cells through EMT in the absence of other immune effectors.

- *Experiment 2: To determine if NK cell T cells can induce EMT.*

Based on Experiment 3 in Task 1A, an experiment was designed to test whether NK cell-derived molecules could induce the loss of neu expression as well as induce EMT. Thus, NK cells were purified from mice and activated in the presence of IL-2 and IL-12. After 2 days, the conditioned cell-free media was collected from the activated NK cells and transferred to wells containing neu+ tumor cells. After 2 additional days, the tumor cells were collected and examined for cell surface expression of neu, E-cadherin and N-cadherin using standard techniques. As shown in **Figure 5**, both neu expression and E-cadherin were down regulated. Unexpectedly, N-cadherin did not increase which suggests either that NK do not induce EMT or induce an incomplete EMT. Nonetheless, the results show that NK cells can induce significant changes in protein expression in tumor cells, but may require additional factors to induce EMT.

Task 2. To determine if breast tumor cells, induced by CD8 T cells to undergo EMT, demonstrate increased immunosuppression compared to native epithelial breast cancer cells.

Task 2a: Perform multiplexed cytokine analysis of five distinct mesenchymal cell lines.

Cytokine analysis was done using multiplexing as described in our prior publication (7). The tumor cells were cultured for 48 hours after which a sample of the cell culture media was removed and assessed for cytokine content. The cytokines analyzed included TGF-β, IL-1β, GM-CSF, MIP-1β, IL-10, IFN-γ, TNF-α, IL-1α, IL-6; IL-12 (p40); IL-12, MCP-1, MIP-1α, IL-9, eotaxin, RANTES, IL-13 and VEGF. TGF-β and VEGF were done independently due to a different technical step (**Figures 6 and 8**). The results show considerable differences amongst the various tumor cell types. In general, the inflammatory cytokines (IL-1β, GM-CSF, MIP-1β, IFN-γ, IL-1α, IL-12 (p40); IL-12, MCP-1, MIP-1α, IL-9, eotaxin, RANTES and IL-13) are nearly universally downregulated in the mesenchymal cells with the exception of GM-CSF which was elevated (**Figure 7**). In contrast, the potent immunosuppressive molecule, TGF-β is highly upregulated in 3 of the four mesenchymal lines. Similarly, VEGF, also an immunosuppressive cytokine, was release at higher levels from the mesenchymal cells **(Figure 8)**. IL-10 and TNF-α were not considered produced since all values were at the limit of detection.

Using microarray databases as described in Santisteban et al., (4), it was observed that the hormone, adrenomedullin (ADM), and its receptor (ADMR) were expressed specifically by mesenchymal cells but not by parental epithelial tumor cells. Prior work has already shown that adrenomedullin is a potent immune suppressive factor (8, 9). The expression profile of ADM, ADMR (heterodimer of RAMP3 and CRLR) in the murine epithelial and mesenchymal tumor cell lines was examined as is shown in **Figure 9A**. Reverse

transcriptase PCR (RT-PCR) showed upregulation of ADM and ADMR in mesenchymal (M) cell compared to epithelial (E) cells. Expression was confirmed was also confirmed by western blotting and immunofluorescence staining using polyclonal antibodies (not shown). To determine if the ADM pathway is functional in the mesenchymal cells, we measured changes in the intracellular levels of cAMP in cell lysate from control or RAMP3 siRNA transfected cells treated with or without ADM by using a non-acetylation, enzyme immunoassay system (The HitHunter™ Enzyme Fragment Complementation (EFC) cAMP Assay from GE Healthcare Life Sciences). The results indicated an increase in intracellular cAMP levels after ADM treated but not in lysates from ADM treated cell lacking RAMP3. This suggests that the ADM pathway is functional in these breast cancer stem cell lines and that RAMP3 mediates the ADM signaling. The addition of a truncated form of calcitonin gene-related peptide (CGRP 8-37) blocked (albeit not efficiently) the production of cAMP by adrenomedullin (**Figure 9B**). Subsequent studies using grant support generated from this preliminary data have revealed an important role of adrenomedullin in maintaining the mesenchymal phenotype (See Reportable Outcomes) (not shown).

Based on these findings, we conclude that the mesenchymal cells are far less inflammatory and immune suppressive as compared to the parental epithelial cells. Furthermore, the immune suppressive agents that are produced by the mesenchymal cells may act in an autocrine or paracrine fashion leading to functional changes in the tumor cells themselves.

Task 2b: Perform flow cytometry assessing for immunosuppressive cell surfaces receptors on mesenchymal cells.

The expression of immune suppressive molecules B7-H1, PD-1, B7-H3, and B7-H4 was assessed using microarray analysis as described in Santisteban et al. There was no expression noted for any of these molecules on any of the cell lines (data not shown). These molecules are not longer being considered at this time.

KEY RESEARCH ACCOMPLISMENTS

- CD8 T cell depletion prevents immunoediting *in vivo*. In contrast, CD4 T cell depletion prevents initiation of the immune response suggesting that CD4 T cells are indirectly involved in immunoediting (Reported in Santisteban, et al., (4) and Behrens et al. (3)).

- CD8 T cells appear to actively induce EMT and not just support their growth once established (Reported in Santisteban, et al., (4) and Behrens et al. (3)).

- Monoclonal anti-neu antibodies generate antigen loss variants that appear to have undergone EMT and possess breast cancer stem cell properties. Data suggests that NK cells (which are like CD8 T cells) may be responsible for relapse of animals with immunoedited tumor cells.

- Mesenchymal tumor cells produce lower levels of inflammatory cytokines and higher levels of immunosuppressive cytokines.

- Mesenchymal cells specifically produce the immune suppressive cytokine hormone, Adrenomedullin, which acts in an autocrine fashion on the mesenchymal tumor cells.

REPORTABLE OUTCOMES:

The following papers and grants contain data generated using funds from this BCRP concept award.

Manuscripts:

Behrens, M.D., J. Reiman, C.J. Krco, I.T. Lamborn, and K.L. Knutson. CD8 T cells promote relapse of breast cancer by inducing epithelial to mesenchymal transition. J Immunother 2006;29:682 (Abstract).

Santisteban, M., J.M. Reiman, M.K. Asiedu, M.D. Behrens, A. Nassar, K.R. Kalli, P. Haluska, J.N. Ingle, L.C. Hartmann, M.H. Manjili, D.C. Radisky, S. Ferrone, and K.L. Knutson. Immune-induced epithelial to mesenchymal transition in vivo generates breast cancer stem cells. Cancer Res 2009;69(7):2887-95.

Grants:

Atwater Award 12/31/2007 – 12/30/2011
Mayo Foundation
Title: Breast Cancer Stem Cell Targeted Therapies
Identification of targets and development of biologics against breast cancer stem cells.

BCRP Postdoctoral Fellowship 9/30/2010 -- 9/29/2013
Department of Defense
Delineating the pathologic role of the RAMP3 in breast cancer stem cells

CONCLUSION:

In conclusion, we have found that CD8 T cells may be able to directly immunoedit tumor cells through the induction of EMT. Furthermore, this ability of CD8 T cells may be shared by NK cells. The resulting immunoedited tumor cells have a reduced inflammatory signature and produce immune suppressive substances. The immune suppressive substances produced by the mesenchymal tumor cells may act in an autocrine or paracrine fashion to modulate tumor functions in addition to their immune suppressive actions. These findings could provide an explanation for how an immune or inflammatory response in breast cancers may drive disease progression rather than regression. Understanding these mechanisms may lead to the discovery of immune modulators which could modify the immune response to favor tumor regression.

REFERENCES:

1. Bilik, R., C. Mor, B. Hazaz, and C. Moroz. Characterization of T-lymphocyte subpopulations infiltrating primary breast cancer. Cancer Immunol Immunother 1989;28(2):143-7.

2. Georgiannos, S.N., A. Renaut, A.W. Goode, and M. Sheaff. The immunophenotype and activation status of the lymphocytic infiltrate in human breast cancers, the role of the major histocompatibility complex in cell-mediated immune mechanisms, and their association with prognostic indicators. Surgery 2003;134(5):827-34.

3. Behrens, M.D., J. Reiman, C.J. Krco, I.T. Lamborn, and K.L. Knutson. CD8 T cells promote relapse of breast cancer by inducing epithelial to mesenchymal transition. J Immunother 2006;29:682 (Abstract).

4. Santisteban, M., J.M. Reiman, M.K. Asiedu, M.D. Behrens, A. Nassar, K.R. Kalli, P. Haluska, J.N. Ingle, L.C. Hartmann, M.H. Manjili, D.C. Radisky, S. Ferrone, and K.L. Knutson. Immune-induced epithelial to mesenchymal transition *in vivo* generates breast cancer stem cells. Cancer Res 2009;69(7):2887-95.

5. Knutson, K.L., H. Lu, B. Stone, J. Reiman, E. Gad, A. Smorlesi, and M.L. Disis. Immunoediting of cancers may lead to epithelial to mesenchymal transition. J. Immunol. 2006;177:1526-1533.

6. Knutson, K.L., B. Almand, Y. Dang, and M.L. Disis. Neu antigen-negative variants can be generated after neu-specific antibody therapy in neu transgenic mice. Cancer Res 2004;64(3):1146-51.

7. Behrens, M.D., W.M. Wagner, C.J. Krco, C.L. Erskine, K.R. Kalli, J. Krempski, E.A. Gad, M.L. Disis, and K.L. Knutson. The endogenous danger signal, crystalline uric acid, signals for enhanced antibody immunity. Blood 2007;111:1472-1479.

8. Gonzalez-Rey, E., A. Chorny, F. O'Valle, and M. Delgado. Adrenomedullin protects from experimental arthritis by down-regulating inflammation and Th1 response and inducing regulatory T cells. Am J Pathol 2007;170(1):263-71.

9. Lopez, J. and A. Martinez. Cell and molecular biology of the multifunctional peptide, adrenomedullin. Int Rev Cytol 2002;221:1-92.

APPENDICES:

Santisteban, M., J.M. Reiman, M.K. Asiedu, M.D. Behrens, A. Nassar, K.R. Kalli, P. Haluska, J.N. Ingle, L.C. Hartmann, M.H. Manjili, D.C. Radisky, S. Ferrone, and K.L. Knutson. Immune-induced epithelial to mesenchymal transition *in vivo* generates breast cancer stem cells. Cancer Res 2009;69(7):2887-95.

Knutson, K.L., H. Lu, B. Stone, J. Reiman, E. Gad, A. Smorlesi, and M.L. Disis. Immunoediting of cancers may lead to epithelial to mesenchymal transition. J. Immunol. 2006;177:1526-1533.

Behrens, M.D., W.M. Wagner, C.J. Krco, C.L. Erskine, K.R. Kalli, J. Krempski, E.A. Gad, M.L. Disis, and K.L. Knutson. The endogenous danger signal, crystalline uric acid, signals for enhanced antibody immunity. Blood 2007;111:1472-1479.

SUPPORTING DATA:

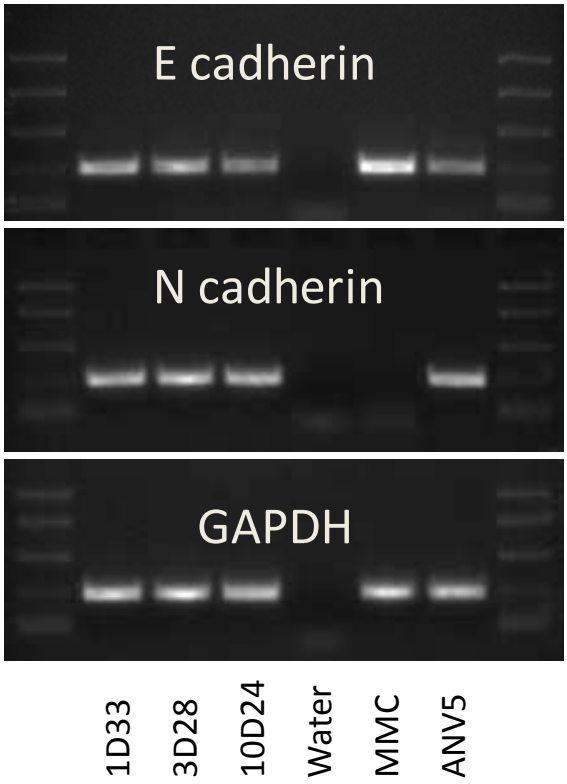

Figure 1. neu-antibody induced neu-negative tumor cells have undergone epithelial to mesenchymal transition. Shown are the RT-PCR analyses of 3 neu-negative cell lines (1D33, 3D28, and 10D24), the epithelial cell line MMC, and ANV5 (an established mesenchymal cell line). Water without RNA was used as a control.

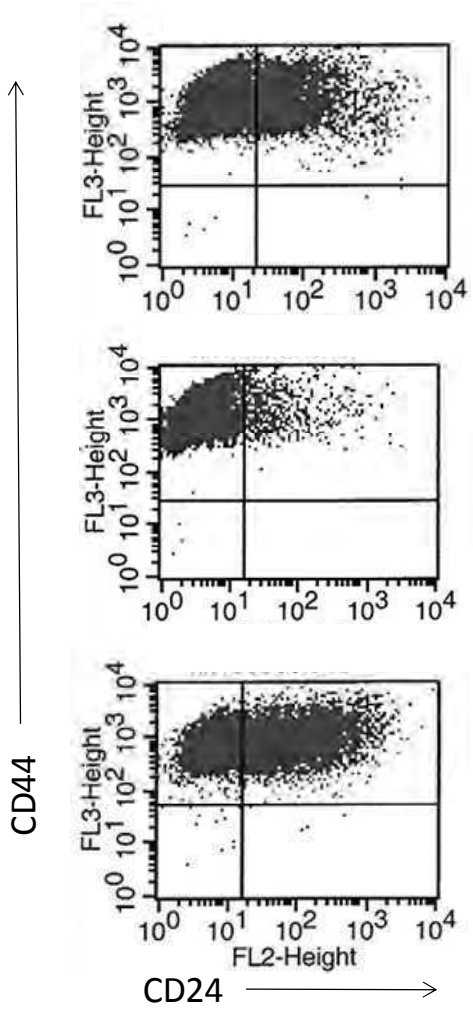

Figure 2. Tumor cell lines generated from anti-neu antibody treated mice have $CD24^{lo/int}CD44^{hi}$ phenotype. Shown are neu-negative cell lines dual stained for CD44 (Y-axis) and CD24 (X-axis) and examined by using a flow cytometer.

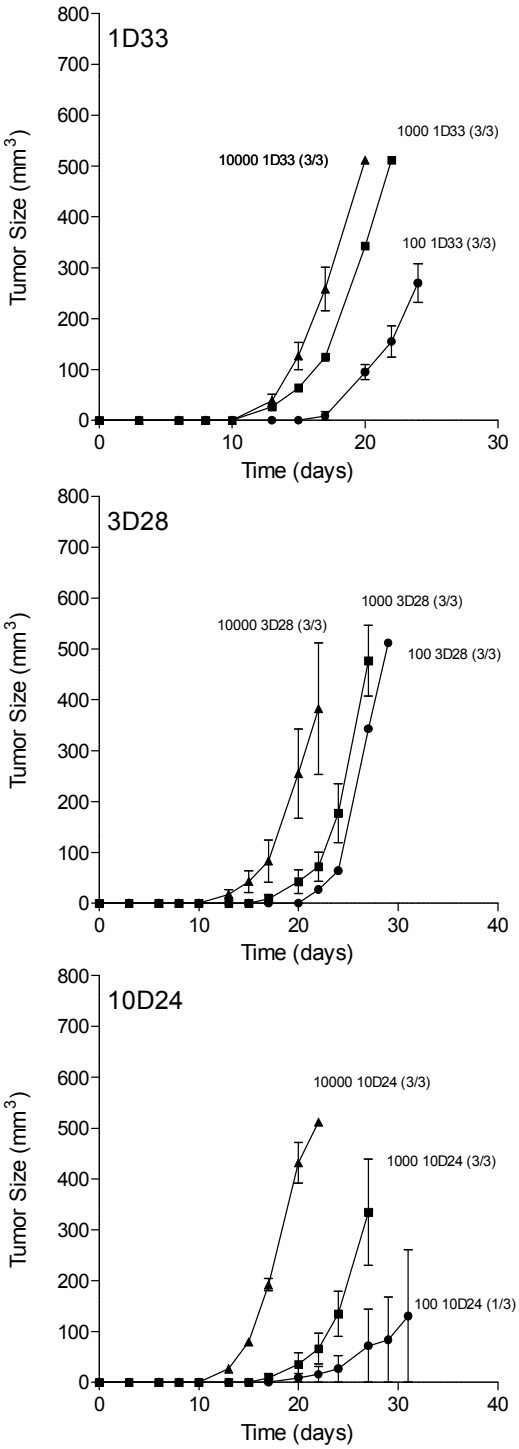

Figure 3. neu- variants are highly tumorigenic. Cells derived from tumors from mice treated with a neu-specific were injected into tumor free mice at various doses (10000, 1000, and 100) for each of three cell lines. Shown are the tumor growth curves and the fraction of mice that developed tumors at each dose. Each data point is the mean (s.e.m.)

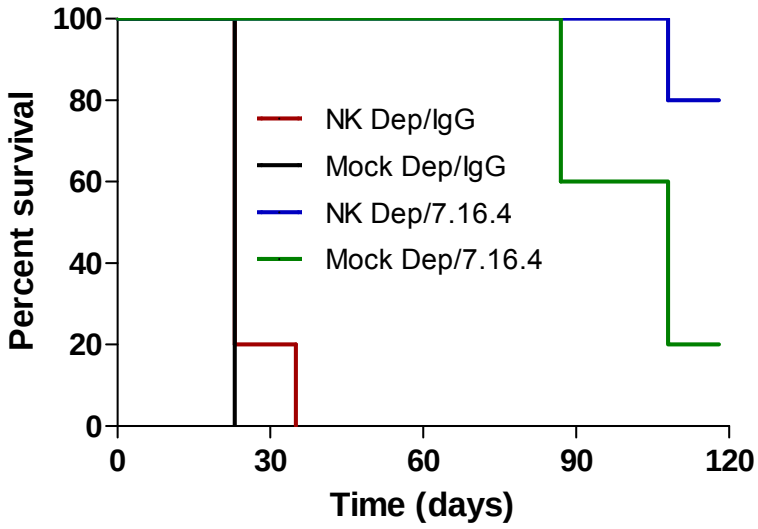

Figure 4. Mice depleted of NK cells relapse less frequently than nondepleted mice. Five mice/group were challenged with neu+ tumor cells and treated with either anti-neu antibody or an irrel IgG (IgG). Two of the four group were depleted of NK prior to tumor challenge and anti-neu treatments. Shown is the percent survival over time. Note that 80% of mice depleted of NK and treated with anti-neu antibody survived tumor free while only 20% of NK replete mice treated with ant-neu antibody survived.

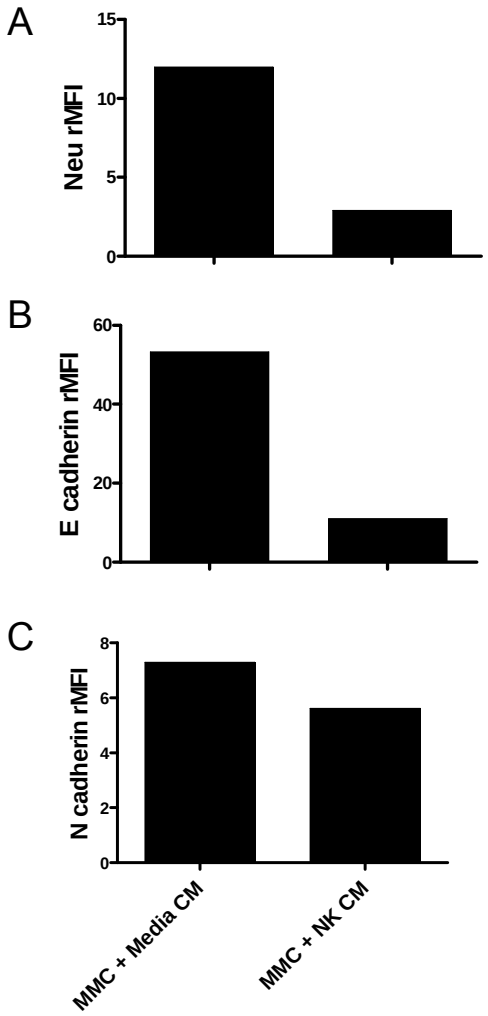

Figure 5. Treatment of neu+ tumor cells with NK cell-conditioned media induces loss of neu and E-cadherin. Shown are the relative mean flourescent intensities of cell surface staining of (A) neu, (B) E-cadherin, and (C) N-cadherin of neu+ tumor cells (MMC) treated for 2 days with media conditioned (CM) for 2 days by activated (IL-2 (1000 U/ml) and 10 ng/ml IL-12) NK cells. rMFI=relative mean intensity.

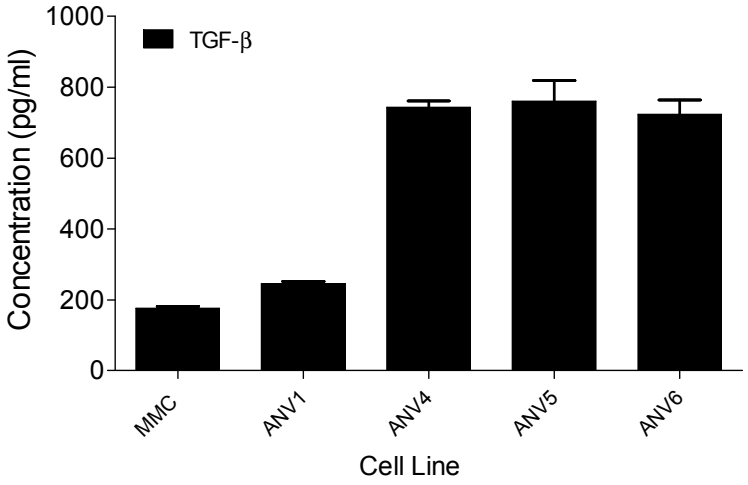

Figure 6. Mesenchymal tumor cells produce immuno-suppressive TGF-β. Shown are the concentrations of TGF-β. Each bar is the mean (± s.e.m) of duplicate samples. MMC is the neu+ cell line and ANV1, 4, 5, and 6 are the neu- tumor cell lines. The content of each cytokine in fresh media is also shown.

Figure 7a

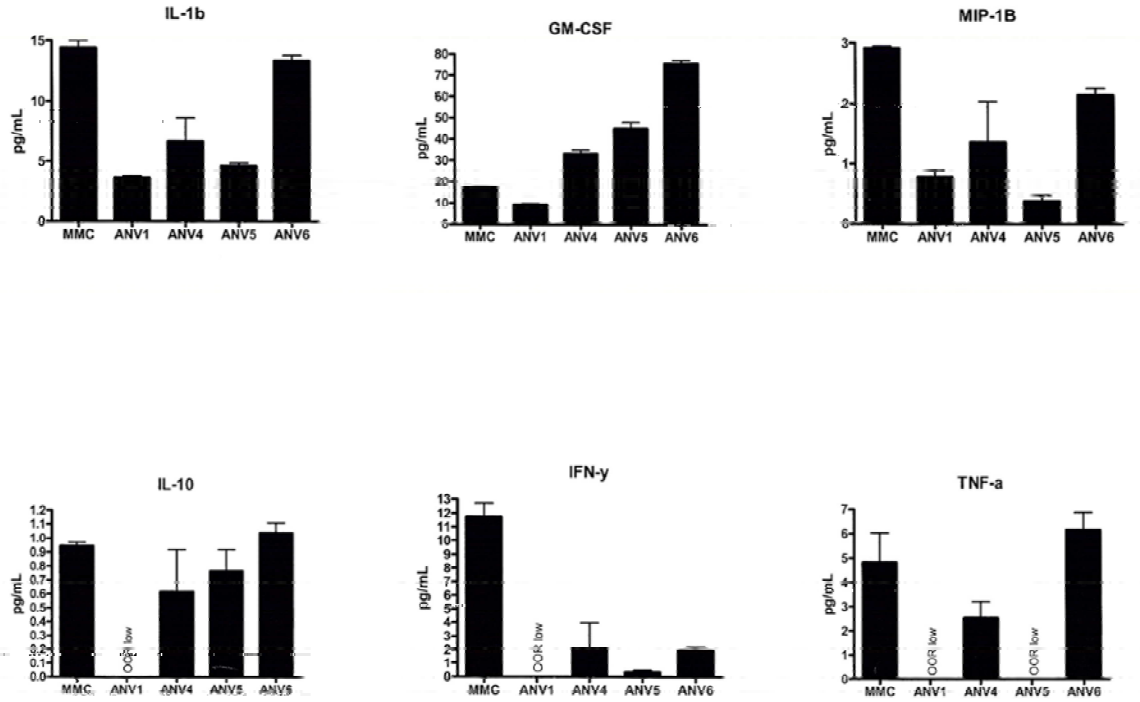
IL-1b
pg/mL
MMC
ANV1
ANV4
ANV5
ANV6
GM-CSF
MIP-1B
IL-10
OOR low
IFN-y
TNF-a

Figure 7b

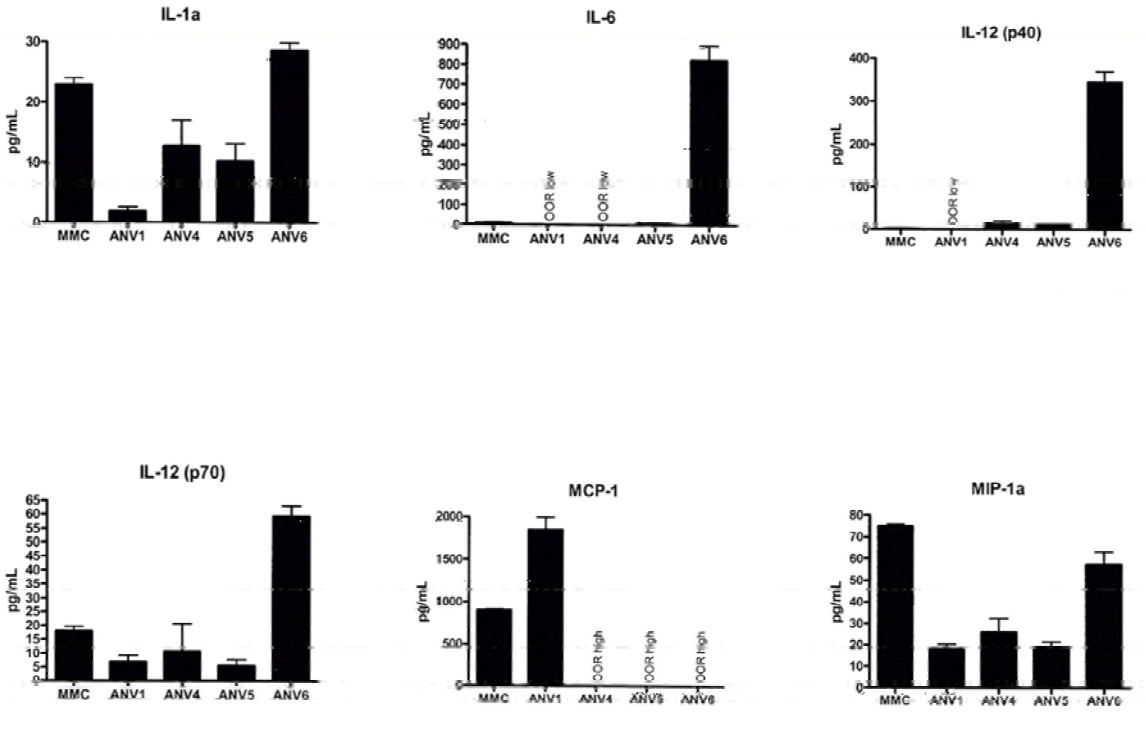
IL-1a
pg/mL
MMC
ANV1
ANV4
ANV5
ANV6
IL-6
pg/mL
OOR low
OOR low
IL-12 (p40)
pg/mL
OOR low
IL-12 (p70)
pg/mL
MCP-1
pg/mL
OOR high
OOR high
OOR high
MIP-1a
pg/mL

Figure 7c

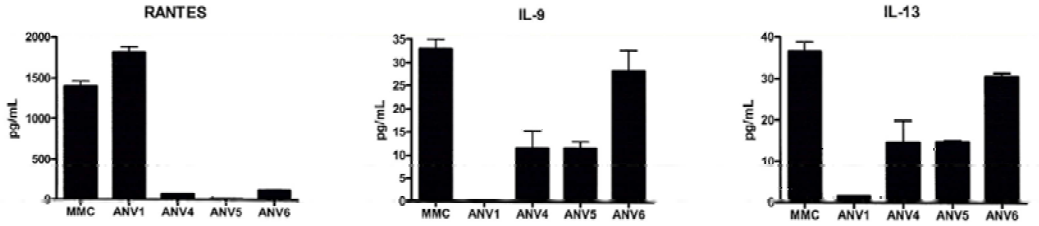

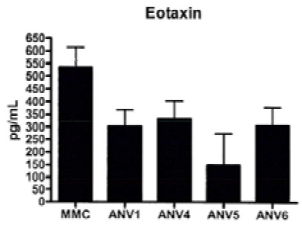

Figure 7. Cytokine profiles of mesenchymal cell lines (ANV) relative to parental epithelial tumor cell line (MMC). Shown are the levels of cytokines in the cell culture supernatants obtained after 48 hrs culture. Each bar is the mean (±sem) of duplicate samples. The cytokine analyzed in named above each graph. OOR low = Not detectable, OOR high concentration above standard curve range. IL-1b = interleukin 1 beta; GM-CSF = granulocyte macrophage colony stimulating factor; MIP-1B = monocyte inhibitory protein 1 beta; IL-10 = interleukin 10; IFN-y = interferon gamma; TNF-a = tumor necrosis factor alpha; IL-1a = interleukin1 alpha; IL-6 = interleukin 6; IL-12 (p40) = interleukin 12 p40; IL-12 (p70) = interleukin 12 p70; MCP-1 = macrophage chemotactic protein 1; MIP-1a = macrophage inhibitory protein alpha; IL-9 = interleukin 9; IL-13 = interleukin 13.

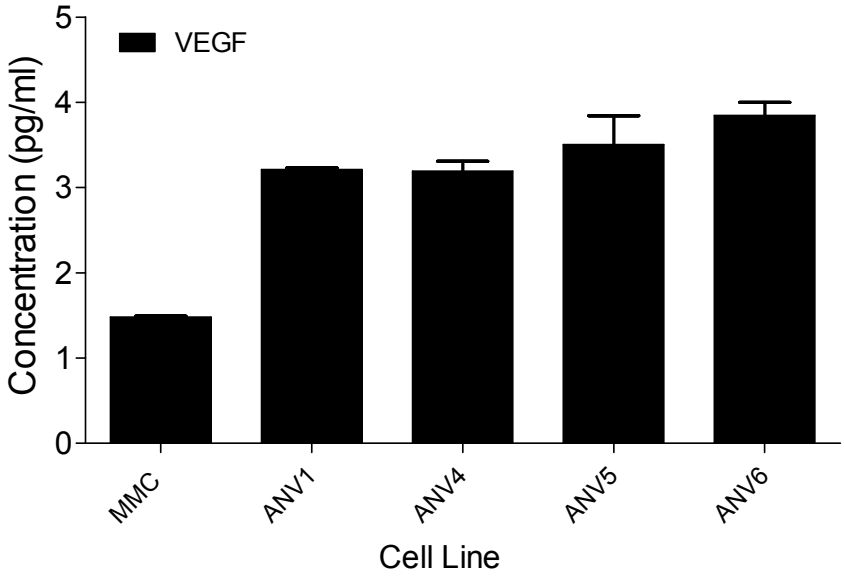

Figure 8. Mesenchymal tumor cells produce immuno-suppressive VEGF. Shown are the concentrations of VEGF. Each bar is the mean (± s.e.m) of duplicate samples. MMC is the neu+ cell line and ANV1, 4, 5, and 6 are the neu- tumor cell lines. The content of each cytokine in fresh media is also shown.

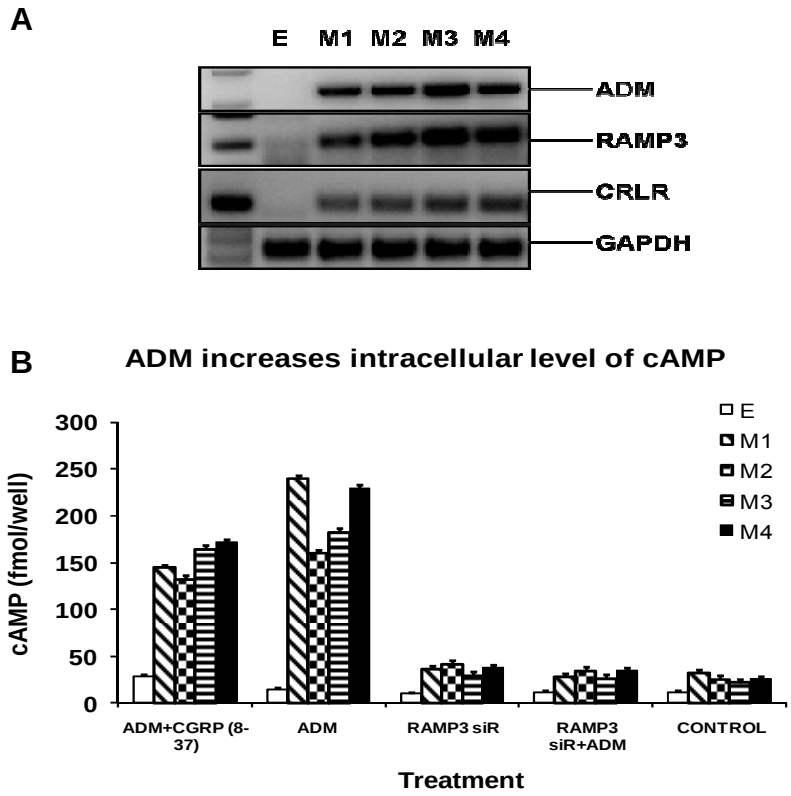

Figure 9. Murine mesenchymal (M) tumor cells possess a functional adrenomedullin pathway. Panel A shows western blot analysis of adrenomedullin (ADM), Receptor activity modifying protein 3 (RAMP3), Calcitonin receptor like receptor (CRLR), and GAPDH expression in epithelial (E) tumor cells and immunoedited mesenchymal (M) cells. Panel B shows that mesenchymal tumor cells have a functional ADM pathway as assessed by the production of cyclic AMP. Shown are the concentrations of cAMP in the cell lysates after 48 hrs culture in presence of ADM (100 ng/ml), CGRP(8-37) (an ADM antagonist), RAMP3 siRNA, or combinations thereof. Control well contained media alone. Each bar is the mean (± sem) of 3 replicates.

Immune-Induced Epithelial to Mesenchymal Transition *In vivo* Generates Breast Cancer Stem Cells

Marta Santisteban,[1,4] Jennifer M. Reiman,[2] Michael K. Asiedu,[2] Marshall D. Behrens,[2] Aziza Nassar,[3] Kimberly R. Kalli,[1] Paul Haluska,[1] James N. Ingle,[1] Lynn C. Hartmann,[1] Masoud H. Manjili,[5] Derek C. Radisky,[6] Soldano Ferrone,[7] and Keith L. Knutson[2]

Departments of [1]Oncology, [2]Immunology, and [3]Anatomic Pathology, Mayo Clinic, Rochester, Minnesota; [4]Department of Oncology, Clinica Universidad de Navarra, Pamplona, Spain; [5]Department of Microbiology and Immunology, VCU School of Medicine, Massey Cancer Center, Richmond, Virginia; [6]Department of Biochemistry and Molecular Biology, Mayo Clinic, Jacksonville, Florida; and [7]Departments of Surgery, Immunology and Pathology, University of Pittsburgh Cancer Institute, Pittsburgh, Pennsylvania

Abstract

The breast cancer stem cell (BCSC) hypotheses suggest that breast cancer is derived from a single tumor-initiating cell with stem-like properties, but the source of these cells is unclear. We previously observed that induction of an immune response against an epithelial breast cancer led *in vivo* to the T-cell–dependent outgrowth of a tumor, the cells of which had undergone epithelial to mesenchymal transition (EMT). The resulting mesenchymal tumor cells had a $CD24^{-/lo}CD44^{+}$ phenotype, consistent with BCSCs. In the present study, we found that EMT was induced by CD8 T cells and the resulting tumors had characteristics of BCSCs, including potent tumorigenicity, ability to reestablish an epithelial tumor, and enhanced resistance to drugs and radiation. In contrast to the hierarchal cancer stem cell hypothesis, which suggests that breast cancer arises from the transformation of a resident tissue stem cell, our results show that EMT can produce the BCSC phenotype. These findings have several important implications related to disease progression and relapse. [Cancer Res 2009;69(7):2887–95]

Introduction

A current goal among breast cancer scientists worldwide is to reduce the risk of breast cancer recurrence following therapy (1). This risk, which remains high for at least one decade, suggests that treated patients still maintain a small population of tumorigenic, albeit dormant, cancer stem cells. Although previously described (2), it was not until 2003 that interest in breast cancer stem cells (BCSC) was renewed (3). In that study, identification of the $CD24^{-/lo}CD44^{+}$ tumorigenic breast cancer cells provided a valuable marker framework for testing hypotheses on BCSC involvement in the clinical course of breast cancer and its pathogenesis.

A prevalent BCSC hypothesis proposes that breast tumors are initiated and maintained by a small fraction of tumorigenic cells (4). What remains unclear about the BCSC hypothesis is the origin of the tumorigenic cells. One hypothesis is that transformed resident tissue stem cells undergo asymmetrical division, occasionally renewing a copy of themselves but most often generating proliferative epithelial daughter progeny with limited tumorigenicity. An alternative hypothesis is that BCSCs are derived from transformed, differentiated epithelial cells by acquisition of stem cell attributes. Determining the origin and biology of BCSCs is important for the development of therapies to reduce the risk of breast cancer relapse.

In prior work, we found that immunoediting of breast tumors in the neu-transgenic (neu-tg) mouse resulted in neu antigen-loss variant tumors (5–8). Our first observation was that the variants had a different proteomic profile and reduced inflammatory and danger signals (7). Subsequent analyses revealed that antigen-loss tumor cells had undergone T-cell–dependent epithelial to mesenchymal transition (EMT; refs. 5, 6). EMT, a dedifferentiation program that converts epithelial cells into a mesenchymal phenotype, is involved in embryogenesis and used pathologically during cancer progression (9). Because our studies showed that mesenchymal antigen-loss variants were $CD24^{-/lo}$, we assessed whether these antigen-loss tumor cells had characteristics of $CD24^{-/lo}$ BCSCs observed by Al-Hajj and colleagues (3, 6). Furthermore, we aimed to determine what T-cell subset was involved in the induction of EMT. Herein, we show that EMT induction *in vivo* involves CD8 T cells and generates BCSCs.

Materials and Methods

Animals. Female neu-tg mice on the FVB background and FVB/N mice were maintained as a colony in accordance with institutional policy.

Cell lines. The epithelial cell line (E) was derived as previously described (10). Four cell lines (M1, M2, M3, and M4) were obtained from relapsed tumors that underwent EMT following injection of E tumor cells into parental nontransgenic FVB/N mice (6). All cell lines were maintained in RPMI 1640 containing 10% fetal bovine serum (FBS), 1% penicillin/streptomycin, 1% sodium pyruvate, 2.5% HEPES, and 2 mmol/L L-glutamine.

***In vivo* tumorigenicity assays.** Neu-tg mice were inoculated s.c. on the mid-dorsum unless otherwise specified, with doses of tumors cells ranging from 100 to 10^6 cells. Tumors were measured every other day with vernier calipers, and volumes were calculated as the product of length × width × height × 0.5236.

Antibodies for *in vivo* cell depletion. Anti-CD4 (GK1.5) and anti-CD8 (53.6.72) monoclonal antibodies were prepared by the Mayo Antibody Core Facility (Rochester, MN). Mice were injected daily for 5 d with 100 μg of antibody i.v. and E tumor cells were injected 48 h later. For secondary depletion of CD8s, mice previously injected with E tumor cells received five more daily doses of anti-CD8 and were rechallenged with tumors.

Proliferation of M3 cells in response to CD8 T-cell conditioned media. CD8 T cells were derived from lymph nodes and spleens of naïve FVB mice with a mouse $CD8a^{+}$ T-cell isolation kit per manufacturer's recommendations using an autoMACS Separator (Miltenyi Biotec, Inc.).

Note: Supplementary data for this article are available at Cancer Research Online (http://cancerres.aacrjournals.org/).

M. Santisteban and J.M. Reiman are equal co-first authors and S. Ferrone and K.L. Knutson are senior authors.

Requests for reprints: Keith L. Knutson, College of Medicine, Mayo Clinic, 342C Guggenheim, 200 First Street Southwest, Rochester, MN 55905. Phone: 507-284-0545; Fax: 507-266-0981; E-mail: knutson.keith@mayo.edu.

doi:10.1158/0008-5472.CAN-08-3343

Two million untouched $CD8^+$ T cells per well were plated in six-well plates. Unstimulated wells contained CD8s and media. CD8s were treated with 2 million irradiated splenocytes (3,300 rad) and 250 μg of concanavalin A. Anti-CD3/CD28 received 400,000 mouse Dynabeads (Invitrogen) per well (~1 bead/5 T cells). One hundred microliters of 18-h conditioned media were added to mesenchymal (M) cells previously seeded into 96-well plates. [^{3}H]Thymidine was added at 0.273 nCi per well; 24 h later, cells were harvested and read on a TopCount NXT scintillation counter (Perkin-Elmer).

Flow cytometry. Cells were incubated with primary antibodies at 4°C for 20 to 30 min, washed, followed by secondary antibody (if needed) for 20 min, washed, and fixed with 0.5% formaldehyde. Samples were run on a BD FACScan or a FACSCalibur flow cytometer (BD Bioscience). Sorting of M3 cells was done on a BD FACSVantage Cell Sorter and data were analyzed using BD CellQuest Pro software (version 4.0.2). Occasionally, results depicted the relative mean fluorescent intensity (ratio of specific marker intensity to the isotype or secondary antibody staining).

Flow cytometry reagents. Antibodies and reagents from BD Pharmingen included anti-CD24 FITC (M1/9), anti-CD44 FITC, phycoerythrin (PE)-Cy5 (IM7), anti-Sca1 FITC (D7), anti–Annexin V allophycocyanin, and 7-amino-actinomycin D (7-AAD). Antibodies from eBioscience were anti-CD24 PE (30-F1), anti-CD34 FITC (RAM34), and anti-CD133/Prominin I FITC (13A4). Rabbit anti–claudin 3 (Z23.JM) was from Zymed/Invitrogen. The mouse monoclonal antibody against rat neu (7.16.4) was previously described (6). Secondary antibodies from Jackson ImmunoResearch Laboratories were FITC goat anti-rabbit IgG and FITC anti-mouse IgG. Antimouse IgG2a/2b FITC (R2-40) was from BD Pharmingen. Isotype antibodies were PE Rat IgG2b (eBioscience), FITC Rat IgG2b (BD Pharmingen), and PE-Cy5 Rat IgG2b (195-1, BD Pharmingen). BD Cytofix/Cytoperm Fixation/Permeabilization solution kit (BD Pharmingen) was used for claudin-3 staining.

***In vitro* coculture of E cells with primed CD8s.** FVB mice were injected with 5 million E tumor cells, and spleens removed 7 d later to isolate primed CD8 T cells as described above. In six-well plates, 2.5×10^5 E cells and 2×10^6 CD8 T cells were added per well. CD8 T cells were irradiated to 3,300 rad. Cells were cocultured for 24 h, T cells washed off, and tumor cells stained for neu and CD24 and analyzed by flow cytometry.

PCR analysis. RNA was isolated using RNeasy (Qiagen). PCR primers, selected with MacVector software (MacVector, Inc.), were from Invitrogen. Reverse transcription-PCR (RT-PCR) used SuperScript One-Step RT-PCR with Platinum Taq (Invitrogen) using 100 or 200 ng of RNA in a Bio-Rad MyCycler. Samples were electrophoresed on 1% agarose gels, imaged on a Gel Doc XR (Bio-Rad), and band intensities quantified with Quantity One software (version 4.5.2). DNA repair gene expression analysis was done using DNA Damage Signaling RT^2 Profiler PCR Array qPCR kit (SuperArray Bioscience) according to the manufacturer's protocol and run on a Mx3005P thermal cycler (Stratagene). Expression was normalized to housekeeping genes and expressed as fold expression relative to the E cell line.

Cell photography. Images of cell lines at ×40 magnification were taken using an Axiovert 200M inverted microscope and AxioCam HRm camera interfaced with Axiovision software (Carl Zeiss). Images of spheroids at ×20 magnification were obtained with a Leica DC 200 microscope (Leica Microsystems) and Fujifilm FinePix 6800 Zoom camera (Fujifilm).

Histology. M3 and E tumors from neu-tg mice were frozen in optimum cutting temperature compound (Tissue-Tek, Sakura Finetek USA), cryosectioned, and stained with H&E. Images (20×) were gathered using a NanoZoomer Digital Pathology (Bacus Laboratories, Inc.) slide scanner and captured using WebSlide Enterprise software. Staining and imaging of frozen tumor sections was done by the Tissue and Cell Molecular Analysis of the Mayo Clinic Cancer Center using standard techniques.

Western blotting. Protein was isolated from whole cell lysates using cell extraction buffer (Invitrogen), and concentration determined using the BCA assay (Pierce/Thermo Fisher Scientific, Inc.). Protein (80–150 μg) was subjected to SDS-PAGE electrophoresis and transferred onto polyvinylidene difluoride membranes, which were blocked for 1 h with skim milk (3% w/v of PBS with Tween 20) and incubated overnight (4°C) with monoclonal antibodies against BCRP (BXP-21) or PGP (C219) from Calbiochem diluted 1:50 and 1:500, respectively. Membranes were washed and incubated with alkaline phosphatase–conjugated antimouse IgG (Chemicon/Millipore) for 1 h (1:8,000 dilution) followed by detection with enhanced chemiluminescence (GE Healthcare). Anti–β-actin was used as loading control (AC-74, Sigma Aldrich).

Chemotherapy assays. Mitoxantrone dihydrochloride was from Sigma Aldrich; 1,3-bis(2-chloroethyl)-1-nitrosourea (BCNU) from the Chemical Synthesis Branch of National Cancer Institute; and etoposide from Biomol International. 3-(4,5-Dimethylthiazol-2-yl)-2,5-diphenyltetrazolium bromide (MTT) cellular proliferation assays were used (11) for mitoxantrone chemosensitivity. E and M cells (5,000) were plated in 96-well plates in complete medium overnight and thereafter in serum-free medium. Cell lines were exposed to increasing concentrations (0, 2.5, 5, 10, and 20 μmol/L) of mitoxantrone (diluted in 95% ethanol) for 72 h. Medium was aspirated from wells and 15 μL/well of MTT reagent (Sigma Aldrich) were added and incubated for 4 h at 37°C followed by 100 μL of stop solution. The following day, plate absorbances were measured at 562 nm in an ELISA SpectraMax 190 reader (Molecular Devices). Percent inhibition of growth was measured as a percentage of control (no mitoxantrone). For apoptotic assays, cells were plated and treated with 2 μmol/L etoposide for 24 h followed by staining with Annexin V and 7-AAD. The percentage of apoptotic cells was determined by flow cytometry as described (12).

Clonogenic assays. Five hundred cells were plated in P35 dishes and treated 24 h later with irradiation or BCNU. Irradiation was done with a ^{137}Cs laboratory irradiator to generate a dose curve of 0, 4, 8, 16, and 32 Gy, or cells were exposed to increasing doses (0, 2.5, 5, 10, and 20 μmol/L) of BCNU. After 8 d, cells were washed, stained with crystal violet, and colonies counted.

Matrix metalloproteinase activity assay. The EnzoLyte 520 Generic MMP Fluorometric Assay Kit (AnaSpec) was used according to the manufacturer's directions. Cell culture supernatants were incubated with 1 mmol/L of 4-aminophenylmercuric acetate for 24 h at 37°C to activate pro-MMPs. Fluorescence was measured at 490/520 nm Ex/Em using a Victor V plate reader (Perkin-Elmer).

RNA microarray. Affymetrix microarray analysis was done by Mayo Advanced Genomic Technology Center as previously described (6) using GeneChip Mouse Genome 430 2.0 arrays. The expression analysis was done with Affymetrix GeneChip Operating Software with a scaling target signal of 500 and normalization of 1. Microarray data are posted on Gene Expression Omnibus as GSE13259.

Spheroids. Cells from monolayer cultures were harvested and resuspended at a density of 4×10^4 viable cells/mL in serum-free MEBM (Cambrex Bioscience) supplemented with 2% B27 (Invitrogen), 20 ng/mL epidermal growth factor EGF (BD Biosciences), 100 μL mercaptoethanol, 4 μg/mL insulin (Sigma), 1 ng/mL hydrocortisone, 1% penicillin/streptomycin, 0.25 μg/mL amphotericin B, and 20 μg/mL gentamicin sulfate and then seeded into 10-cm dishes coated with 1% agarose. Cultures were fed weekly.

Statistical analyses. Statistical analysis was done using Prism 4 for Windows (version 4.03, GraphPad Software). Data were analyzed using one-way ANOVA when comparing E with each of the M cell lines with the Bonferroni multiple comparison test (Kruskal-Wallis as nonparametric) or one-tailed Student's t tests. Statistical significance was set at $P \leq 0.05$. The number of replicates is indicated with each figure.

Results

Induction of EMT *in vivo* requires CD8 T cells. Immune rejection of neu^+ epithelial (E) breast tumors in the FVB/N mouse, where neu is a foreign antigen, results in T-cell– and IFN-γ–dependent induction of neu antigen-loss (neu^-) variant tumors that have undergone EMT (5, 6). To determine which T-cell subset was responsible, we depleted CD4 or CD8 T cells from FVB/N mice before challenge with neu^+ E tumor cells. Control mice developed tumors at ~40 days, whereas those depleted of CD4 T cells developed tumors at ~20 days (Fig. 1*A*; ref. 6). Consistent with

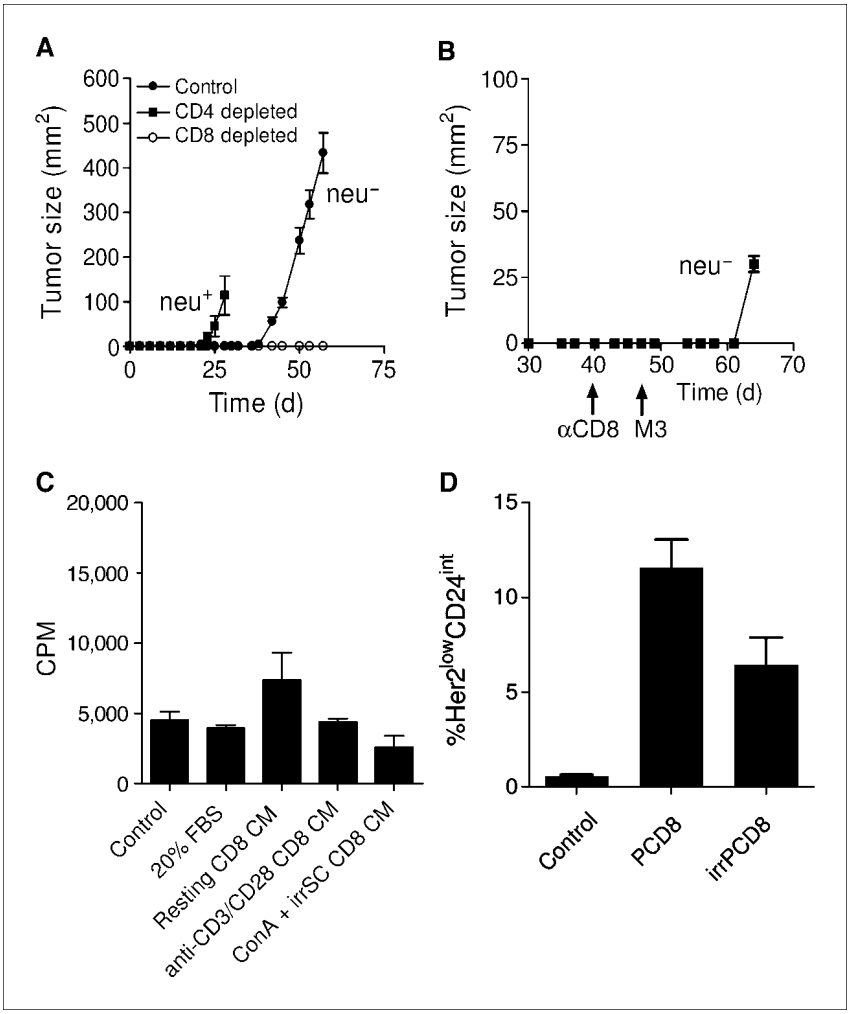

Figure 1. Induction of EMT *in vivo* requires CD8 T cells. *A,* tumor growth in control, CD4-depleted, and CD8-depleted mice. *Points,* mean of measurements from three tumors; *bars,* SE. A repeat experiment yielded identical results. *B,* tumor growth in CD8-depleted mice that had been injected with parental E cells on day 0 and rechallenged at day 47 with antigen-loss variant tumor cells (M3). *Points,* mean ($n = 3$); *bars,* SE. *C,* proliferation rates (counts per minute of incorporation of thymidine) of antigen-negative tumor cells incubated with RPMI 1640 + 10% FBS (control medium), medium with 20% FBS, conditioned medium from resting CD8 T cells (resting CD8 CM), conditioned medium from anti-CD3/anti-CD28–stimulated T cells, or conditioned medium from concanavalin A–stimulated T cells cocultured with irradiated splenocytes. *Columns,* mean ($n = 3$); *bars,* SE. *D,* percentages of tumor cells that lost neu and had reduced CD24 (epithelial marker) expression following exposure of E tumor cells to control (regular) medium, tumor-primed CD8 T cells (*PCD8*) or irradiated tumor-primed CD8 T cells (*irPCD8*). *Columns,* mean of three separate samples; *bars,* SE.

prior work, control mice developed neu$^-$ variants, whereas those depleted of CD4 T cells had neu$^+$ tumors (data not shown). Mice depleted of CD8 T cells, however, remained disease-free (Fig. 1*A*). Long-term observation (>100 days) suggested complete tumor rejection (data not shown). Four possible reasons could explain why tumors did not grow in CD8 T-cell–depleted mice. The first is that CD8 T-cell depletion permitted a more robust immune response against neu$^-$ EMT variants. To test this, CD8 T-cell–depleted mice that rejected tumor were rechallenged with neu$^-$ EMT variants. If robust immunity against neu$^-$ EMT variants existed, these mice should reject tumor, which we did not observe (Fig. 1*B*). The second possible reason is that CD8 T cells preferentially support enhanced growth of the neu$^-$ EMT variants contained as a small population within the E cell line. To test this, conditioned culture medium from CD8 T cells was applied to neu$^-$ EMT variants *in vitro*. Neu$^-$ EMT variant tumor cells exposed to conditioned medium did not grow any better than those incubated with control medium ($P > 0.05$), ruling out the likelihood that growth of these cells was enhanced by growth factors derived from CD8 T cells (Fig. 1*C*). A third possibility is that CD8 T cells promote the malignant transformation of stromal cells that associate with the nascent tumor. This is ruled out because these mesenchymal tumors contain the *neu* oncogene, which is not in the FVB/N genome (5). The only remaining possibility is that CD8 T cells directly induce neu$^-$ EMT variants. These findings, along with prior work, show that the generation of neu$^-$ EMT variants in the FVB/N mice is an active, rather than a selective, process (5). To further support this, we found that E cells cultured with tumor-primed CD8 T cells lost neu and CD24 expression ($P = 0.0009$; Fig. 1*D*). This was partially ablated by prior irradiation of the CD8 T cells, which is known to blunt T-cell proliferation and cytokine production. Naïve CD8 T cells failed to generate antigen-negative tumor cells (data not shown).

Stable mesenchymal cell lines were established. Four neu$^-$ EMT variant cell lines (M1, M2, M3, and M4) were established from four different tumors. All were neu$^-$ as assessed by RT-PCR (data not shown). Consistent with having undergone EMT, the M cell lines had significantly reduced levels of the epithelial markers E-cadherin and claudin 3 ($P = 0.0001$; Fig. 2*A*). Moreover, mesenchymal markers N-cadherin and Snail were up-regulated in M cell lines (Fig. 2*B*). Increased mesenchymal function, as measured by matrix metalloproteinase (MMP) activity, was increased significantly ($P < 0.01$) in all lines, except M1 relative to the parental E cell line (Fig. 2*B*). Visual inspection (Fig. 2*C*) showed that M cell lines had a scattered, spindle-shaped appearance, whereas the E cell line had strong cellular junctions with a cobblestone appearance. Fluorescence *in situ* hybridization karyotyping revealed that each M cell line contained, like the parental E cells, a single integration site for rat neu within chromosome 3 (Supplementary Fig. S1).

Mesenchymal cells are $CD24^{-/lo}CD44^{+}$ and highly tumorigenic. Human BCSCs have been distinguished from nontumorigenic cells by the cell surface marker profile $CD24^{-/lo}CD44^{+}$ (3). Because our prior work showed that CD24 was down-regulated in neu^{-} EMT variant tumors, we hypothesized that M cells may have a BCSC profile. As shown in Fig. 3*A*, the M cell lines were largely $CD24^{-/lo}$ and $CD44^{+}$ in contrast to the $CD24^{+}CD44^{+}$ E cells. CD24 expression was significantly lower in all M cells relative to the E cells ($P = 0.004$). CD34, a sialomucin expressed on mesenchymal stem cells (13), was not significantly elevated ($P = 0.63$) in M cell lines relative to E cells (Supplementary Fig. S2). Consistent with prior work, the M cells had low and intermediate expression of stem cell antigen-1 (Sca1), and although elevated relative to E cells, it was not statistically significant ($P = 0.23$; Supplementary Fig. S2). CD133, a marker of hematopoietic stem cells, was also examined given its association with human cancer stem cells (14). Staining revealed similarly low expression in both tumor types ($P = 0.74$; Supplementary Fig. S2).

A key property of cancer stem cells is their ability to seed tumors at very low numbers. *In vivo* studies showed that M tumor cells were far more tumorigenic than E cells (Fig. 3*B*; Table 1). M cells formed tumors in 100% of mice at doses of ≥1,000 cells, and M3 formed tumors with as few as 100 cells. E cells only formed tumors when 10^6 cells were injected (Fig. 3*B*; Table 1). Despite large differences in tumorigenicity, both cell types were able to form spheroids *in vitro* under conditions that prevented attachment (Supplementary Fig. S3). However, the M cells generated spheroids with greater efficiency than E cells ($P < 0.0001$; Fig. 3*B*).

Mesenchymal tumor cells generate $neu^{+}CD24^{hi}CD44^{+}$ tumors in neu-tg mice. Another unique feature of BCSCs is the ability to give rise to epithelial progeny that constitute the bulk of a tumor. To examine whether the mesenchymal cells could reconstitute an epithelial tumor, M tumor cells were injected into the neu-tg mouse, which carries the *neu* transgene and will not reject neu^{+} tumors. Because some M cells showed a minor population with moderate CD24 expression, we sorted $CD24^{-}$ tumor cells from $CD24^{lo/int}$ tumor cells. Both fractions formed tumors on injection of 10^5, 10^4, or 10^3 cells with nearly equal efficacy (data not shown). M cells were able to reconstitute tumors that regained CD24 expression and maintained high CD44 expression levels (Fig. 3*C*). Histologic analysis of tumors from E and M3 cells shows no remarkable differences (Supplementary Fig. S4). However, neu expression was poorly up-regulated, a finding consistent with our prior study showing that the neu-transgene mouse mammary tumor virus (MMTV) promoter in the neu^{-} EMT variant tumors is heavily methylated (5). Indeed, neu expression could be regained by injection of M tumor cells into the mammary fat pad, a site of preferential activation of the MMTV promoter. In fact, M1 cells regained complete neu expression in the mammary fat pad but not in the flank ($P = 0.002$; Fig. 3*C*). CD24 and neu expression were also induced, albeit moderately, in M1 cells grown under spheroid forming conditions (Supplementary Fig. S5).

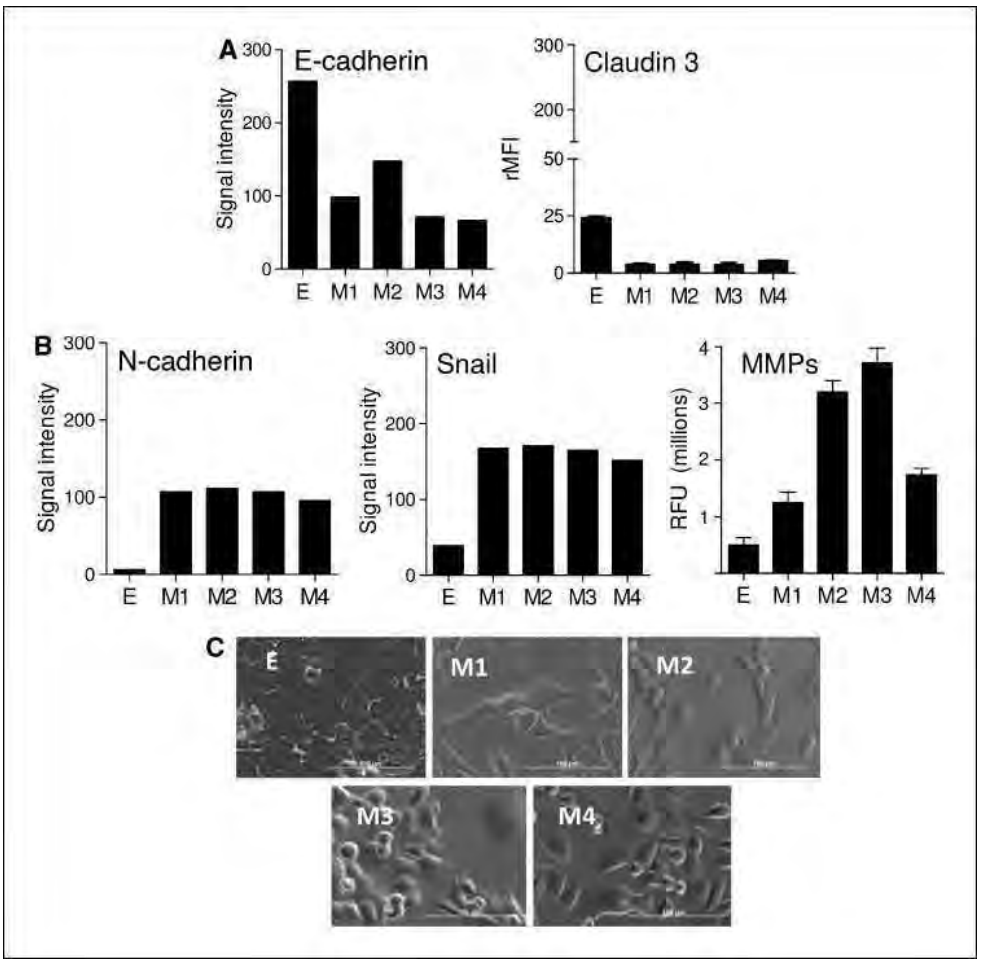

Figure 2. Stable cell lines from tumor cells that underwent EMT were established. *A,* expression levels of E-cadherin and claudin 3 in E and M cell lines. The E-cadherin experiments were repeated independently thrice with similar results. Claudin 3 was measured by flow cytometry; *columns,* mean of two separate experiments; *bars,* SE. *B,* N-cadherin and Snail expression and MMP activity for all cell lines. *Columns,* signal intensity derived using RT-PCR. RT-PCR results are representative of two experiments that gave nearly identical results. For MMP activity, each column is the mean of three samples; *bars,* SE. *C,* light microscope pictures (×40) of the cell lines. *Bar,* 100 μm.

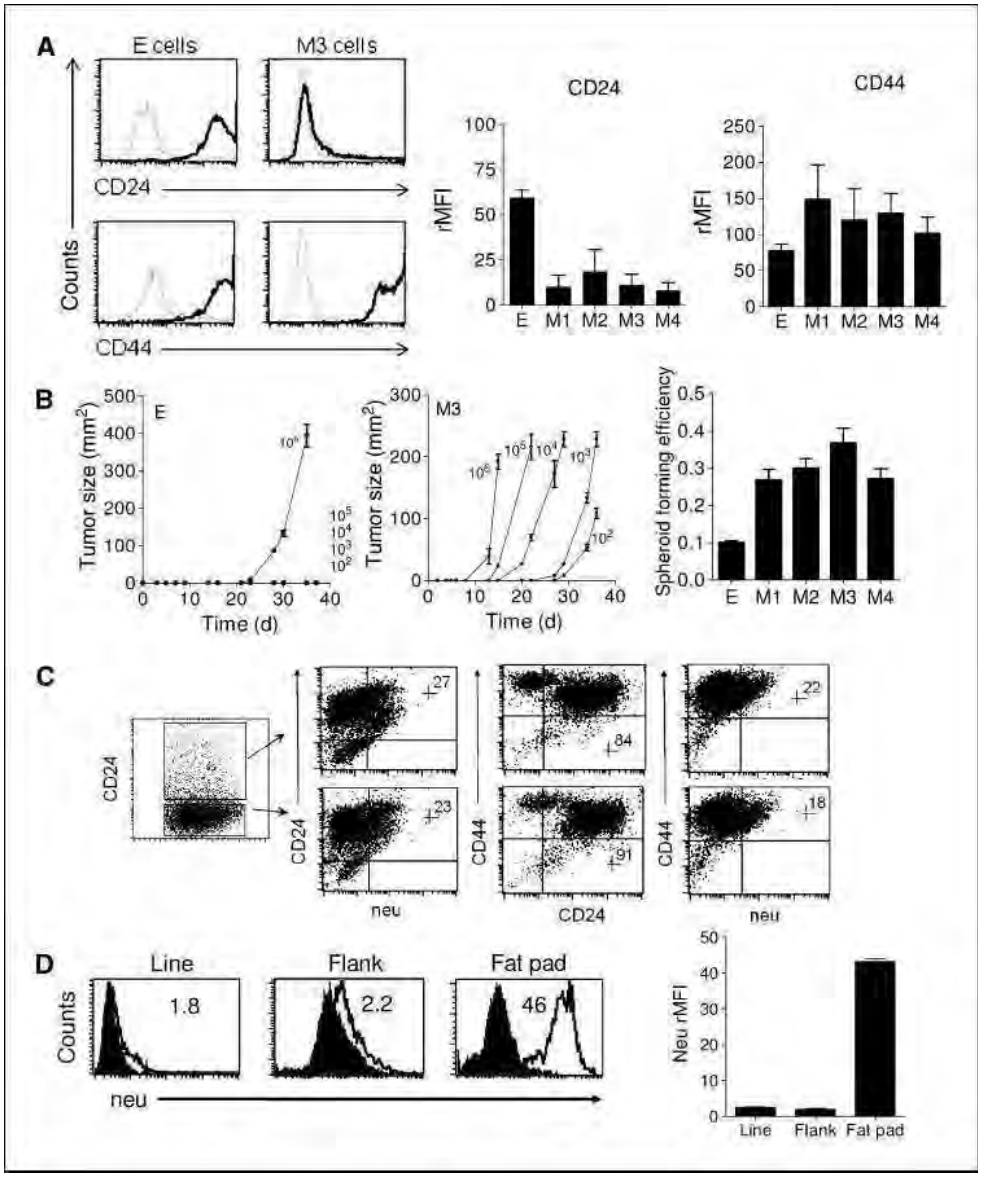

Figure 3. Mesenchymal cells are $CD24^{-/lo}CD44^{+}$ and highly tumorigenic. *A,* a representative histogram showing that M tumor cells are $CD24^{-/lo}$ $CD44^{+}$. Dark and light tracings represent specific and isotype fluorescence, respectively. The graphs summarize the CD24 and CD44 expression in the E and M cells. *Columns,* average relative mean fluorescent intensities (*rMFI*) calculated from three experiments; *bars,* SE. *B,* tumor growth curves of the E (*left*) and M3 (*middle*) cell lines injected into neu-tg mice. *Points,* mean tumor size calculated from three mice; *bars,* SE. Numbers indicate the dose of cells injected. The right graph shows the mean (n = 5 independent experiments) spheroid forming efficiency of each line; *bars,* SE. *C, left,* a summary of dot plots from CD24, CD44, and neu expression in tumors derived from sorted $CD24^{-}CD44^{+}$ M3 mesenchymal cells. This experiment is representative of four similar experiments done with each of the mesenchymal cells lines. Quadrants were established using M3 cell line cells (data not shown). Inset numbers indicate percentage of gated cells in top right quadrants. *D,* histograms of neu expression in cells from a mesenchymal cell line (*Line*), flank tumors (*Flank*), and mammary fat pad tumors (*Fat pad*). Inset numbers represent the relative mean fluorescent intensity. Nearly identical results were seen with four different samples of each cell type, which are shown averaged in accompanying graph.

Mesenchymal cell lines have elevated expression of drug pumps and DNA repair enzymes and are resistant to cytotoxic agents. Another hallmark of BCSCs is their ability to resist environmental insults. Both mesenchymal cells and BCSCs have been linked to resistance to drugs and radiation in recent studies (15). Cytotoxic resistance is often due to elevated expression of drug pumps. Two pumps associated with resistance in breast cancer are BCRP and PGP (16). We observed higher expression of both pumps in mesenchymal cells relative to parental cells (Fig. 4*A*). Enhanced chemoresistance of M cells to mitoxantrone or etoposide (substrates for BCRP and PGP, respectively) suggests that these pumps are active (Fig. 4*A*).

Our mesenchymal tumor cells also have elevated expression of key DNA repair enzymes. One enzyme involved in drug resistance in human cancers is O^6-methylguanine-DNA methyltransferase (MGMT), a ubiquitous DNA repair protein that removes O^6-alkylguanine lesions from damaged DNA and contributes to the resistance of brain cancers to α-chloro-nitrosourea (BCNU; ref. 17). Figure 4*B* shows that M cells have high expression of MGMT (>200-fold higher relative to E cells) and are resistant to BCNU treatment (P = 0.0002 at 20 μmol/L). Because human BCSCs are resistant to ionizing radiation (18), we evaluated this and the expression of double-stranded DNA repair pathway components (i.e., *Brca2, H2afx, Mre11a, Prkdc, Rad52*, and *Xrcc6*). Relative to E cells, M tumor cell lines showed elevated expression of *H2afx* and *Xrcc6* (Fig. 4*C*). Activation of H2afx enhances DNA repair efficiency (19), and the KU-70 protein (encoded by *Xrcc6*) has a key role by recruiting the DNA-dependent protein kinase (20). In general, levels of double-stranded DNA repair genes were similar to E cells, except *Prkdc*, the gene encoding the catalytic subunit of the DNA-dependent protein kinase, whose expression was reduced in two M cell lines. Nonetheless, this altered expression of the double-stranded DNA repair pathway was associated with the strong resistance of M cells to γ-irradiation (P = 0.003 at 16 Gy; Fig. 4*C*). Additional irradiation experiments showed that E cells were more sensitive to irradiation as compared with M cells when assessed by apoptosis assays (data not shown).

Gene expression of luminal or basal epithelial markers in mesenchymal cells suggests that EMT is incomplete. The normal mammary epithelium contains two layers, basal and luminal.

Table 1. Frequency of tumor development following injection of E and M cell lines

Cell line	Dose of cells injected*				
	10^6	10^5	10^4	10^3	10^2
E	6/6 †	0/6	0/6	0/6	0/6
M1	n.d.	n.d.	3/3	3/3	0/3
M2	n.d.	n.d.	3/3	3/3	0/3
M3	6/6	6/6	6/6	6/6	3/6
M4	n.d.	n.d.	3/3	3/3	0/3

*Tumors were injected s.c.
†Numerator represents number of mice developing tumor; Denominator is number of mice injected; n.d.: not done.

These layers are distinguished by unique cytokeratins (Ck; ref. 21). Ck5 and Ck14 are expressed by the basal layer and Ck8 and Ck18 by the luminal layer (21, 22). Because Ck expression is confined to epithelial cells, we investigated whether EMT was complete based on loss of Ck expression in our cell lines. E tumor cells have the characteristic signature of high Ck8 and low Ck14 expression consistent with their luminal differentiation (Fig. 5*A*). There was no consistent pattern of modulation of Cks observed in the mesenchymal cells. Whereas the M1 cell line showed loss of Ck8 and maintained low level of Ck14 expression, M2, M3, and M4 cell lines maintained Ck8 and increased Ck14 expression. Other frequently cited markers of luminal (EpCAM, MUC1, galectin 3, claudin 4, and Ck18) and basal (CD10, osteonectin, S100, myosin light chain, and integrin α_6) epithelial phenotypes were also assessed (Fig. 5*B* and *C*). Of the luminal markers, EpCAM ($P < 0.0001$) and claudin 4 ($P < 0.0001$) were consistently down-regulated in all M lines relative to the E lines, and MUC1 was not expressed by any line. Like Ck8, Ck18 expression was inconsistent. Of the basal markers, only osteonectin was convincingly elevated ($P < 0.0001$), an expected finding given its expression in mesenchymal stem cells (ref. 23; Fig. 5*C*). The other basal markers did not change and failed to distinguish E from M tumor cells. Collectively, the results show that EMT is incomplete.

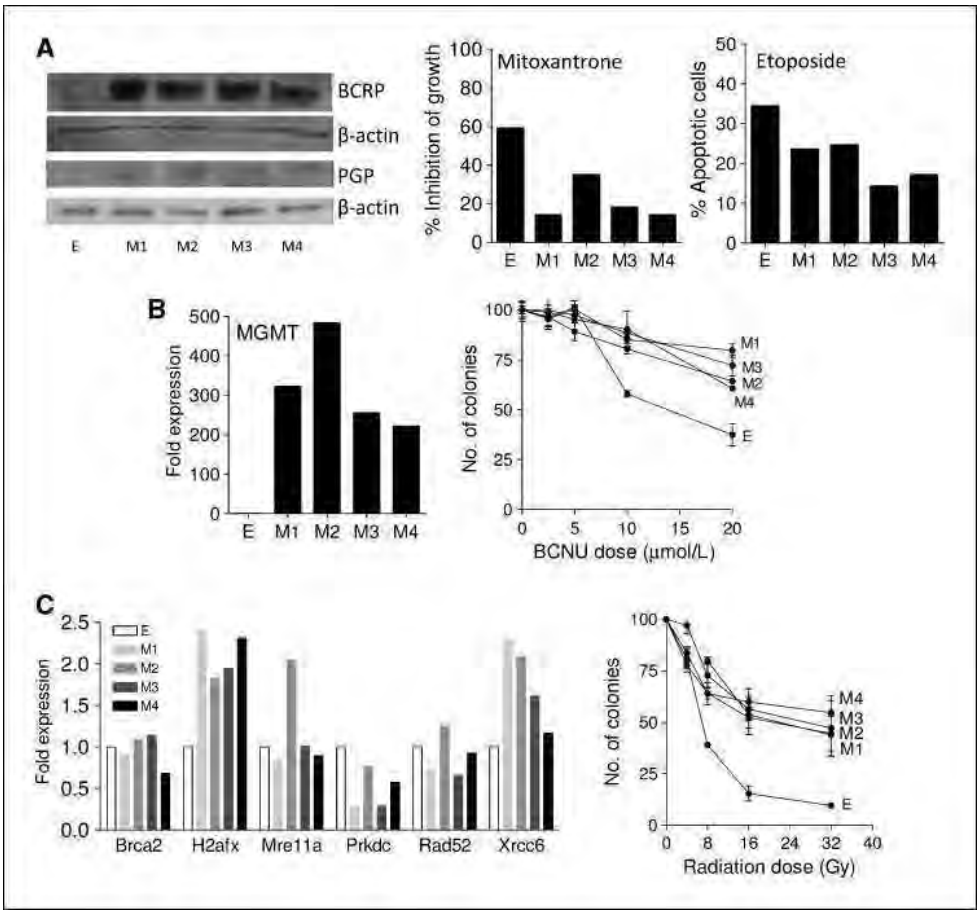

Figure 4. Mesenchymal cell lines have elevated expression of drug pumps and DNA repair enzymes and are resistant to environmental insults. *A, left,* Western blot analysis of BCRP and PGP drug pumps in all cell lines. β-Actin was used as a loading control. Western blots are representative of three experiments for each protein. *Middle,* inhibition of growth (i.e., compared with control treated cells) of the tumor cells lines after *in vitro* treatment with mitoxantrone. *Right,* apoptotic response to etoposide as assessed using flow cytometry. *Columns,* percentage of apoptotic cells following treatment. A representative experiment is shown for MTT and apoptotic assays, both done twice. *B, left,* expression levels of MGMT in the tumor cell lines by real-time PCR. Results are expressed as fold expression over E and represent one experiment. *Right,* results of a clonogenic assay of the tumor cells following exposure to escalating doses of BCNU; *points,* mean of three replicates; *bars,* SE. *C, left,* results of real-time PCR analysis of the double-stranded DNA repair genes. Results are expressed as fold expression over E. *Right,* results of clonogenic assay after escalating doses of γ-irradiation; *points,* mean of three replicate plates; *bars,* SE.

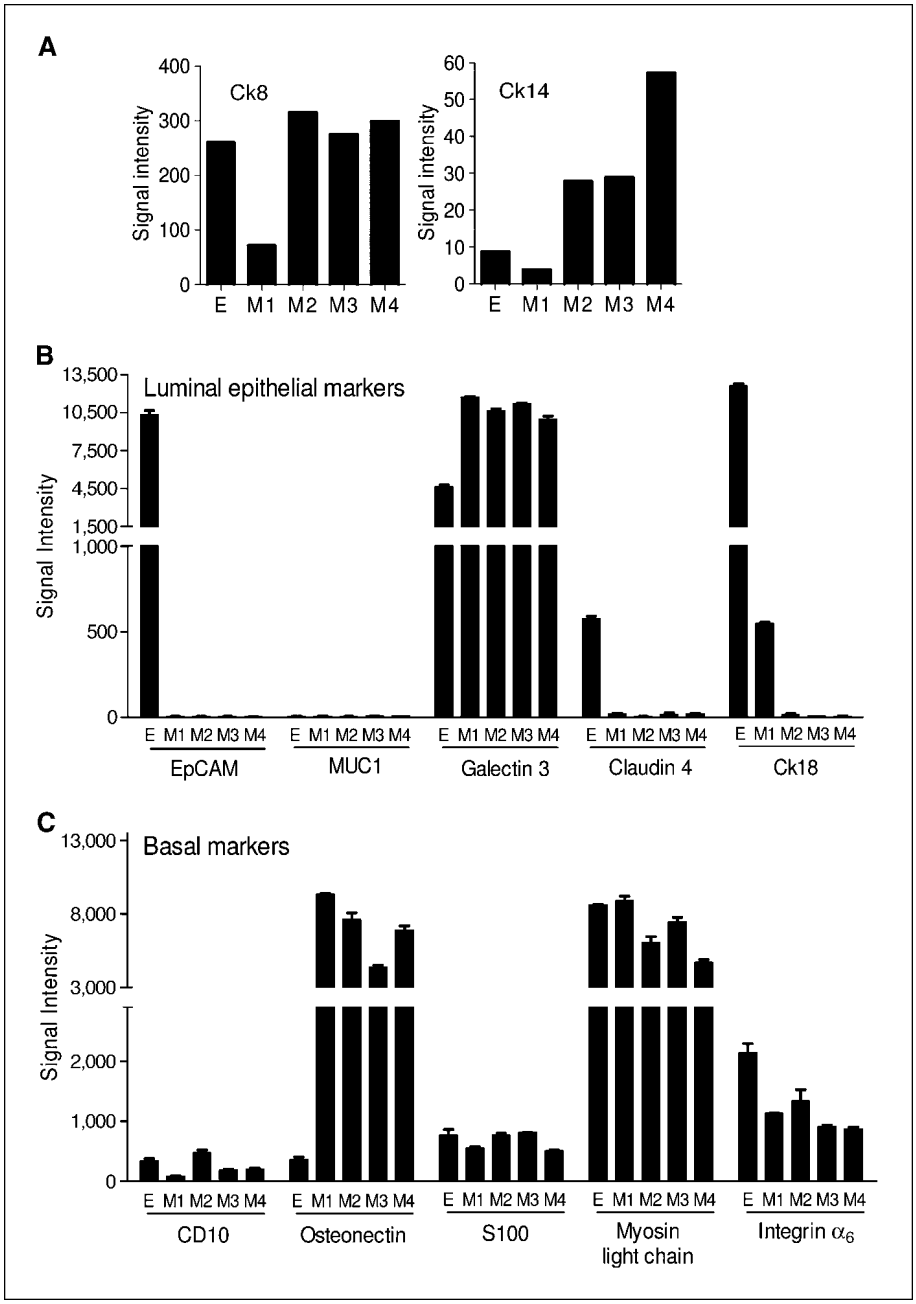

Figure 5. Gene expression of luminal or basal epithelial markers in mesenchymal cells suggests that EMT is incomplete. *A,* RT-PCR results depicting expression of Ck8 (*left*) and Ck14 (*right*) in the tumor cell lines. Results are representative of three independent experiments. *B* and *C,* RNA microarray analyses of common luminal epithelial and basal markers in the cell lines, respectively. *Columns,* mean signal intensities of two microarray analyses for each cell line; *bars,* SE. Each columns represents the signal intensity for a unique probe.

Discussion

Whereas great strides in breast cancer treatment have been made, women treated for the disease remain at high risk for recurrence. Recent hypotheses suggest that recurrence (and possibly tumor initiation) is caused by a subset of tumor cells with stem cell qualities including self renewal, ability to differentiate and reconstitute a tumor, and resistance to chemotherapeutic drugs and radiation. Whereas studies have confirmed the existence of this tumorigenic subset, their origin is unclear. Understanding the origin and biology of these cells may reveal strategies for targeting them therapeutically. In this study, we made three novel observations that provide an additional framework for BCSCs. These observations are that (*a*) EMT was induced *in vivo* by CD8 T cells; (*b*) EMT generates mesenchymal tumor cells with BCSC properties; and (*c*) EMT (and BCSC genesis) is not associated with complete loss of epithelial characteristics.

Although much evidence shows the importance of EMT in embryogenesis, investigation of its role in cancer has been confined mainly to *in vitro* model systems. As a result, the relevance of natural EMT to *in vivo* malignancy is controversial. In the current study, we found that EMT was induced *in vivo* without prior manipulation of tumor cells. Our conclusion that the tumor cells had undergone EMT was based on a number of molecular and cellular changes, including (*a*) loss of the epithelial markers CD24, E-cadherin, and claudin 3; (*b*) gain of validated mesenchymal markers N-cadherin and Snail; (*c*) gain of MMP activity; and (*d*) acquisition of a scattered phenotype. Prior studies showed that mesenchymal tumors develop in the neu-tg mouse, but it remained unclear whether the appearance of the mesenchymal tumors was

due to selection or induction (5, 6, 24). Our findings clarify this by showing CD8 T-cell–dependent EMT induction *in vivo*.

Various immune effector cells are known to produce factors capable of inducing EMT, such as transforming growth factor-β (TGF-β) and tumor necrosis factor-α (TNF-α; refs. 25, 26). Of those, the notable example is TGF-β. Whereas CD4 T regulatory cells are the predominant source of TGF-β among T cells, newer studies show that chronically stimulated effector CD8 T cells can also become regulatory and produce TGF-β (27). Another potential mediator is the recently discovered product of the *FAM3C* gene, interleukin-like EMT inducer (ILEI). Although little is known of ILEI, it seems to be highly expressed in lymphocytes associated with chronic inflammatory lesions (e.g., arthritis and tumors; ref. 24). Bates and Mercurio (25) observed that TGF-β and TNF-α synergistically induced EMT in human colon cancer cells. The requirement of multiple stimuli for EMT is supported by our prior studies showing that engagement of the IFN-γreceptor is necessary for the generation of antigen-loss variants *in vivo*, but IFN-γ stimulation *in vitro* leads only to a modest loss of neu antigen (5). Whatever mechanism is operative, the induction of EMT and the generation of the BCSC phenotype were observed *in vivo*, suggesting that our results may be biologically relevant events. Our findings in mice are also consistent with prior studies showing that CD8 T-cell infiltration is associated with lymph node metastasis in breast cancer patients (28).

EMT was accompanied by the acquisition of the BCSC properties, including tumorigenicity, resistance to environmental insults, ability to redifferentiate into an epithelial tumor, and ability to form spheroids. These findings are consistent with those of Mani and colleagues (29) who recently showed that forced expression of EMT-associated molecules such as Snail and Twist or treatment with TGF-βresulted in cells with a cancer stem cell phenotype. Similarly, Morel and colleagues (30) showed with the same cell lines that adding active Ras generated a population of $CD24^{-}CD44^{+}$ cells that underwent EMT and had BCSC attributes. One key characteristic of cancer stem cells called into question by our studies is the need for self-renewal, a property that ensures preservation of cancer stem cells in the tumor. Our hypothesis offers an alternative to self renewal, suggesting that a tumor cell with cancer stem cell properties could be generated from differentiated epithelial tumor cells through the aberrant use of EMT. This premise of dedifferentiation is supported by the recently described generation of pluripotent stem cells from seemingly terminally differentiated somatic cells (31, 32). Inducing a cancer stem cell from differentiated daughter cells could likely explain the shortcomings of the hierarchal self-renewing BCSC hypothesis. That hypothesis does not easily explain why relapse is closely associated with metastasis and invasion, features not readily linked to normal mammary stem cells (33, 34). Based on the current study and hallmarks of these prior studies, a likely alternative explanation for relapse and disease progression is that a few of the tumor cells within the primary tumor separate from the primary lesion via EMT and are not eliminated by conventional therapies, due in part to physical separation but primarily to the inherent drug and radio-resistance of the mesenchymal tumor cells. Such a hypothesis is supported by Moody and colleagues (24) who showed that the EMT inducer Snail is linked to relapse in human breast cancer. EMT might also explain why relapse in breast cancer is linked with a wound response signature (35). Mesenchymal tumor cells may have several characteristics in common with normal healthy mesenchymal stem cells, which have roles in the wound repair and healing response (36).

Stemness has been associated with the $CD24^{+}$ phenotype in murine mammary models including $CD24^{+}CD29^{hi}$ (37) and $CD24^{+}Sca1^{-}$ (21). In contrast to these data, we have found stemness associated with the $CD24^{-/lo}$ cells. Although not directly addressed by our study, there are at least two possibilities to explain these discrepancies. First, there may be multiple types of cells generated during malignant transformation and progression that have BCSC-like properties. Second, markers used to identify BCSC traits may be variable and reflect the context or microenvironment from which the cells were derived, as has been described by Bissell and colleagues (38).

Although our results show that the tumor cells underwent EMT, as assessed using well-established markers, gene transcription analysis suggests that EMT was incomplete because luminal and basal epithelial associated genes remained expressed. These results are consistent with the observation that EMT is associated with some, but not all, genetic changes ordinarily associated with the stromal or mesenchymal phenotype (39). In other words, EMT may be incomplete or aberrant. Our results are also consistent with a recent study in human breast cancer that revealed that a small fraction (<10%) of the disseminated Ck-expressing tumor cells show the $CD24^{-/lo}CD44^{+}$ BCSC phenotype (40). The implications of our findings could be important for identifying evidence of EMT in breast cancer lesions with strict marker paradigms that include the absence of Cks and E-cadherin expression.

Disclosure of Potential Conflicts of Interest

No potential conflicts of interest were disclosed.

Acknowledgments

Received 8/27/08; revised 1/19/09; accepted 1/19/09; published OnlineFirst 3/10/09.

Grant support: Martha and Bruce Atwater (K.L. Knutson and L.C. Hartmann) and Mayo Breast Specialized Program of Research Excellence grants P50-CA116201 (J.N. Ingle and K.L. Knutson), K01-CA100764 (K.L. Knutson), and R01-CA113861 (K.L. Knutson and S. Ferrone).

The costs of publication of this article were defrayed in part by the payment of page charges. This article must therefore be hereby marked *advertisement* in accordance with 18 U.S.C. Section 1734 solely to indicate this fact.

We thank the Cytogenetics Shared Resource at Mayo Clinic.

References

1. Group EBCTC. Effects of chemotherapy and hormonal therapy for early breast cancer on recurrence and 15-year survival: an overview of the randomised trials. Lancet 2005;365:1687–717.
2. Pierce GB, Nakane PK, Martinez-Hernandez A, Ward JM. Ultrastructural comparison of differentiation of stem cells of murine adenocarcinomas of colon and breast with their normal counterparts. J Natl Cancer Inst 1977;58:1329–45.
3. Al-Hajj M, Wicha MS, Benito-Hernandez A, Morrison SJ, Clarke MF. Prospective identification of tumorigenic breast cancer cells. Proc Natl Acad Sci U S A 2003;100:3983–8.
4. Cho RW, Wang X, Diehn M, et al. Isolation and molecular characterization of cancer stem cells in MMTV-Wnt-1 murine breast tumors. Stem Cells 2008;26:364–71.
5. Kmieciak M, Knutson KL, Dumur CI, Manjili MH. HER-2/neu antigen loss and relapse of mouse mammary carcinoma are actively induced by T cell-mediated anti-tumor responses. Eur J Immunol 2007;37:675–85.
6. Knutson KL, Lu H, Stone B, et al. Immunoediting of cancers may lead to epithelial to mesenchymal transition. J Immunol 2006;177:1526–33.
7. Manjili MH, Arnouk H, Knutson KL, et al. Emergence of immune escape variant of mammary tumors that has distinct proteomic profile and a reduced ability to induce "danger signals." Breast Cancer Res Treat 2006;96:233–41.

8. Worschech A, Kmieciak M, Knutson KL, et al. Signatures associated with rejection or recurrence in HER-2/neu-positive mammary tumors. Cancer Res 2008; 68:2436–46.

9. Thiery JP, Sleeman JP. Complex networks orchestrate epithelial-mesenchymal transitions. Nat Rev Mol Cell Biol 2006;7:131–42.

10. Knutson KL, Almand B, Dang Y, Disis ML. Neu antigen-negative variants can be generated after neu-specific antibody therapy in neu transgenic mice. Cancer Res 2004;64:1146–51.

11. Parrizas M, Saltiel AR, LeRoith D. Insulin-like growth factor 1 inhibits apoptosis using the phosphatidylinositol 3′-kinase and mitogen-activated protein kinase pathways. J Biol Chem 1997;272:154–61.

12. Herault O, Colombat P, Domenech J, et al. A rapid single-laser flow cytometric method for discrimination of early apoptotic cells in a heterogenous cell population. Br J Haematol 1999;104:530–7.

13. Nadri S, Soleimani M. Isolation murine mesenchymal stem cells by positive selection. In Vitro Cell Dev Biol Anim 2007;43:276–82.

14. Richardson GD, Robson CN, Lang SH, Neal DE, Maitland NJ, Collins AT. CD133, a novel marker for human prostatic epithelial stem cells. J Cell Sci 2004;117: 3539–45.

15. Dean M, Fojo T, Bates S. Tumour stem cells and drug resistance. Nat Rev Cancer 2005;5:275–84.

16. Hait WN, Yang JM. Clinical management of recurrent breast cancer: development of multidrug resistance (MDR) and strategies to circumvent it. Semin Oncol 2005;32:S16–21.

17. Liu L, Gerson SL. Targeted modulation of MGMT: clinical implications. Clin Cancer Res 2006;12:328–31.

18. Phillips TM, McBride WH, Pajonk F. The response of $CD24^{-/low}/CD44^{+}$ breast cancer-initiating cells to radiation. J Natl Cancer Inst 2006;98:1777–85.

19. Vidanes GM, Bonilla CY, Toczyski DP. Complicated tails: histone modifications and the DNA damage response. Cell 2005;121:973–6.

20. Meek K, Gupta S, Ramsden DA, Lees-Miller SP. The DNA-dependent protein kinase: the director at the end. Immunol Rev 2004;200:132–41.

21. Liu JC, Deng T, Lehal RS, Kim J, Zacksenhaus E. Identification of tumorsphere- and tumor-initiating cells in HER2/Neu-induced mammary tumors. Cancer Res 2007;67:8671–81.

22. Deugnier MA, Faraldo MM, Janji B, Rousselle P, Thiery JP, Glukhova MA. EGF controls the *in vivo* developmental potential of a mammary epithelial cell line possessing progenitor properties. J Cell Biol 2002; 159:453–63.

23. Silva WA, Jr., Covas DT, Panepucci RA, et al. The profile of gene expression of human marrow mesenchymal stem cells. Stem Cells 2003;21:661–9.

24. Moody SE, Perez D, Pan TC, et al. The transcriptional repressor Snail promotes mammary tumor recurrence. Cancer Cell 2005;8:197–209.

25. Bates RC, Mercurio AM. Tumor necrosis factor-α stimulates the epithelial-to-mesenchymal transition of human colonic organoids. Mol Biol Cell 2003;14:1790–800.

26. Zavadil J, Bottinger EP. TGF-β and epithelial-to-mesenchymal transitions. Oncogene 2005;24:5764–74.

27. Mahic M, Henjum K, Yaqub S, et al. Generation of highly suppressive adaptive $CD8^{+}CD25^{+}FOXP3^{+}$ regulatory T cells by continuous antigen stimulation. Eur J Immunol 2008;38:640–6.

28. Bilik R, Mor C, Hazaz B, Moroz C. Characterization of T-lymphocyte subpopulations infiltrating primary breast cancer. Cancer Immunol Immunother 1989;28:143–7.

29. Mani SA, Guo W, Liao MJ, et al. The epithelial-mesenchymal transition generates cells with properties of stem cells. Cell 2008;133:704–15.

30. Morel AP, Lievre M, Thomas C, Hinkal G, Ansieau S, Puisieux A. Generation of breast cancer stem cells through epithelial-mesenchymal transition. PLoS ONE 2008;3:e2888.

31. Takahashi K, Tanabe K, Ohnuki M, et al. Induction of pluripotent stem cells from adult human fibroblasts by defined factors. Cell 2007;131:861–72.

32. Yu J, Vodyanik MA, Smuga-Otto K, et al. Induced pluripotent stem cell lines derived from human somatic cells. Science 2007;318:1917–20.

33. Liu R, Wang X, Chen GY, et al. The prognostic role of a gene signature from tumorigenic breast-cancer cells. N Engl J Med 2007;356:217–26.

34. Wang Y, Klijn JG, Zhang Y, et al. Gene-expression profiles to predict distant metastasis of lymph-node-negative primary breast cancer. Lancet 2005;365:671–9.

35. Chang HY, Sneddon JB, Alizadeh AA, et al. Gene expression signature of fibroblast serum response predicts human cancer progression: similarities between tumors and wounds. PLoS Biol 2004;2:E7.

36. Galie M, Konstantinidou G, Peroni D, et al. Mesenchymal stem cells share molecular signature with mesenchymal tumor cells and favor early tumor growth in syngeneic mice. Oncogene 2008;27:2542–51.

37. Shackleton M, Vaillant F, Simpson KJ, et al. Generation of a functional mammary gland from a single stem cell. Nature 2006;439:84–8.

38. Bissell MJ,Labarge MA. Context, tissue plasticity, and cancer: are tumor stem cells also regulated by the microenvironment? Cancer Cell 2005;7:17–23.

39. Turley EA, Veiseh M, Radisky DC, Bissell MJ. Mechanisms of disease: epithelial-mesenchymal transition-does cellular plasticity fuel neoplastic progression? Nat Clin Pract Oncol 2008;5:280–90.

40. Balic M, Lin H, Young L, et al. Most early disseminated cancer cells detected in bone marrow of breast cancer patients have a putative breast cancer stem cell phenotype. Clin Cancer Res 2006;12:5615–21.

Immunoediting of Cancers May Lead to Epithelial to Mesenchymal Transition[1]

Keith L. Knutson,[2]* Hailing Lu,† Brad Stone,‡ Jennifer M. Reiman,* Marshall D. Behrens,* Christine M. Prosperi,* Ekram A. Gad,† Arianna Smorlesi,[3]† and Mary L. Disis†

Tumors evade both natural and pharmacologically induced (e.g., vaccines) immunity by a variety of mechanisms, including induction of tolerance and immunoediting. Immunoediting results in reshaping the immunogenicity of the tumor, which can be accompanied by loss of Ag expression and MHC molecules. In this study, we evaluated immunoediting in the neu-transgenic mouse model of breast cancer. A tumor cell line that retained expression of rat neu was generated from a spontaneous tumor of the neu-transgenic mouse and, when injected into the non-transgenic parental FVB/N mouse, resulted in the development of a strong immune response, initial rejection, and ultimately the emergence of neu Ag-loss variants. Morphologic and microarray data revealed that the immunoedited tumor cells underwent epithelial to mesenchymal transition accompanied by an up-regulation of invasion factors and increased invasiveness characteristic of mesenchymal tumor cells. These results suggest that immunoediting of tumor results in cellular reprogramming may be accompanied by alterations in tumor characteristics including increased invasive potential. Understanding the mechanisms by which tumors are immunoedited will likely lead to a better understanding of how tumors evade immune detection. ***The Journal of Immunology*****, 2006, 177: 1526–1533.**

A key function of the immune system is to survey for dysfunctional tissues such as cancers. Research indicates that tumors evade the immune system following immunosurveillance by either directly inducing tolerance or by altering their phenotype to suppress or evade immunity. This latter mechanism has been termed immunoediting (1). The occurrence of immunoediting is becoming more frequent as our ability to modulate antitumor immunity improves. Some important examples of immunoediting are modulation of Ag expression (Ag-loss variants) and loss of immune recognition molecules. The ability of a tumor cell to modulate or reduce levels of expression of Ags has been increasingly reported using a variety of different immunotherapy approaches to demonstrate that immunoediting can be induced pharmacologically (2–7). Natural immunoediting is supported by studies that have demonstrated that as tumors age, the expression of important recognition molecules decrease. For example, studies in breast cancer have revealed that most advanced tumors have little or no expression of MHC class I molecules unlike normal breast epithelium or early cancers, which typically express an abundance of the molecule (8).

The mechanisms by which immunoediting occurs remain largely unknown. The loss of Ags could simply reflect changes such as gene mutagenesis, which leads to loss of specific gene expression. Alternatively, the immune system could lead to the activation of pathways that lead to rapid, sustained changes in broad gene expression profiles in tumor cells (i.e., cellular reprogramming). This ability of tumors to adapt to a new microenvironment by reprogramming reflects an important property of tumors called plasticity (9).

We, and others, have found that tumors arising in the FVB/N rat neu-transgenic (neu-tg)[4] mouse are capable of rapid immune escape when treated with any of a variety of immune-based approaches including mAb therapy, vaccines, or T cell therapy (2, 10). Furthermore, this immunoescape phenomenon can also be observed when transplanting tumors into the syngeneic non-transgenic parental FVB/N mouse (11). Immune escape observed when transplanting tumors from the neu-tg mouse into the FVB/N parental animals is manifest as the loss of neu Ag expression (2). In this study, we evaluated the phenotypic differences (i.e., immunoediting) between native neu-expressing tumor cells, derived from the neu-tg mouse, and those that resulted from immunoediting following transplantation in the FVB/N parental strain. Our results suggest that immunoedited tumors have undergone reprogramming through epithelial to mesenchymal transition (EMT).

Materials and Methods

Animals

Mice were from an established colony of neu-tg mice (strain FVB/N-TgN (MMTVneu)202Mul) or FVB/N mice (12). The neu-tg mice develop spontaneous tumors after a long latency (e.g., >50 wk), and in the current studies, our previously described transplantable model was used in mice between the ages of 6 and 12 wk (2). As previously described by others and us, the neu-tg mice are tolerant of the neu transgene. This tolerance can be circumvented with vaccines and other immune manipulations (10, 13–17). Animal care and use was in accordance with the institutional guidelines at both the Mayo Clinic (Rochester, MN) and the University of Washington (Seattle, WA).

*Department of Immunology, Mayo Clinic, Rochester, MN 55905; †Tumor Vaccine Group, Center for Translational Medicine in Women's Health, Seattle, WA 98195; and ‡Benaroya Research Institute, Seattle, WA 98101

Received for publication January 17, 2006. Accepted for publication May 16, 2006.

The costs of publication of this article were defrayed in part by the payment of page charges. This article must therefore be hereby marked *advertisement* in accordance with 18 U.S.C. Section 1734 solely to indicate this fact.

[1] This study was supported by Grants R01 CA-113861 (to K.L.K.) and R01 CA-85374 (to M.L.D.) from the National Institutes of Health. K.L.K. is supported by a National Cancer Institute Howard Temin Award K01-CA100764. M.L.D. is supported by a National Cancer Institute Career Award K24-CA85218.

[2] Address correspondence and reprint requests to Dr. Keith L. Knutson, Mayo Clinic College of Medicine, 342C Guggenheim, Mayo Clinic, 200 First Street Southwest, Rochester, MN 55905. E-mail address: knutson.keith@mayo.edu

[3] Current address: Dipartimento Ricerche, Istituto Nazionale Riposo e Cura Anziani, via Birarelli 8, 60100 Ancona, Italy.

[4] Abbreviations used in this paper: neu-tg, neu-transgenic; EMT, epithelial to mesenchymal transition; MMP, matrix metalloproteinase; TJP, tight junction protein; SI, stimulation index; MMC, mouse mammary carcinoma; ANV, Ag-negative variant.

0022-1767/06/$02.00

Cell lines

The mouse mammary carcinoma (MMC) cell line was established from a spontaneous tumor harvested from the neu-tg mice. MMC cells were grown and maintained in RPMI 1640 supplemented with 20% FCS (Gemini Bio-Products) as well as penicillin/streptomycin and L-glutamine (Invitrogen Life Technologies). Ag-negative variants (ANV) are cell lines derived from neu-loss variant tumors in FVB/N mice and are maintained in culture identical with MMC. The cell lines were not used continuously, but rather replaced with low-passage cultures every 2 mo. The microarrays were performed with different cultures to avoid intraculture artifact and biasing. Both cell lines have been previously used in other studies in the same mouse model (2, 11).

Tumor growth in vivo

The tumor cells were harvested from culture plates using 2 mM EDTA and washed before injection. FVB/N or neu-tg mice were inoculated with MMC or ANV1 cells s.c. on the right mid-dorsum with a 23-gauge needle. Tumors were measured every other day with vernier calipers, and tumor size was calculated as the product of length times width. In some cases, mice were pretreated with mAbs to deplete either $CD8^+$ or $CD4^+$ T cells before tumor injection. In these cases, mice were i.v. administered 100 μg of purified monoclonal GK1.5 (anti-CD4; American Type Collection Culture (ATCC)) or 53.6.72 (anti-CD8; ATCC) for 5 consecutive days. Mice were allowed to rest 48 h before tumor injection. Peripheral blood was analyzed for $CD4^+$ and $CD8^+$ T cells on day 5 to verify depletion as described below.

Flow cytometry

Cultured cell line cells, tumor-harvested tumor cells, and T cells were stained in PBS containing 1% FCS before labeling. Cells ($0.5–1.0 \times 10^6$) were incubated in primary anti-rat neu Ab (mAb 7.16.4, a mouse IgG2a Ab reactive with the rat neu oncogene-encoded p185 molecule was generously provided by Dr. M. Greene and has been previously described (18)), anti-CD24 FITC (BD Pharmingen), anti-MHC class I FITC (TIB-139, ATCC), anti-CD4 FITC (GK1.5), and anti-CD8 FITC (53.6.72) at 4°C for 30 min and washed three times, and in some cases, followed by secondary labeling with FITC-conjugated rat anti-mouse Ab (BD Pharmingen) at 4°C for 30 min followed by three washes. Samples were run on a FACScan II and analyzed using CellQuest software (BD Biosciences). Control cells received nonspecific mouse IgG. The relative mean fluorescence intensity was calculated as the ratio of the geometric mean of the fluorescence intensities of rat neu stained to the control IgG-stained control cells.

Proliferation assays

Proliferation assays were done essentially as previously described with minor modifications (19). Splenocytes (3–12 replicates) were plated at 5×10^5 splenocytes per well and treated with media alone, 2 μg of Con A, 1:1 irradiated (3300 rad) Con A-elicited blasts (16 h at 5 μg/ml Con A), or freeze-thaw tumor lysates (three freezes). [^{3}H]Thymidine (1.5 μCi/well) was added at 24 h following antigenic stimulation and the incorporation into the DNA was measured at 48 h by liquid scintillation. The stimulation indices (SI) were calculated as the ratio of the sample cpm to the control cpm.

Microarray analysis

RNA was extracted using an RNeasy kit (Qiagen) or RNA4 aqueous kit from Ambion. Biotinylated cRNA probes were synthesized using a MessageAmp II kit from Ambion. Two different types of microarray were used, Affymetrix and dual-label expression arrays. For the Affymetrix analysis, 15 μg of each labeled probe was mixed with Affymetrix hybridization spike controls in a standard hybridization solution and heated to 95°C for 5 min, 45°C for 5 min, centrifuged to pellet particulates, and hybridized to Affymetrix Mouse430_2 chips. Chips were washed using the supplied eukGE-WS5v2 protocol and stained using Ab amplification on a GeneChip 450 Fluidics station. Chips were immediately scanned using a GeneChip 3000 scanner. Affymetrix global scaling was used to normalize results from each sample.

For the dual-label arrays, RNA was labeled with Cy3-dUTP and Cy5-dUTP (Amersham Biosciences) by reverse transcription. For each reverse transcription reaction, 30 μg of total RNA was mixed with random hexamer in a total volume of 18.5 μl, heated at 70°C for 10 min, and placed on ice for 10 min. Unlabeled nucleotide pool with either Cy3- or Cy5-conjugated dUTP, 5× first-strand Superscript II buffer, 0.1 M DTT, Superscript II reverse transcriptase (Invitrogen Life Technologies) were added to a final volume of 30 μl. After incubation at 42°C for 2 h, RNA was hydrolyzed by adding 10 μl of 0.5 M EDTA and 10 μl of 1 N NaOH and incubated at 65°C for 15 min. The mixture was neutralized by adding 25 μl of 1 M Tris-HCl (pH 7.4) and by adjusting the volume to 500 μl with Tris-EDTA. Labeled cDNA was purified by centrifugation in a Microcon-30 concentrator (Amicon; Millipore) and eluted in water. The Cy3- and Cy5-labeled cDNAs were then quenched with hydroxylamine to prevent cross-coupling. Qiaquick PCR purification kit (Qiagen) was used to remove unincorporated/quenched dye. Hybridization and washing of the slides were done using standard protocol. Then the arrays were dried by centrifugation. Fluorescence intensities for both dyes (Cy3 and Cy5) and local background subtracted values for individual spots were obtained using the GenePix 4000 microarray scanner and accompanying software (Axon Instruments). The data were imported into Microsoft Excel spreadsheets for analysis. Defective spots that are substandard on the scanned image or have negative background subtracted values were first excluded. Then the Cy3:Cy5 ratio values were log transformed, and global equalization to remove a deviation of the signal intensity between whole Cy3 and whole Cy5 fluorescences was performed by subtracting a median of all log(Cy3/Cy5) values from each log(Cy3/Cy5) value.

Migration assay

NeuroProbe 96-well plates (5-μm pore size) were coated with 10 μg/ml fibronectin (Sigma-Aldrich) at 37°C for 1 h. Next followed removing the excess fibronectin with HBSS. Tumor cells were suspended in HBSS with 0.1% BSA at a concentration of 10^6/ml. Calcein-AM (Molecular Probes) was added to cells at a final concentration of 2 μM and incubated for 30 min at 37°C in free calcein-AM-incubated cells in RPMI 1640 and resuspended at 10^6 in RPMI 1640 and 1% DMSO. Fifty thousand cells were added to the upper chamber of the NeuroProbe plate and incubated for 90 min at 37°C. The cells that moved through the fibronectin were then quantified on a PerkinElmer Victor V using 485 nm excitation/535 nm emission program. A standard curve was generated by measuring the fluorescent intensity of varying concentrations of calcein-AM-stained cells.

RT-PCR analysis

E-cadherin, tight junction protein 1 (TJP1), vimentin transcript, and rat neu were detected in MMC and ANV cells by RT-PCR on a Bio-Rad MyCycler. Total RNA was extracted from MMC and ANV cells as already described. cDNA was synthesized from 100 ng of total RNA by SuperScript One-Step RT-PCR with Platinum Taq as per manufacturer's instructions (Invitrogen Life Technologies). RT-PCR was performed using the following primers: E-cadherin forward GGTCTTTGAGGGATTCGTTGC and reverse CAGCCTGAACCACCAGA-GTGTATG, which yielded a 248-bp product; TJP-1 forward GACTTTTGTCCCACTTGAATCCC and reverse CCACCGTCCGC ATAAACATCTC; vimentin forward TAGCCGCAGC CTCTATTCCTCATC and reverse AGAAGTCCACCGAGTCTT-GA AGC; and rat HER2/neu forward TGAGCACCATGGAGCTGGC and reverse TCCGGCAGAAATGCCAGGCTC that yielded a 1144-bp product. The PCR conditions for all primer pairs, except neu, were cDNA synthesis and predenaturation: 1 cycle at 50°C, 30 min, 94°C, 2 min; PCR amplification: 40 cycles at 94°C, 15 s (denaturation), 57.5°C, 30 s (annealing), 70°C, 15 s (extension); and final extension: 1 cycle at 72°C, 10 min. For rat neu, the PCR conditions were cDNA synthesis and predenaturation: 1 cycle at 50°C for 30 min, 94°C for 2 min; PCR amplification: 40 cycles at 94°C for 30 s (denaturation), 55.8°C for 45 s (annealing), 70°C for 3 min (extension); and final extension: 1 cycle at 72°C for 10 min. These samples were electrophoresed on a 1% agarose gel with ethidium bromide and imaged on a Gel Doc XR (Bio-Rad). The results for E-cadherin were analyzed with Quantity One software (v.4.5.2; Bio-Rad).

Western blotting

Probing for rat neu expression in tumors and tumor cell lines was performed as previously described (2).

Results

The MMC cell line is immunogenic in parental FVB/N mice and elicits a protective T cell response

The ability of the neu^+ MMC to generate tumors was examined in the neu-tg and parental rat neu^- FVB/N mice. As shown in Fig. 1*A*, tumors that were initially rejected in FVB/N parental mice emerged after a longer latency compared with the neu-tg mouse. As previously reported, implantation of the MMC tumor cells in the FVB/N is accompanied by a strong immune response, which was confirmed in this study (Fig. 1*B*) (11). Splenocytes derived

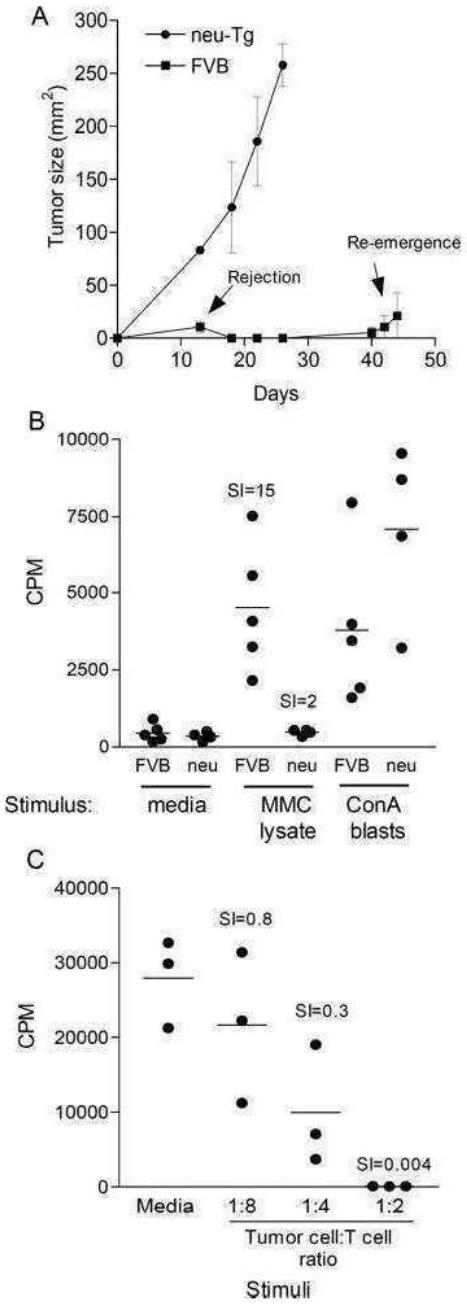

FIGURE 1. The MMC cell line is immunogenic in parental FVB/N mice and elicits a protective T cell response. *A*, Initial rejection of the MMC cells (6×10^5) in the FVB/N parental mice but not the neu-tg mice. Each time point is the mean (± SEM) of six independent measurements. Similar results were also observed in other experiments. *B*, FVB/N but not neu-tg mice demonstrate an immune response to irradiated tumor cells as assessed by proliferation assays (in cpm). Animals received an injection of live 5×10^6 MMC tumor cells and immunity was examined 1 wk later and before tumor development. The proliferation responses to irradiated Con A-elicited splenic blasts are shown as a positive control. Each data symbol represents the mean of 12 replicates from an individual mouse and is representative of two independent experiments. The solid line within each group represents the mean. Tumor cell lysates were added at a tumor cell-to-T cell ratio of 1:4. *C*, MMC-immunized FVB/N mice do not respond to tumors that emerge following rejection. Each scattergram symbol (●) represents the mean basal proliferation response (in cpm) of splenocytes incubated with either medium alone or varying concentrations of tumor cell lysates. Each dot is calculated from three dots and represents a unique mouse. The horizontal line represents the mean of the groups of three mice. The splenocytes were analyzed 2 wk after MMC tumor challenge but before the development of measurable tumors. SI values are shown in *B* and *C*.

from FVB/N mice injected with tumor demonstrated a proliferation response (SI = 15 ± 5, $n = 5$) to tumor in vitro that was significantly ($p = 0.026$) greater than the proliferation response observed by the splenocyte derived from tumor-bearing neu-tg mice (SI = 2 ± 0.5, $n = 4$). To determine whether FVB/N mice that had rejected MMC tumor challenge developed an immune response to the relapse tumors, splenocytes were assessed for reactivity, following MMC tumor rejection, to lysates derived from the relapse tumors (Fig. 1*C*). As shown, MMC-immunized mice do not demonstrate an immune proliferation response but rather are inhibited. The addition of relapse tumor lysate to splenocytes, at a 1:2 tumor cell-to-splenocyte ratio, led to a decline in baseline proliferation (SI = 0.004 ± 0.0006, $n = 3$, $p < 0.001$). This decrease was specific for the relapse tumor cells as it was observed that the addition of Con A to splenocytes from the same mice resulted in enhanced proliferation (data not shown). Although the precise mechanism by which blockade of proliferation occurs is unclear, it is possible that tumors produce immune suppressive molecules (e.g., IL-10) that dampen the splenocytes baseline growth response to serum-derived immune stimulatory molecules, which would be consistent with previous findings that Ag-loss variants that arise in these mice produce reduced "danger signals" (11). Nonetheless, what is apparent is that unlike MMC lysates (Fig. 1*B*), which stimulate proliferation, the relapsing tumors do not.

Tumors that emerge in FVB/N parental mice following MMC rejection are Ag-low variants or ANVs

The phenotype (i.e., neu expression) of the tumors derived from the neu-tg and the FVB/N mice was compared by flow cytometric analysis. Fig. 2*A* shows neu expression in the MMC cell line that was used for tumor transplant. As shown in Fig. 2, *B* and *C*, and *E* and *F*, tumors that emerged in the FVB/N mice (Fig. 2, *D–F*) had significantly less neu expression than those that emerged in the neu-tg (Fig. 2, *B* and *C*). Cell lines established from the ANVs maintained low Ag expression in vitro in all cases, an example (i.e., ANV1) of which is shown in Fig. 2*D*. The loss or reduction in neu expression was due, at least in part, to reductions in rat neu-specific mRNA (Fig. 2*G*). To verify that neu was not just simply internalized, we also evaluated for expression in ANV cell lines using Western blotting. Only a very weak neu-specific signal was observed in the cell lysates from various ANVs, which is consistent with flow cytometry results (Fig. 2*H*). Quantitative analysis of the ANVs compared with the fresh tumors from the neu-tg mouse, as assessed by flow cytometry, is shown in Fig. 2*I*. Unlike MMC (Fig. 1*A*), these ANV rapidly gave rise to tumor in both the neu-tg and the FVB/N parental mice (Fig. 2*J*). Because the possibility existed that the ANV tumors were derived from the FVB/N parental mice and not the transplanted tumor, PCR analysis was done, which confirmed that the ANVs contained a copy of the rat neu gene demonstrating its origin in the neu-tg (data not shown). Furthermore, the observation that these cells are tumorigenic when reimplanted (Fig. 2*J*) demonstrates that the cells were not contaminating stroma. Tumors have also been reported to lose MHC class I expression, which could lead to immune escape. Therefore, we also examined for expression of MHC class I, both basal levels and following IFN treatment. ANV cells retain MHC class I expression and can be induced to express more with either IFN-γ or IFN-α. Representative histograms for MMC and ANV1 are shown in Fig. 3, *B* and *C*.

Ag loss requires $CD4^+$ T cells

To determine the T cell subset that is primarily responsible for rejection of MMC tumor, either the $CD8^+$ or $CD4^+$ T cell subsets were depleted using mAbs before tumor injections. As shown in

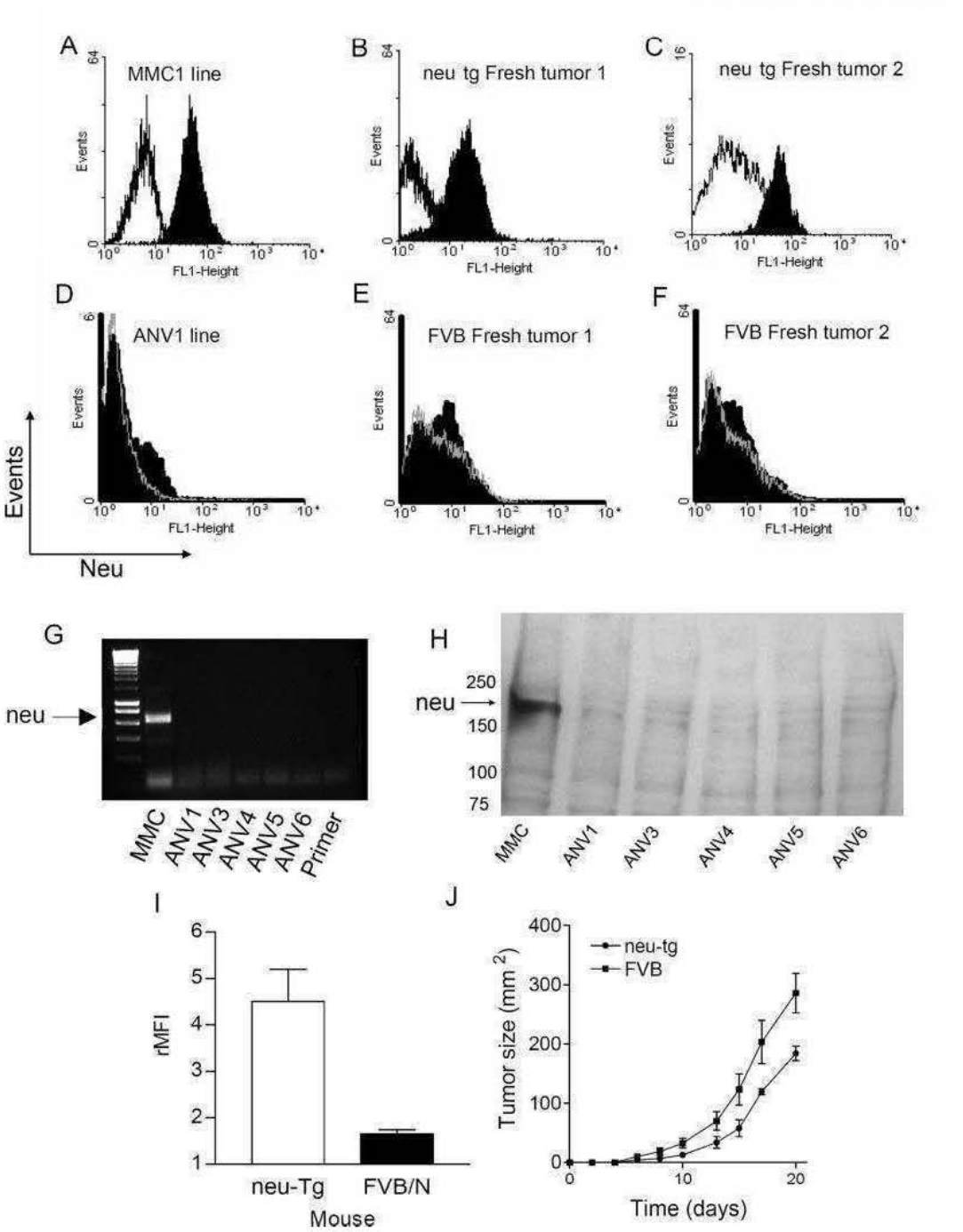

FIGURE 2. Tumors that emerge in FVB/N parental mice following MMC rejection are Ag-low variants or ANVs. *A–F*, Histograms of neu expression in either cell lines (*A* and *D*) or fresh tumors derived from neu-tg mice (*B* and *C*) and FVB/N mice (*E* and *F*). Data shown are representative of three similar and independent experiments. *A–C*, Control data are shown as open black line histogram. *D–F*, Control data are shown as gray line histogram. *G*, RT-PCR analysis of rat neu expression of MMC and several Ag-low or ANV lines (ANV1, 3, 4, 5, and 6). The DNA ladder (*far left lane*) is shown. *H*, Protein expression, as assessed by immunoblotting, of rat neu in the ANV cells lines of *G* relative to expression of expression in MMC. The arrow indicates the band corresponding to rat neu. Values (*left*) are the positions of the molecular weight markers. *I*, The average (± SEM) relative mean fluorescent intensity (rMFI) of neu staining in tumors derived from either the neu-tg or FVB/N mice. *J*, An example ANV cell line growing unimpeded in both FVB/N and neu-tg mice. Each measurement represents the mean (± SEM) of three mice. The experiment was repeated twice with similar results.

Fig. 4*A*, only those animals depleted of $CD4^+$ T cells were unable to reject the tumor cells. Tumors removed from these animals showed levels of neu expression that were comparable to the MMC tumor cells, demonstrating that T cells are required for rejection and Ag-loss (Fig. 4*B*).

ANV are derived from MMC as a result of EMT

Compared with MMC, the ANV cells were morphologically distinct, being more spindle-shaped (Fig. 5, *A* and *B*). The ANV also formed less tight junctions than did the MMC, which suggested that the cells underwent EMT. Thus, an EMT cluster was derived

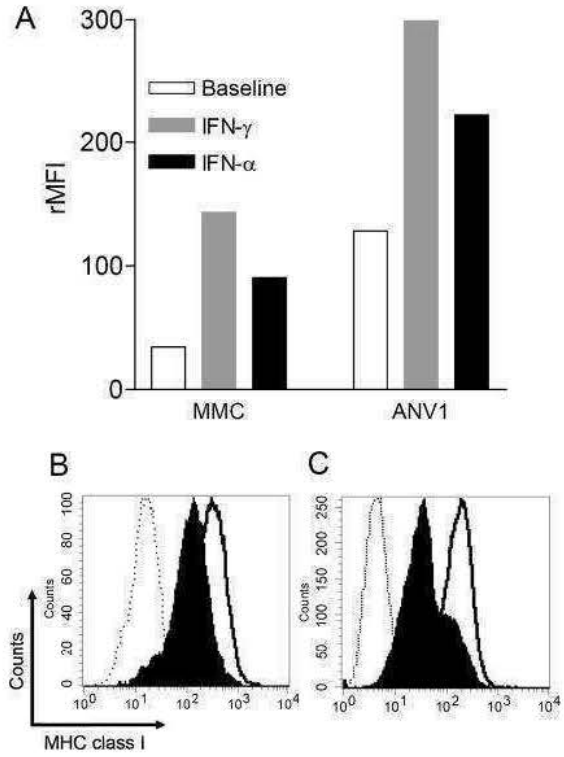

FIGURE 3. ANV cells retain MHC class I expression and responsiveness to IFN treatment. *A*, The relative mean fluorescent intensity (rMFI) of MHC class I expression on cultured MMC and ANV1 in response to IFN-γ (▩) or IFN-α as compared with baseline expression. MMC (*B*) and ANV (*C*) stained with either an irrelevant Ab (dotted histogram) or with anti-MHC class I Abs (filled and open histograms) following treatment with either medium alone (filled histogram) or IFN-γ (open histogram).

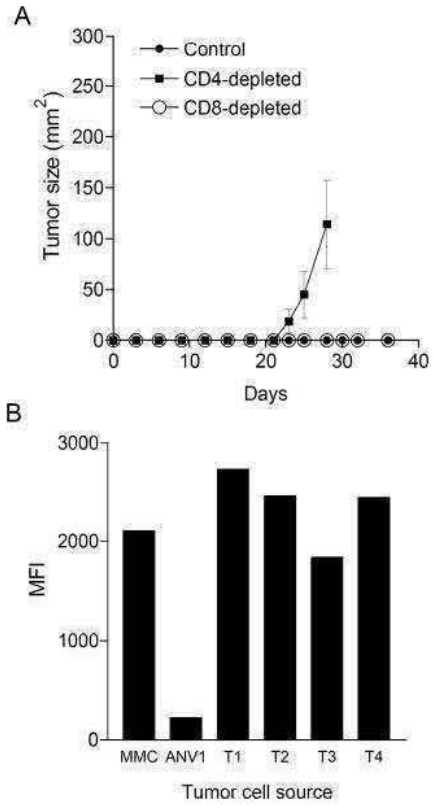

FIGURE 4. Tumor rejection and immunoediting can be eliminated by prior depletion of FVB/N mice with anti-CD4 mAbs. *A*, Tumor growth in groups of mice ($n = 4$ per group) pretreated with PBS (Control), anti-CD4 Ab, or anti-CD8 Ab. Each plot is calculated from four mice, each injected with 3×10^6 MMC tumor cells. In this experiment, the animals were not followed to relapse. The symbols for the control and the CD8-depleted T cell subsets overlap. *B*, Mean fluorescence intensity (MFI) of tumor cells (T1-T4), derived from anti-CD4 treated mice and stained with rat neu-specific Abs as compared with either MMC (neu^+) or ANV1 (neu^-).

from a RNA microarray and used to examine for evidence of EMT. The cluster consisted of E-cadherin (Fig. 5*C*) and TJP1 (ZO1) (Fig. 5*D*) for epithelial cell markers and N-cadherin (Fig. 5*E*) and vimentin (Fig. 5*F*) for mesenchymal cell markers (20–22). As shown, the pattern of gene expression demonstrates that ANVs are mesenchymal, having reduced expression of E-cadherin and TJP1 and elevated levels of N-cadherin and vimentin. PCR confirmed the results of the microarray by showing that TJP is down-regulated and vimentin is up-regulated in the ANV (Fig. 5*G*). Analysis of five other independent Ag-loss variant cell lines by RT-PCR demonstrated loss of E-cadherin confirming loss of epithelial characteristics (Fig. 5*H*). Lastly, we also examined for cell surface expression of CD24, a marker whose level of expression in the mammary gland distinguishes epithelial cells from nonepithelial cells (23). As shown in Fig. 5, *I* and *J*, the transition of MMC to ANV was accompanied by a reduction in CD24 expression.

ANV demonstrate a more invasive phenotype than MMC

EMT is a cellular reprogramming strategy that is used early in the course of embryonic development to impart a migratory and invasive phenotype to epithelial cells so that they may migrate to other regions to give shape to the developing embryo (24). Furthermore, EMT has recently been implicated as a mechanism important for local tumor invasion and metastasis (25, 26). Thus, we speculated that ANV cell lines because of EMT may express molecules associated with increased invasion. Using microarray, again we examined expression of a panel of matrix metalloproteinases (MMPs), enzymes that are involved in their increased invasive potential (27). Of the eight metalloproteinases in the cluster, the MMC expressed two predominantly, MMP2 and MMP9 (Fig. 6*A*). Consistent with a more invasive phenotype, the ANV acquired expression of MMP3, MMP10, MMP11, MMP13, and MMP14, which were not expressed at all in the MMC cells. Furthermore, the ANV also demonstrated expression, in contrast to MMC, of other tumor invasion-associated proteins such as Twist (20), Slug (20), and SDF-1 (28) (as shown in Fig. 2*B*). Both Twist and Slug are also intricately involved in the EMT process (20). The ANV cells were also more invasive as assessed by in vitro migration assays as shown in Fig. 6*C*. The expression of these increased invasion markers, however, did not appear to confer an increased growth advantage because MMC and ANV grew largely at the same rate following transplantation, indicating that EMT may result in increased invasion without altering overall growth rate (Fig. 6*D*).

Discussion

According to the premise of immunosurveillance and immunoediting, immunoescape is a multifaceted event. Tumors can either shut off the immune response (e.g., tolerance induction) or alter their phenotype to lose or avoid recognition (e.g., immunoediting). Past research demonstrating that strong immune responses can lead to the generation of Ag-loss variants has suggested that immunoediting is frequent and can lead to the generation of tumors to which the immune system is tolerant. Using the neu-tg mouse model of epithelial breast cancer, in the present study, we have investigated the phenotype of tumor cells that have undergone immunoediting.

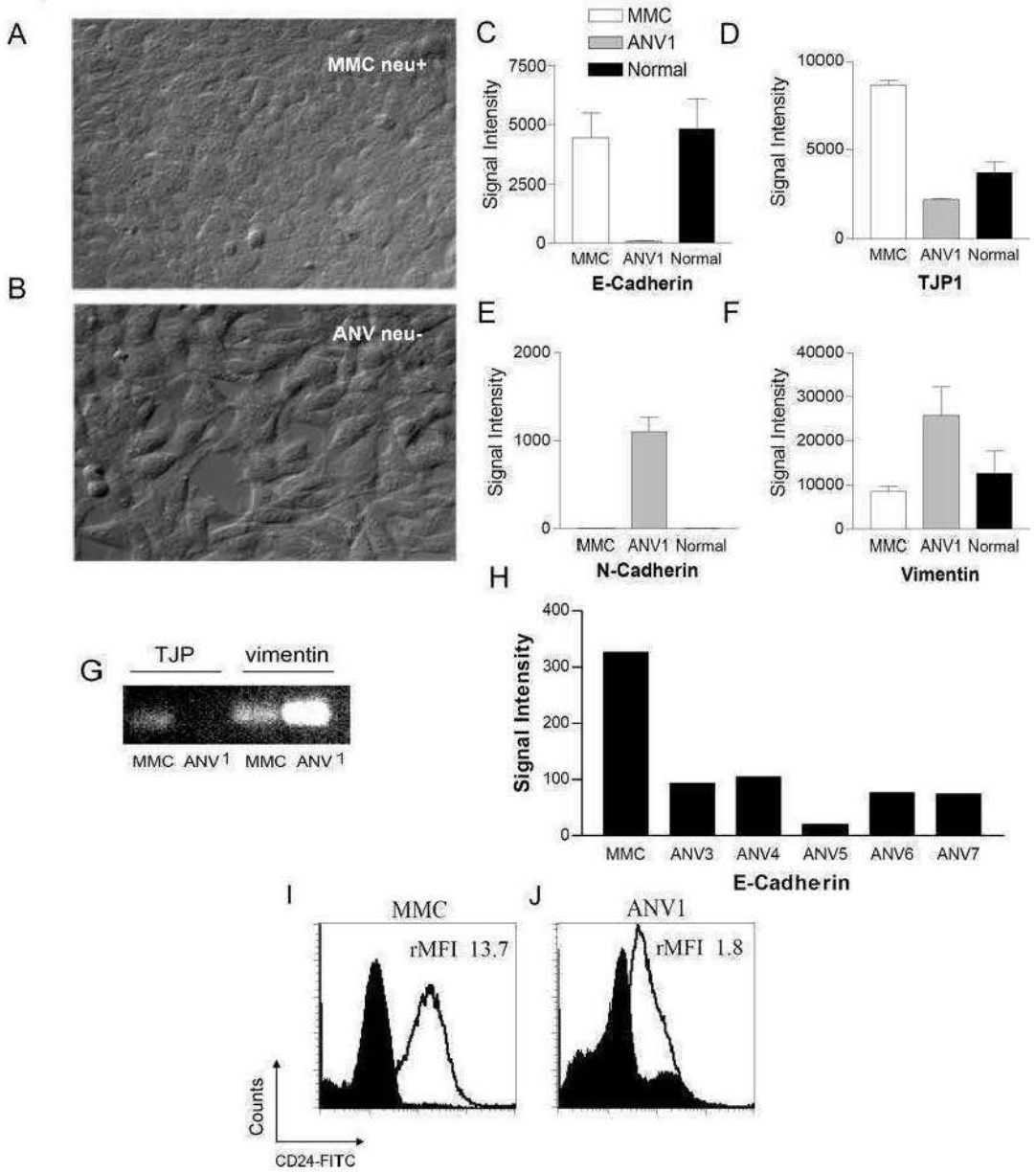

FIGURE 5. ANV are derived from MMC as a result of EMT. Microscope view of the MMC (*A*) and ANV1 (*B*) are shown. *C–F*, Microarray data for EMT markers, E-cadherin, TJP1, N-cadherin, and vimentin are shown. Data represent the mean (± SEM) of two signal intensity measurements from the Affymetrix 420 2.0 array. Similar results were repeated in similar independent experiments using two different microarray analyses. *G*, PCR confirmation of the microarray results for TJP1 and vimentin in the MMC and ANV1 cells. *H*, Quantitative PCR analysis of E-cadherin loss, compared with MMC cell line, in various tumor cell lines generated from tumors derived following immunoediting. The experiment was repeated twice with similar results. *I* and *J*, Histograms of MMC and ANV1 cells stained for CD24 expression are shown. Value shown (*inset*) is the relative mean fluorescence intensity (rMFI) for each cell line.

Specifically, we have found that the tumor cells lost Ag expression, had an altered morphology, and up-regulated genes associated with EMT.

In recent years, the concept of immunoediting has become important because the generation of ANVs in vivo with immune-based approaches is being reported more frequently by a number of laboratories not only in breast cancer but also other cancers following immune-based therapies using a number of different strategies. For example, we have previously reported that mAb therapy can lead to the rapid emergence of tumor ANVs in the neu-tg mouse (2). The phenotype of the resulting Ag-negative tumors was a stable phenotype and not simply due to Ab-induced protein degradation. Furthermore, we also observed in a prior study, that Ag-loss variants generated in FVB/N mice had a unique proteomic profile compared with the tumors generated in the neu-tg mouse model, which was associated with reduced immune danger signals (11). Similarly, Zhou et al. (5) recently reported that mouse renal adenocarcinoma cells can undergo Ag-loss in response to Ag-specific CD4 Th cell therapy. In that study, they observed that the model Ag of influenza hemagglutinin is lost due to down-modulation of the influenza hemagglutinin mRNA, suggesting immunoediting works at the nucleotide level. Our finding that endogenous $CD4^+$ T cells are important in immunoediting corroborates the importance of $CD4^+$ T cells in immunoediting. In humans, adoptive T cell therapy and cancer vaccines have demonstrated the potential for Ag-loss variants to emerge (3, 6, 29). For example, Dudley et al. (29) showed in clinical trials of adoptive T cell therapy with expanded melanoma-derived

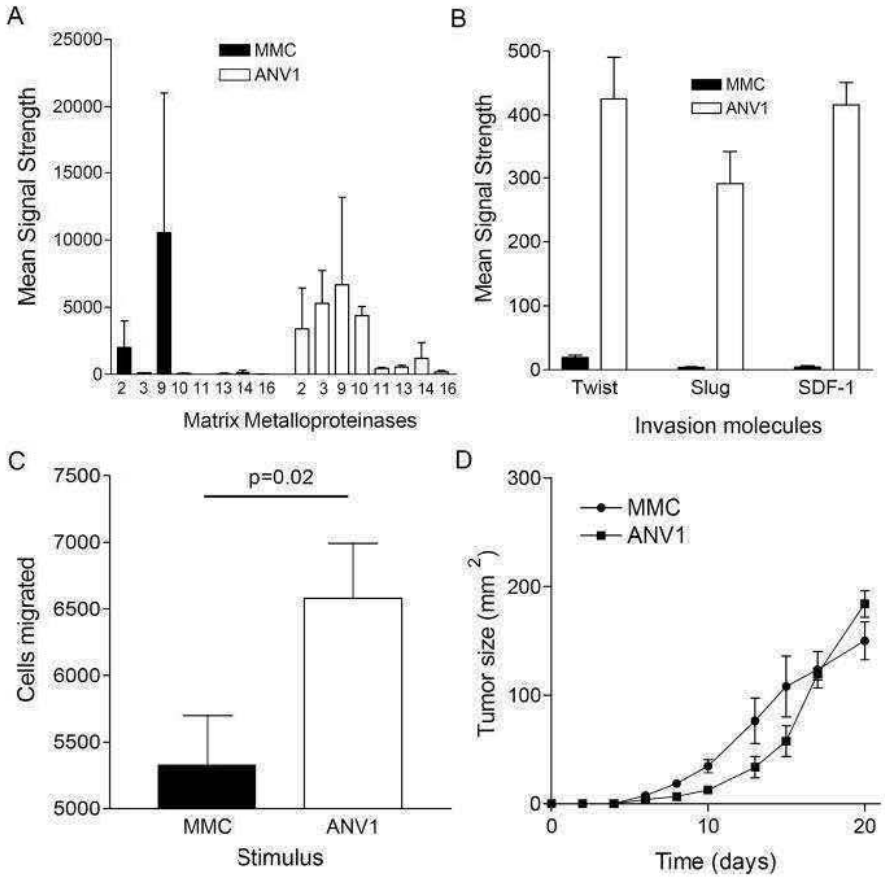

FIGURE 6. ANV tumor cells display a more invasive phenotype than MMC tumor cells. *A*, Levels of MMPs in both the MMC (■) and the ANV (□). Data are the mean (± SEM) of two integrated measurements from two independent gene chip experiments. The results for MMP2 were confirmed using dual-staining microarray. *B*, Increased expression of three proteins involved in breast cancer invasion potential. The results for stromal cell derived factor-1 were confirmed using dual-staining microarray. *C*, Invasive potential of MMC (■) and ANV (□) is represented measured as the relative mean fluorescence intensity (rMFI). Data represent the mean of six determinations. *D*, The comparative tumor development and growth of 3×10^6 MMC or ANV in neu-tg mice. Each time point is the mean (± SEM) of triplicate determinations.

tumor-infiltrating lymphocytes that responding patients, but not nonresponding patients, developed both Ag- and MHC-loss variants following treatment, demonstrating that immunoediting is important in human tumors as well. Although the mechanisms by which Ag expression is lost is not clear (i.e., genetic or epigenetic), mouse studies have begun to answer some questions. Sanchez-Perez et al. (4) have shown in the B16 melanoma model that, rather than selecting for mutants, gene expression is lost epigenetically through DNA methylation following immunoediting. Collectively, the observations that the altered phenotypes are stable and that gene expression is modulated, suggest that immunity activates cellular reprogramming pathways.

Our study suggests that one potential reprogramming mechanism activated during immunoediting is EMT, a gene expression program that has long been known to be important in embryonic development but only suspected recently to have a role in the pathogenesis of cancer (26). Embryonic epithelial tissue cells use EMT to dedifferentiate and transition into a more motile cell type to give rise to specialized tissues including the mammary glands, somites, and heart endocardium (26). Although it is unclear what role EMT plays in cellular motility in a fully developed healthy mammal, EMT is a reprogramming strategy that is used pathologically in breast cancer, which may permit nonmigratory epithelial cancer cells to acquire motility to seed other tissues within the body (30). Similar to that observed in embryonic development, the transition of breast epithelial cells to the mesenchymal state is also accompanied by a loss of epithelial characteristics (e.g., E-cadherin, TJPs) as well as tissue-specific proteins (our unpublished observations). Thus, these results suggest that the interaction of tumor cells with the immune system may not only result in loss of immune recognition but also may have a role in the pathogenesis of the disease.

With the exception that $CD4^+$ T cells are required, at present we can only speculate on the potential in vivo mechanisms by which the immune system could lead to EMT. In a recent report, Bates and Mercurio (31) demonstrated a connection between the immune system and the induction of EMT by showing that activated macrophages could directly facilitate EMT in human colonic tumor cells in vitro. Further analysis revealed that TNF-α was a critical factor produced by the macrophages that led to accelerated EMT. Thus, a plausible scenario that may explain our findings is that the immune effectors (T cell, macrophages, etc) at the tumor site led to increased levels of TNF-α. Indeed, this result may have a correlate in human breast cancer where increased TNF-α in the tumor microenvironment in the periphery is associated with increased metastatic potential (32, 33). Alternatively, other immune factors are also associated with EMT. For example, EMT is typically induced by TGF-β in a variety of different cell types including breast cancer cells in vitro (34). Furthermore, several immune effectors such as regulatory T cells are known to produce high levels of TGF-β (35). Thus, the development of a strong immune response may also be accompanied by chemoattraction or induction of TGF-β producing regulatory T cells that may also promote EMT. Nonetheless, understanding the mechanisms of EMT induction in the immune microenvironment will improve our understanding of tumor-immune interactions and the development of immune escape variants.

In conclusion, our findings suggest that immunoediting of breast tumors in mice may involve EMT. Thus, immune escape may be more than incremental changes in gene expression resulting in the chance loss of Ag expression. Rather, breast cancer may actively escape immune detection through the pathologic use of cellular reprogramming.

Acknowledgments

The expert technical assistance of Shay Park and Dr. Christopher Krco is gratefully acknowledged. We gratefully acknowledge helpful discussions from Dr. Masoud Manjili.

Disclosures

The authors have no financial conflict of interest.

References

1. Dunn, G. P., A. T. Bruce, H. Ikeda, L. J. Old, and R. D. Schreiber. 2002. Cancer immunoediting: from immunosurveillance to tumor escape. *Nat. Immunol.* 3: 991–998.
2. Knutson, K. L., B. Almand, Y. Dang, and M. L. Disis. 2004. Neu antigen-negative variants can be generated after neu-specific antibody therapy in neu transgenic mice. *Cancer Res.* 64: 1146–1151.
3. Yee, C., J. A. Thompson, D. Byrd, S. R. Riddell, P. Roche, E. Celis, and P. D. Greenberg. 2002. Adoptive T cell therapy using antigen-specific $CD8^+$ T cell clones for the treatment of patients with metastatic melanoma: in vivo persistence, migration, and antitumor effect of transferred T cells. *Proc. Natl. Acad. Sci. USA* 99: 16168–16173.
4. Sanchez-Perez, L., T. Kottke, R. M. Diaz, A. Ahmed, J. Thompson, H. Chong, A. Melcher, S. Holmen, G. Daniels, and R. G. Vile. 2005. Potent selection of antigen loss variants of B16 melanoma following inflammatory killing of melanocytes in vivo. *Cancer Res.* 65: 2009–2017.
5. Zhou, G., Z. Lu, J. D. McCadden, H. I. Levitsky, and A. L. Marson. 2004. Reciprocal changes in tumor antigenicity and antigen-specific T cell function during tumor progression. *J. Exp. Med.* 200: 1581–1592.
6. Khong, H. T., Q. J. Wang, and S. A. Rosenberg. 2004. Identification of multiple antigens recognized by tumor-infiltrating lymphocytes from a single patient: tumor escape by antigen loss and loss of MHC expression. *J. Immunother.* 27: 184–190.
7. Lozupone, F., L. Rivoltini, F. Luciani, M. Venditti, L. Lugini, A. Cova, P. Squarcina, G. Parmiani, F. Belardelli, and S. Fais. 2003. Adoptive transfer of an anti-MART-1_{27-35}-specific $CD8^+$ T cell clone leads to immunoselection of human melanoma antigen-loss variants in SCID mice. *Eur. J. Immunol.* 33: 556–566.
8. Madjd, Z., I. Spendlove, S. E. Pinder, I. O. Ellis, and L. G. Durrant. 2005. Total loss of MHC class I is an independent indicator of good prognosis in breast cancer. *Int. J. Cancer* 117: 248–255.
9. Bissell, M. J., and M. A. Labarge. 2005. Context, tissue plasticity, and cancer: are tumor stem cells also regulated by the microenvironment? *Cancer Cell* 7: 17–23.
10. Ercolini, A. M., B. H. Ladle, E. A. Manning, L. W. Pfannenstiel, T. D. Armstrong, J.-P. Machiels, J. G. Bieler, L. A. Emens, R. T. Reilly, and E. M. Jaffee. 2005. Recruitment of latent pools of high-avidity $CD8^+$ T cells to the antitumor immune response. *J. Exp. Med.* 201: 1591–1602.
11. Manjili, M. H., H. Arnouk, K. L. Knutson, M. Kmieciak, M. L. Disis, J. R. Subjeck, and A. L. Kazim. 2006. Emergence of immune escape variant of mammary tumors that has distinct proteomic profile and a reduced ability to induce "danger signals". *Breast Cancer Res. Treat.* 96: 233–241.
12. Guy, C. T., M. A. Webster, M. Schaller, T. J. Parsons, R. D. Cardiff, and W. J. Muller. 1992. Expression of the neu protooncogene in the mammary epithelium of transgenic mice induces metastatic disease. *Proc. Natl. Acad. Sci. USA* 89: 10578–10582.
13. Ercolini, A. M., J.-P. Machiels, Y. C. Chen, J. E. Slansky, M. Giedlen, R. T. Reilly, and E. M. Jaffee. 2003. Identification and characterization of the immunodominant rat HER-2/neu MHC class I epitope presented by spontaneous mammary tumors from HER-2/neu-transgenic mice. *J. Immunol.* 170: 4273–4280.
14. Reilly, R. T., J.-P. Machiels, L. A. Emens, A. M. Ercolini, F. I. Okoye, R. Y. Lei, D. Weintraub, and E. M. Jaffee. 2001. The collaboration of both humoral and cellular HER-2/neu-targeted immune responses is required for the complete eradication of HER-2/*neu*-expressing tumors. *Cancer Res.* 61: 880–883.
15. Reilly, R. T., M. B. Gottlieb, A. M. Ercolini, J.-P. Machiels, C. E. Kane, F. I. Okoye, W. J. Muller, K. H. Dixon, and E. M. Jaffee. 2000. HER-2/*neu* is a tumor rejection target in tolerized HER-2/*neu* transgenic mice. *Cancer Res.* 60: 3569–3576.
16. Knutson, K. L., and M. L. Disis. 2001. Expansion of HER2/neu-specific T cells ex vivo following immunization with a HER2/neu peptide-based vaccine. *Clin. Breast Cancer* 2: 73–79.
17. Knutson, K. L., Y. Dang, H. Lu, J. Lukas, B. Almand, E. Gad, E. Azeke, and M. L. Disis. 2006. IL-2 immunotoxin therapy modulates tumor-associated regulatory T cells and leads to lasting immune-mediated rejection of breast cancers in neu-transgenic mice. *J. Immunol. In press.*
18. Drebin, J. A., V. C. Link, and M. I. Greene. 1988. Monoclonal antibodies reactive with distinct domains of the neu oncogene-encoded p185 molecule exert synergistic anti-tumor effects in vivo. *Oncogene* 2: 273–277.
19. Knutson, K. L., and M. L. Disis. 2004. IL-12 enhances the generation of tumour antigen-specific Th1 CD4 T cells during ex vivo expansion. *Clin. Exp. Immunol.* 135: 322–329.
20. Huber, M. A., N. Kraut, and H. Beug. 2005. Molecular requirements for epithelial-mesenchymal transition during tumor progression. *Curr. Opin. Cell Biol.* 17: 548–558.
21. Larue, L., and A. Bellacosa. 2005. Epithelial-mesenchymal transition in development and cancer: role of phosphatidylinositol 3′ kinase/AKT pathways. *Oncogene* 24: 7443–7454.
22. Thomson, S., E. Buck, F. Petti, G. Griffin, E. Brown, N. Ramnarine, K. K. Iwata, N. Gibson, and J. D. Haley. 2005. Epithelial to mesenchymal transition is a determinant of sensitivity of non-small-cell lung carcinoma cell lines and xenografts to epidermal growth factor receptor inhibition. *Cancer Res.* 65: 9455–9462.
23. Sleeman, K. E., H. Kendrick, A. Ashworth, C. M. Isacke, and M. J. Smalley. 2006. CD24 staining of mouse mammary gland cells defines luminal epithelial, myoepithelial/basal and non-epithelial cells. *Breast Cancer Res.* 8: R7.
24. Hay, E. D. 1995. An overview of epithelio-mesenchymal transformation. *Acta Anat. (Basel)* 154: 8–20.
25. Gotzmann, J., M. Mikula, A. Eger, R. Schulte-Hermann, R. Foisner, H. Beug, and W. Mikulits. 2004. Molecular aspects of epithelial cell plasticity: implications for local tumor invasion and metastasis. *Mutat. Res.* 566: 9–20.
26. Thiery, J. P. 2003. Epithelial-mesenchymal transitions in development and pathologies. *Curr. Opin. Cell Biol.* 15: 740–746.
27. Vihinen, P., R. Ala-aho, and V. M. Kahari. 2005. Matrix metalloproteinases as therapeutic targets in cancer. *Curr. Cancer Drug Targets* 5: 203–220.
28. Kang, H., G. Watkins, C. Parr, A. Douglas-Jones, R. E. Mansel, and W. G. Jiang. 2005. Stromal cell derived factor-1: its influence on invasiveness and migration of breast cancer cells in vitro, and its association with prognosis and survival in human breast cancer. *Breast Cancer Res.* 7: R402–R410.
29. Dudley, M. E., J. R. Wunderlich, J. C. Yang, R. M. Sherry, S. L. Topalian, N. P. Restifo, R. E. Royal, U. Kammula, D. E. White, S. A. Mavroukakis, et al. 2005. Adoptive cell transfer therapy following non-myeloablative but lymphodepleting chemotherapy for the treatment of patients with refractory metastatic melanoma. *J. Clin. Oncol.* 23: 2346–2357.
30. Vincent-Salomon, A., and J. P. Thiery. 2003. Host microenvironment in breast cancer development: epithelial-mesenchymal transition in breast cancer development. *Breast Cancer Res.* 5: 101–106.
31. Bates, R. C., and A. M. Mercurio. 2003. Tumor necrosis factor-α stimulates the epithelial-to-mesenchymal transition of human colonic organoids. *Mol. Biol. Cell* 14: 1790–1800.
32. Ardizzoia, A., P. Lissoni, F. Brivio, E. Tisi, M. S. Perego, M. G. Grassi, S. Pittalis, S. Crispino, S. Barni, and G. Tancini. 1992. Tumor necrosis factor in solid tumors: increased blood levels in the metastatic disease. *J. Biol. Regul. Homeostatic Agents* 6: 103–107.
33. Leek, R. D., R. Landers, S. B. Fox, F. Ng, A. L. Harris, and C. E. Lewis. 1998. Association of tumour necrosis factor α and its receptors with thymidine phosphorylase expression in invasive breast carcinoma. *Br. J. Cancer* 77: 2246–2251.
34. Huber, M. A., N. Azoitei, B. Baumann, S. Grünert, A. Sommer, H. Pehamberger, N. Kraut, H. Beug, and T. Wirth. 2004. NF-κB is essential for epithelial-mesenchymal transition and metastasis in a model of breast cancer progression. *J. Clin. Invest.* 114: 569–581.
35. Buckner, J. H., and S. F. Ziegler. 2004. Regulating the immune system: the induction of regulatory T cells in the periphery. *Arthritis Res. Ther.* 6: 215–222.

blood

2008 111: 1472-1479
Prepublished online Nov 20, 2007;
doi:10.1182/blood-2007-10-117184

The endogenous danger signal, crystalline uric acid, signals for enhanced antibody immunity

Marshall D. Behrens, Wolfgang M. Wagner, Christopher J. Krco, Courtney L. Erskine, Kimberly R. Kalli, James Krempski, Ekram A. Gad, Mary L. Disis and Keith L. Knutson

Blood (print ISSN 0006-4971, online ISSN 1528-0020), is published semimonthly by the American Society of Hematology, 1900 M St, NW, Suite 200, Washington DC 20036.

The endogenous danger signal, crystalline uric acid, signals for enhanced antibody immunity

Marshall D. Behrens,[1] Wolfgang M. Wagner,[2] Christopher J. Krco,[1] Courtney L. Erskine,[1] Kimberly R. Kalli,[1] James Krempski,[1] Ekram A. Gad,[2] Mary L. Disis,[2] and Keith L. Knutson[1]

[1]Department of Immunology, Mayo Clinic College of Medicine, Rochester, MN; and [2]Tumor Vaccine Group, Center for Translational Medicine in Women's Health, Seattle, WA

Studies have shown that the immune system can recognize self-antigens under conditions (eg, cell injury) in which the self-tissue might elaborate immune-activating endogenous danger signals. Uric acid (UA) is an endogenous danger signal recently identified to be released from dying cells. Prior work has shown that UA activates immune effectors of both the innate and adaptive immune system, including neutrophils and cytotoxic T-cell immunity. However, it was unclear whether UA could enhance antibody immunity, which was examined in this study. When added to dying tumor cells or with whole protein antigen, UA increased IgG1-based humoral immunity. Further, UA blocked growth of tumor in subsequent tumor challenge experiments, which depended on CD4, but not CD8, T cells. Sera derived from UA-treated animals enhanced tumor growth, suggesting it had little role in the antitumor response. UA did not signal for T-cell expansion or altered tumor-infiltrating leukocyte populations. Consistent with the lack of T-cell expansion, when applied to dendritic cells, UA suppressed T-cell growth factors but up-regulated B cell–activating cytokines. Understanding the nature of endogenous danger signals released from dying cells may aid in a better understanding of mechanisms of immune recognition of self. (Blood. 2008; 111:1472-1479)

Introduction

A hallmark of the immune system is the keen ability to distinguish between infected and noninfected self.[1] Immune responses to infected tissues are not due merely to the presence of a microbial-derived antigen but rather the presentation of that antigen to the immune system in the context of another microbial-derived molecule termed a pathogen-associated molecular pattern (PAMP).[2] Unlike antigens, PAMPs are not typically peptides or proteins, but rather molecules such as nucleic acids or glycolipids that are not readily subject to change through mutations. There are several PAMPs including lipopolysaccharide (LPS), unmethylated cytosine-guanosine repeats (CpGs), and double-stranded RNA motifs. PAMPs are recognized by one of several mammalian receptors, most being from the toll-like receptor (TLR) family of pattern-recognition receptors (PRRs).[3] Proof that the immune system relies heavily on PAMPs for the decision about whether to activate comes from studies in which PAMPs are used as adjuvants in vaccines that target self-antigens. For example, cancer vaccines containing a combination of bacterial CpGs along with HER-2/neu-derived peptide epitopes are able to readily overcome tolerance and to provide long-term protection against spontaneous tumor development in the neu-transgenic mouse model of breast cancer.[4] Despite the extensive understanding of PAMPs, it is now clear that the adaptive immune system can become activated against self under sterile conditions such as malignancy, cell death, or cell injury.[5] There are a few stimuli (ie, endogenous danger signals) that have been characterized and identified in recent times that may be capable of driving sterile immune responses.[6,7] One such group of endogenous danger signals is the purines, which include both uric acid (UA) and adenosine triphosphate (ATP).[7-10]

UA has received attention recently due to a series of reports from Rock and colleagues who have recently identified UA as a danger signal that is released from dying cells (Chen et al[5,11]; Shi et al[8,9]). These findings are now being corroborated by studies from other groups. For example, Hu et al found that UA was released from tumor cells undergoing immune rejection and that it had a significant role in the rejection process.[12] UA is a natural product of the purine metabolic pathway and although found in extracellular fluids (eg, blood and interstitial spaces), its release from cells is thought to result in crystallization, which creates the immune bioactive form of UA.[7,8] Crystalline UA has been shown to activate innate immune effectors including dendritic cells (DCs) and macrophages.[8,13] Prior studies have shown that its ability to activate innate effectors can lead ultimately to activation of antigen-specific cytotoxic T-cell immunity.[8]

What has not been addressed is whether UA can also enhance antibody immunity. The primary reason to suggest a role of UA in antibody immunity is that sterile immune responses, such as those seen in rheumatoid arthritis and malignancy are often associated with the development of autoantibodies.[14,15] In the current study, we investigated whether UA could augment antigen-specific antibodies in 2 separate model systems. In the first model, UA was added to dying cells that were injured using irradiation, with the intent of mimicking the purported physiologic role of UA. In the second, the ovalbumin foreign antigen model was used. In both

Submitted October 10, 2007; accepted November 12, 2007. Prepublished online as *Blood* First Edition paper, November 20, 2007; DOI 10.1182/blood-2007-10-117184.

M.D.B. and W.M.W. contributed equally to this work.

The publication costs of this article were defrayed in part by page charge payment. Therefore, and solely to indicate this fact, this article is hereby marked "advertisement" in accordance with 18 USC section 1734.

models, it was found that crystalline UA led to augmented antibody immunity in the absence of significant tumor-specific T-cell expansion.

Methods

Animals

C57BL/6, OT-I, Balb/c, DO11.10, and FVB/N-TgN (MMTVneu)-202Mul (neu-tg mouse) mice were from the Jackson Laboratory (Bar Harbor, ME). OT-I mice are transgenic for a H-2K^b–restricted T-cell receptor that is specific for the chicken ovalbumin epitope Oval(257-264); DO11.10 mice are transgenic for a I-A^d–restricted TCR recognizing Oval(323-339). Only female mice (8-12 weeks old) were used, in accordance with institutional guidelines.

Reagents

UA crystals (> 99% purity; Sigma-Aldrich, St Louis, MO) were prepared as described before.[8] Fluorochrome-conjugated antibodies targeting CD3, CD4, and CD8, CD19, CD14, NKT1.1, and CD11C were from BD Pharmingen (San Diego, CA). Ovalbumin and basic reagents were from Sigma Chemical (St Louis, MO). Synthetic peptides, Oval(323-339) and Oval(257-264), were synthesized by Sigma Genosys (The Woodlands, TX). Rat neu peptide, p420-429, was synthesized by the Mayo Clinic (Rochester, MN). Use of the neu peptide p420-429 H-2^q tetramer has been previously described.[16] The anti–IL-4/biotinylated anti–IL-4 and anti–IFN-γ/biotinylated anti–IFN-γ cytokine antibody pairs were from Endogen (Pierce, Rockford, IL) and BD Pharmingen, respectively. Recombinant murine granulocyte/macrophage-colony stimulating factor (GM-CSF) was obtained from R&D Systems (Minneapolis, MN). The IL-2 immunotoxin, denileukin diftitox (ie, ONTAK), was obtained from Ligand Pharmaceuticals (San Diego, CA).[16] Foxp3 antibody was obtained from eBiosciences (San Diego, CA).

Tumor growth

Mouse mammary carcinoma (MMC) cell line was established from a spontaneous tumor from the neu-tg mice as previously described.[17] For in vivo tumor growth, mice were inoculated with 5×10^6 MMC cells subcutaneously on the middorsum. Tumors were measured every few days with calipers, and tumor volume was calculated as the product of length × width × height × 0.5236. The numbers of mice used in each experiment are stated in "Results." For in vitro experiments, 10^5 MMC cells were plated in 6-well plates with media alone or with various concentrations of sera. Proliferation analysis was done as previously described.[18] In some cases, the tumors were removed for assessment of intracellular trafficking of leukocytes. Leukocyte content was compared between tumors of similar sizes to minimize potential variations due to tumor size such as necrosis and hypoxia.

Adoptive transfer and immunizations

Splenocytes from oval-TCR transgenic donor mice were adoptively transferred into the tail vein of recipient mice one day prior to the immunization. Balb/c mice received 2×10^6 DO11.10 splenocytes per mouse; C57BL/6 received 10×10^6 OT-I splenocytes. Mice were immunized intradermally with 10 μg ovalbumin (or appropriate ovalbumin peptide in the case of TCR transgenic T cells) and 5 μg GM-CSF or 25 μg UA crystals per mouse. Six days later, mice were killed and the Balb/c splenocytes were stained with anti-DO11.10 TCR mab KJ1-26 (Caltag, Burlingame, CA), while B6 splenocytes were stained with (SIINFEKL)-H2-Kb tetramer (Beckman Coulter, Fullerton, CA) followed by flow cytometric analysis. For the antibody studies, Balb/c mice were immunized with whole ovalbumin protein as described for C57BL/6 mice. For dying tumor cell studies in the neu-tg mouse, MMC cells (5×10^6/mouse) were irradiated (150 gray) and injected with or without UA. Two injections were given approximately 7 to 14 days apart, subcutaneously. Seven to 14 days following the last injection, either live MMC tumor cells were injected or splenocytes, lymph node cells, and blood were harvested for examination by flow cytometry. To deplete T regulatory cells (Tregs) prior to immunization, the animals were pretreated with denileukin diftitox as previously described.[16] In some cases, mice were pretreated with monoclonal antibodies to deplete either CD8$^+$ or CD4$^+$ T cells prior to challenge with dying tumor with UA as previously described.[19]

ELIspot assays

Enzyme-linked immunosorbent spot (ELIspot) analysis was conducted essentially as previously described.[20] Splenocytes isolated from treated animals were exposed to media alone, freeze-thawed MMC tumor cells (1 tumor cell per 4 splenocytes), neu peptide p420-429 (10 μg/mL), or concanavalin A (5 μg/mL, concanavalin A, ConA) for 48 hours.

Isolation and in vitro culture of splenic dendritic cells

Minced spleens were incubated with collagenase D (37°C, 30 minutes) and passed through a 70-μm cell strainer. DCs were purified with a CD11c cell purification kit to greater than 90% purity (Miltenyi, Bergisch Gladbach, Germany). TCR transgenic T cells were purified with CD4$^+$ or the CD8$^+$ T-cell isolation kits that produce untouched T cells (Miltenyi). Purified DCs were exposed for 2 hours to peptide antigens and 10 μg/mL UA (in RPMI-1640, 2 mM L-glutamine, 25 mM HEPES, 10% FCS, 50 mM 2-mercaptothanol, and 1% penicillin and streptomycin) after which the media were removed and the DCs washed. TCR-transgenic T cells were then added to the DCs for 48 hours at 37°C after which the T cells were again repurified and placed back into T-cell media for an additional 48 hours. The T cell–conditioned supernatants were then collected and examined for cytokine content using multiplexed microsphere analysis as described in "Multiplexed microsphere cytokine immunoassay." In some cases, DCs were not exposed to T cells but rather allowed to remain in media for 48 hours after which DC-conditioned media were removed and assessed for cytokine content.

Enzyme-linked immuno sorbent assay

For direct enzyme-linked immunosorbent assays (ELISAs), Maxisorp ELISA plates (Nalge Nunc International, Rochester, NY) were coated overnight at 4°C with 5 μg/mL ovalbumin or 10 μg/mL freeze-thawed tumor lysates in 0.05 M carbonate-bicarbonate buffer containing and blocked with 1% BSA. Sera were applied at a 1:120 dilution followed by incubation for 1 hour at room temperature (RT) with horseradish peroxidase–conjugated antibodies against mouse IgG, IgG1, or IgG2a (Zymed, South San Francisco, CA). Serum was omitted from control wells to determine background signals, which were subtracted from each experimental value. In other cases, standard curves were prepared to convert the optical density signals into an estimated antibody concentration by directly plating several concentrations of purified IgG, IgG1, or IgG2a onto the ELISA plates. The plates were developed using tetramethylbenzadine (TMB), which was stopped by the addition of 1 N sulfuric acid. The plates were read at 450 nm on a Victor V 1420 Multilabel Reader (Perkin Elmer, Waltham, MA).

For sandwich ELISA, plates were coated with 100 μL/well of rabbit polyclonal antibodies to rat neu (ab36728; Abcam, Cambridge, MA). After blocking and washing, 20 μg/well of tumor freeze-thawed lysates or assay buffer was added to each well and incubated at RT for 2 hours. After washing, mouse sera were added to the plate at a 1:40 dilution in triplicate and incubated for 1 hour at RT. All other steps were performed as described above.

Multiplexed microsphere cytokine immunoassay

Cytokines (IL-12, IL-2, IFN-γ, IL-4, and IL-5) were measured using multiplex microspheres per the manufacturer's direction (BioRad, San Diego, CA). Briefly, 100 μL Bio-Plex assay buffer (BioRad) was added to each well of a MultiScreen MABVN 1.2-μm microfiltration plate (Millipore, Billerica, MA) followed by the addition of 50 μL of the multiplex bead preparation. Following washing of the beads with 100 μL wash buffer, 50 μL of the samples (ie, cell culture supernatants) or the standards was

added to each well and incubated with shaking for 30 minutes at room temperature. Standard curves were generated with a mixture of cytokine standards and 8 serial dilutions ranging from 0 to 32 000 pg/mL. The plate was washed 3 times followed by incubation of each well in 25 μL premixed detection antibodies for 30 minutes with shaking. The plate was washed and 50 μL streptavidin solution was added to each well and incubated for 10 minutes at RT with shaking. The beads were given a final washing and resuspended in 125 μL Bio-Plex assay buffer. Cytokine levels in the sera were quantitated by analyzing 100 μL of each well on a Bio-Plex using Bio-Plex Manager software (version 4; BioRad).

Flow cytometry

Cell surface molecules and Foxp3 staining and flow cytometry were done essentially as described by Knutson et al.[16] For flow cytometric analysis, a similar number of events, typically 100 000, were collected for all groups.

Immunoprecipitation and Western blotting

Cell lysate preparation, immunoprecipitations, and Western blot analysis were done as previously described by Knutson et al.[21] Sera collected from treatment mice were diluted 50-fold and mixed with 400 μg MMC tumor cell lysates.

Statistical analyses

Statistical analyses were performed using GraphPad InStat for Windows 95/NT (GraphPad Software, San Diego, CA). Data were analyzed using Mann-Whitney or Student *t* tests unless otherwise stated, and the results were considered statistically significant if P was less than .05.

Results

UA signals for enhanced antitumor immunity

The danger signaling properties of UA were examined in a tumor protection model (Figure 1). Crystalline UA, when added with dying (irradiated) tumor cells, led to subsequent suppression of tumor growth in a dose-dependent manner when given prior to tumor challenge, indicating augmentation of memory immune responses. For example, on day 38 after tumor challenge, the size of the tumors in mice pretreated with dying tumor cells containing 100 μg UA was 143 ± 95 mm^3 (mean ± SEM, n = 5), which was significantly smaller than control tumors (25 μg UA only) at the same time point (972 ± 83 mm^3; $P < .001$) and smaller than tumors from animals treated with tumors only (695 ± 200 mm^3; $P = .019$). UA doses of 100 or 20 μg UA led to similar tumor suppression ($P > .05$). UA was ineffective at the 10-μg dose, and at this dose the mean tumor size was not significantly different from control ($P > .05$). UA at lower doses (eg, 1 μg; data not shown) had no impact on tumor growth challenge, likely due to rapid dissolution. In addition to suppressing the growth rate, the inclusion of UA was able to improve overall survival as shown in Figure 1B. Animals that received 20 μg or 100 μg UA had a survival that was more than 35 days longer than that observed in the control mice and approximately 14 days greater than animals treated with tumor cells alone. Depletion of CD4 T cells, but not CD8 T cells, prior to immunization reversed the tumor-suppressive effects of UA (Figure 1C). In fact, CD8 T-cell depletion provided enhanced antitumor activity. Despite its effects on suppressing tumor growth when used in the prevention setting, when injection was begun after the tumors had formed, UA was unable to suppress tumor growth when combined with dying tumor cells (data not shown). Thus, UA added to dying tumor cells augments CD4 T helper cell–dependent antitumor immune responses.

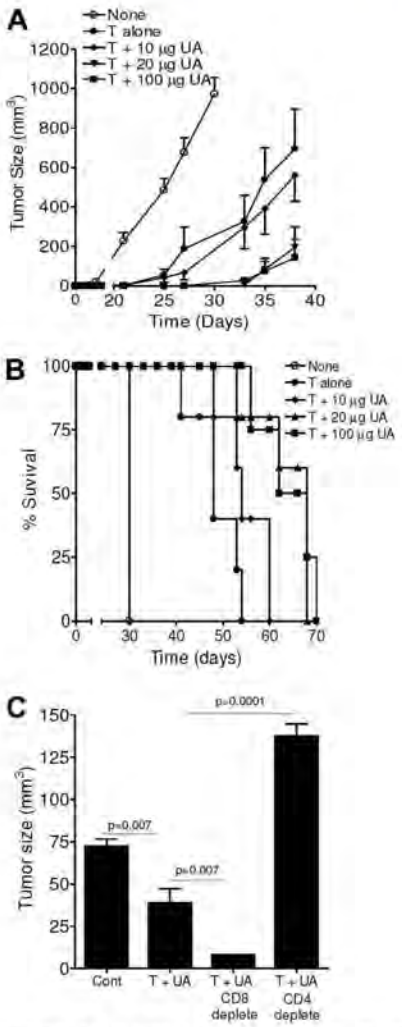

Figure 1. Uric acid signals for enhanced antitumor immunity. (A) Tumor growth measurements for animals treated with dying tumor cells, either alone or along with various concentrations of uric acid (UA) prior to tumor challenge. Control animals (none) received 25 μg UA. Each data point is a mean (± SEM) tumor measurement calculated from 6 animals per group. A similar experiment yielded similar results. (B) Survival curves for mice, treated the same as in panel A, over a course of 75 days. The experiment is representative of 2 similar independent experiments. (C) Tumor growth measurements in animals treated with dying tumor cells and 25 μg UA alone or following depletion of either CD8 or CD4 T cells. Control animals received no treatments. Measurements are the mean (± SEM) of 4 animals per group. A repeat experiment gave identical results.

UA signals for an enhanced IgG1 antibody response

The ability of UA to boost IgG antibody immunity was next examined. As shown in Figure 2A, injection of dying tumor cells alone generated a strong IgG antibody response in the absence of exogenous UA. The inclusion of UA (25 μg) along with the dying tumor cells further boosted this antibody response compared with animals injected with 25 μg UA alone. This level of tumor-specific antibody was significantly higher and nearly double the antibody level achieved following injection of dying tumor cells alone ($P = .001$, n = 12). The increase in tumor-specific IgG antibody was due, at least in part, to a significant increase in tumor-specific IgG1. As shown in Figure 2B, the levels of IgG1 attained with the inclusion of UA were significantly higher compared with the levels achieved with the injection of tumor cells alone ($P = .01$). In contrast, UA did not induce a significant increase in tumor-specific IgG2a (Figure 2C; $P > .05$). Flow cytometric analysis confirmed the finding of elevated IgG by demonstrating that serum from

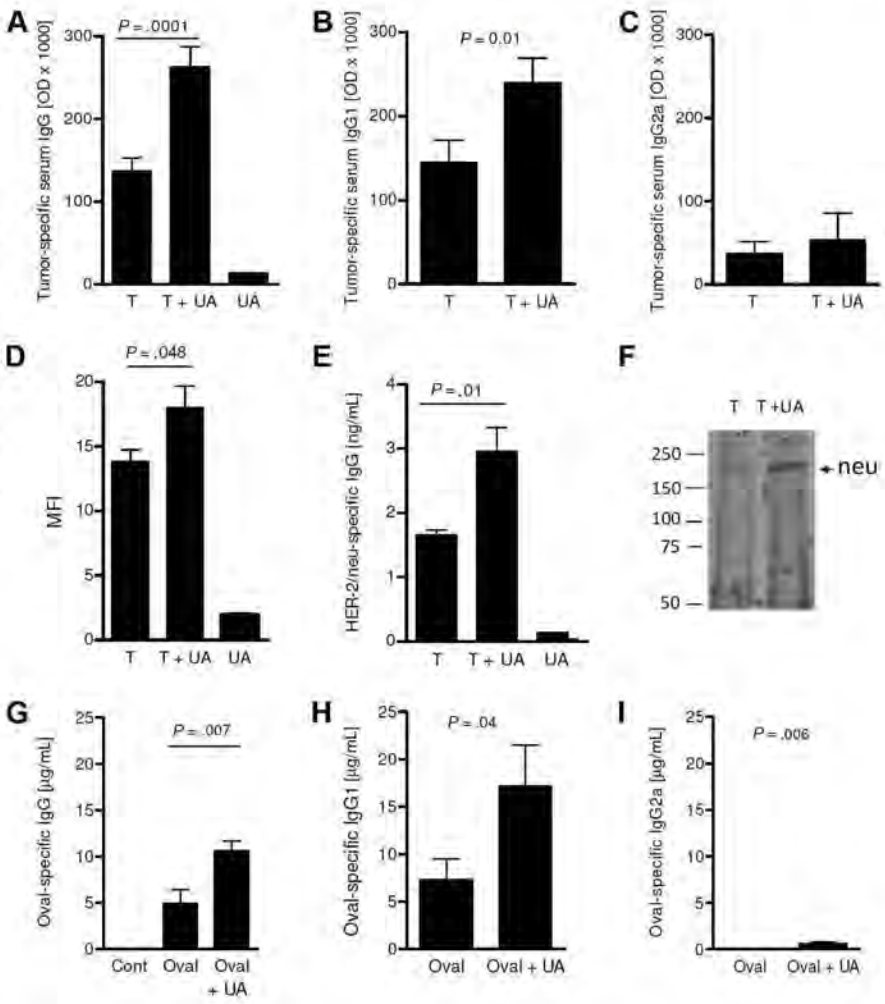

Figure 2. UA signals for enhanced tumor-specific IgG1 antibodies. (A) The tumor-specific antibody concentration in the serum 14 days after 2 injections of dying tumor cells alone (T), tumor cells with UA (T + UA) or with UA alone (UA). Each bar represents the mean (± SEM) of 12 replicates calculated from the optical densities (× 1000) in the ELISA assay. Similar to panel A, panels B and C show the levels of IgG1 and IgG2a, respectively. Each mean (± SEM) is calculated from 2 to 7 replicates. (D) The mean fluorescent intensity (MFI) of tumor cells stained with IgG from sera of animals. Each bar represents the mean (± SEM) of 3 replicates; $^*P = .05$. (E) Rat neu-specific IgG levels in animals treated as determined by capture sandwich ELISA. Each bar is the mean (± SEM) of 3 determinations. (F) Western immunoblot analysis of rat neu immunoprecipitated with sera. Numbers shown are the position of the molecular weight markers (KDa). (G-I) The serum levels of total IgG (F), IgG1 (G), and IgG2a (H) specific for ovalbumin from control mice (Cont), ovalbumin-immunized (Oval), or OVAL/UA-immunized (Oval + UA) mice (n = 5-7). The levels of IgG and IgG1 obtained following ovalbumin immunization were not significantly different ($P > .05$).

animals injected with tumor cells and UA had higher levels of antibodies capable of binding to live tumor cells as assessed by flow cytometry compared with mice pretreated with either UA alone or with dying tumor cells alone (Figure 2D). Binding to tumor-specific antigens was analyzed by neu-specific ELISA and immunoprecipitation. Figure 2E shows that sera from mice exposed to UA and tumor cells have increased levels of neu-specific antibody compared with mice treated with tumor alone. This increase was confirmed by immunoprecipitation assays (Figure 2F). To examine whether UA was able to augment antibody responses in the absence of dying tumor cells, we immunized Balb/C mice with ovalbumin protein with or without UA. Sera taken 28 days after immunization showed that the inclusion of UA with ovalbumin resulted in significantly higher levels of ovalbumin-specific IgG ($P < .05$; Figure 2G). Again, as with dying tumor cells, IgG subtype analysis revealed that UA induced an increase in IgG1 (Figure 2H). There was a minor, albeit significant ($P = .006$), increase in IgG2a induced by UA (Figure 2I). Collectively, these findings show that UA, whether added with self- or foreign antigens, augments IgG1-based antibody immunity.

UA neither augmented T-cell expansion nor altered tumor-infiltrating leukocyte levels

It had been anticipated that because UA resulted in elevated tumor-specific IgG1 antibody immunity that Th2 T cells would also be elevated. However, IL-4 ELIspot showed that the number of tumor-specific IL-4–secreting cells in the spleen of mice treated with both tumor and UA were not augmented compared with spleens of mice treated with tumor alone as shown in Figure 3A ($P > .05$), although tumor alone induced strong Th2 T-cell responses. Tumor cells neither alone nor with UA were able to induce tumor-specific IFN-γ–secreting T cells as assessed by ELIspot (data not shown). UA also did not induce increased levels of neu-specific IFN-γ–secreting T cells (Figure 3B) nor did the numbers of neu-peptide–specific CD8 T cells increase in response to UA as assessed by tetramer analysis (Figure 3C).

Again, these findings were verified using the ovalbumin model. Specifically, DO11.10 TCR transgenic ovalbumin-specific T cells were used to better track T-cell expansion. As shown in Figure 3D, the addition of UA to the ovalbumin immunization used did not change the frequency of ovalbumin-specific $CD4^+$ T cells, which were at similar levels to those in animals that received ovalbumin alone. As a positive control, GM-CSF promoted a strong expansion to more than 2% of all T cells. Similar data were obtained following the infusion of MHC class I–restricted OT-1 CD8 T cells (Figure 3E). To determine whether enhanced tumor rejection was due to increased immune effectors in the tumor microenvironment, tumors either from mice pretreated with dying tumor cells and UA or from untreated control mice were removed, and the tumor-infiltrating leukocyte population was examined. So as to avoid any mass-related differences, leukocyte infiltration was evaluated in similar-size tumors ("Methods"). Thus, when harvested after the harvesting of control tumors (mean size: 466 ± 29 mm^3), the mean tumor size from the mice that were pretreated was

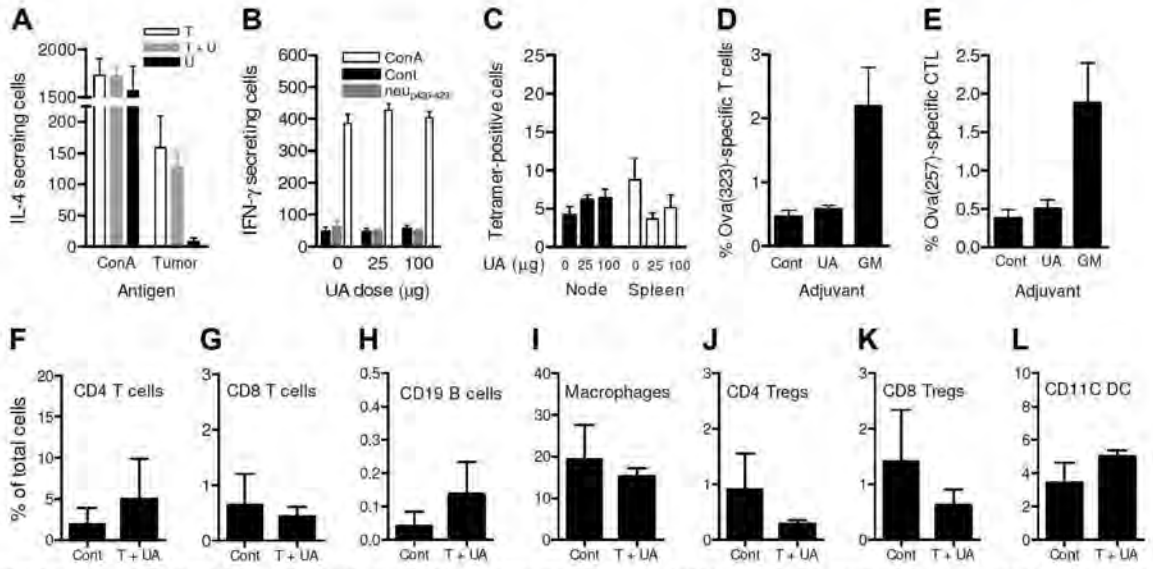

Figure 3. UA did not augment T-cell expansion or alter tumor-infiltrating leukocytes levels. (A) The levels of IL-4–secreting cells that responded to either ConA or tumor cell lysates. Splenocytes for the ELIspot assay were obtained from animals injected with tumor cells alone (□), tumor cells with 25 μg UA (▨), and 25 μg UA alone (■). Each bar represents the mean (± SEM) of 12 determinations. (B) The levels of IFN-γ–secreting T cells responding to no antigen, ConA, or neu-derived MHC class I peptide p420-429. Splenocytes were derived from animals that received dying tumor cells with various levels of UA. Each bar is the mean of 9 determinations. (C) The numbers of neu peptide p420-429 tetramer-positive T cells in draining nodes or splenocytes from mice depicted in panel F. Each is the mean (± SEM) of triplicate determinations calculated from 3 mice. (D,E) The frequencies of Oval(323)-specific CD4$^+$DO11.10 T cells (D) and Oval(257)-specific CD8$^+$OT-I T cells (E) as percentage of all CD3$^+$ splenocytes in untreated control (Cont), ovalbumin cognate peptide/UA (UA), or cognate ovalbumin peptide/GM-CSF (GM). Each bar represents the mean (± SEM) of 7 replicates and represents 2 identical experiments, which yielded similar results. (F-L) The levels of various leukocytes in tumors from mice that received either no treatment (Cont) or pretreatment with tumor cells and 25 μg UA (T + UA), prior to tumor injection. Each bar is the mean (± SEM) of 3 replicates. Each graph represents a unique intratumoral leukocyte population from control, untreated mice and from mice pretreated with dying tumor cells containing UA. All are calculated from 100 000 total events. Results are expressed as the percentage of total cells, both tumor cells and leukocytes, collected following tumor mincing.

544 (± 18) mm^3. As shown in Figure 3F-L, the levels of CD4$^+$ T cells, CD8$^+$ T cells, CD19$^+$ B cells, CD14$^+$ macrophages, CD4$^+$CD25$^+$Foxp3$^+$ Tregs, CD8$^+$CD25$^+$Foxp3$^+$ Tregs, and CD11C$^+$ DCs in the mice treated with dying tumor cells and UA were similar ($P > .05$) relative to tumors derived from untreated animals. There were no measurable levels of natural killer (NK) cells in the tumors of either group (data not shown).

UA favors an IL-5–based Th2 immune response

Increased antibody production in the absence of T-cell expansion suggested that UA somehow skewed the T-cell and DC responses more toward a Th2 phenotype ultimately favoring a B-cell response. This was confirmed with in vitro studies that showed that DO11.10 CD4 T cells that had been stimulated by ovalbumin and UA-pulsed DCs failed to produce IFN-γ and IL-2 (Figure 4A) but maintained expression of IL-4 and even demonstrated elevated secretion of IL-5, a B-cell–stimulating cytokine known to augment antibody production (Figure 4B). DCs, prepared from mice immunized with ovalbumin and UA DCs had reduced IL-2 and IL-12 production compared with DCs from animals treated with ovalbumin alone (Figure 4C). In contrast, these same DCs demonstrated elevated expression of the B-cell growth factors, IL-6 and IL-10 (Figure 4D).

Antibodies induced by UA may not be therapeutic or contribute to the antitumor immune response

To examine whether the antibodies induced by UA were therapeutic by themselves, sera collected from animals treated with tumor and UA, treated with tumor alone, or not treated were injected along with the live tumor cells at the time of tumor challenge. As shown in Figure 5A, although UA increased the levels of antibodies, these antibodies had no impact on tumor growth when used in vivo. Tumors also retained expression of the neu antigen (data not shown). However, when serum derived from animals treated with irradiated tumor cells and UA was applied to tumor cells in vitro, there was a clear enhancement of tumor growth, likely due to an increased level of agonistic antibodies that recognize and cross-link growth factors such as neu (Figure 5B). Such cross-linking may

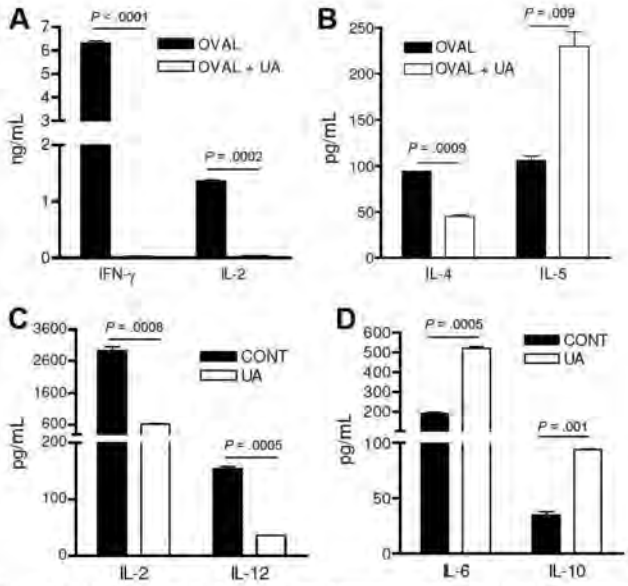

Figure 4. UA favors an IL-5–based Th2 immune response. (A,B) The cytokine concentrations of cell culture supernatants from purified antigen-stimulated DO11.10 CD4 T cells stimulated by DCs stimulated with either control media (control) or 10 μg/mL UA (UA) and ovalbumin antigen (OVAL). Each represents the mean (± SEM) cytokine concentration from duplicate wells. Experiment was reproduced twice with similar results. (C,D) Cytokine concentrations of cell culture supernatants from purified CD11C$^+$ splenic dendritic cells stimulated with UA (UA) or media alone (CONT). Each represents the mean (± SEM) cytokine concentration from duplicate wells. Experiment was reproduced twice with similar results.

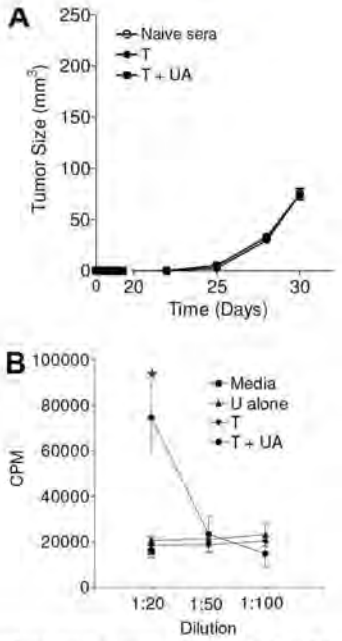

Figure 5. UA may induce growth-promoting antibodies. (A) In vivo tumor growth of MMC tumor cells following intratumoral injection (day 0) of sera from naive animals or from animals from either pretreated with irradiated tumor with (T + UA) or without (T) uric acid. Calculated from 3 separate tumors for each data point. Curves overlap. (B) The thymidine incorporation in live MMC tumor cells exposed to media (■) or various concentrations of serum from animals treated with UA alone (U alone, ▲), irradiated tumor alone (T, ◆), or with UA (T + UA, ●). Each determination represents the mean (± SEM) of 3 determinations; *P = .01.

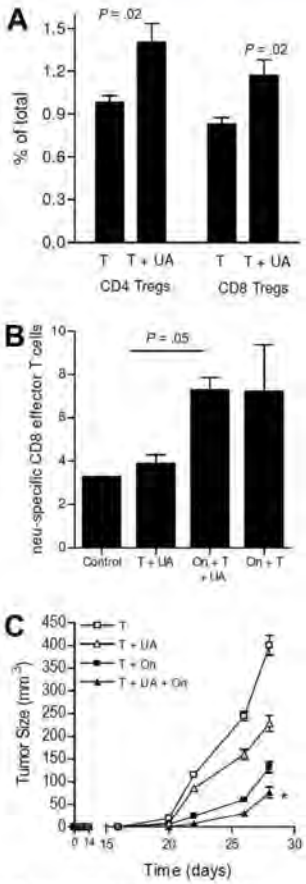

Figure 6. UA does not prevent increased T-cell immunity induced by other means. (A) The peripheral levels of Tregs ($CD4^+CD25^+Foxp3^+$ or $CD8^+CD25^+Foxp3^+$) in animals injected with dying tumor cells alone (T) or with tumor cells with UA (T + UA). Each bar is the mean (± SEM; *$P < .05$) of 3 mice. (B) Levels of neu peptide tetramer$^+$ $CD8^+CD62L^{lo}$ T cells (ie, effector or effector memory) in control animals, or animals injected with tumor cells (T) with or without UA (UA) or ONTAK (On). Each bar is the mean (± SEM) of 3 to 4 mice. (C) The tumor growth rates in mice pretreated with tumor cells alone and tumor cells with or without UA, ONTAK, or both. Each data point is the mean (± SEM) of 3 to 5 mice. *$P < .05$ compared with all other groups.

result in activation and increased proliferation. Thus, antibodies generated by UA appear to be neither therapeutic nor tumor inhibitory.

Treg depletion augments UA induced antitumor responses

Our group has previously observed that regulatory T cells interfere with the endogenous cell–mediated immune responses against breast cancers in the neu-tg mouse. In the current study, we observed that UA led to an increase in both peripheral $CD4^+$ and $CD8^+$ Tregs (ie, $Foxp3^+CD25^+$) (Figure 6A). To determine whether Tregs were involved in preventing T-cell expansion, Tregs were depleted with denileukin diftitox (ONTAK, On) prior to the injection of tumor, with and without UA.[16] As shown in Figure 6B and consistent with our prior studies, Treg depletion with denileukin diftitox led to an expected increase in the level of neu-specific CD8 T cells, as we have previously shown.[16] But, the addition of UA did not further augment CD8 T-cell expansion, suggesting that although UA itself fails to augment T-cell expansion, it does not actively block it. In addition, prior Treg depletion did not impair the ability of UA to induce antitumor responses as shown in Figure 6C. In contrast, both Treg depletion and UA collaborated for enhanced tumor suppression, as was anticipated.

Discussion

Recent evidence shows that mammalian immune systems have evolved mechanisms to respond to uninfected dying or injured cells through a variety of novel ligands.[6,8,9,22-26] The underlying reason for the evolution of such mechanisms for responding to endogenous ligands remains controversial, but one possibility is that they are needed to detect potentially infected cells for which there are no associated PAMPs or other adjuvants.[27] Alternatively, sterile immune responses may be involved in normal tissue homeostasis by providing mechanism to recruit in phagocytic cells of the innate immune system such as macrophages.[28] Regardless of the biologic rationale, further characterization of sterile immunity should have important implications for the treatment of autoimmunity and potentially malignancy. While it is known that UA signaling leads to activation of innate immunity and T lymphocytes, little is known about whether antibody production ensues. We had speculated that since autoantibodies were so prevalent in several diseases associated with sterile immune responses that responses to endogenous danger signals also lead to autoantibody production under some conditions. Indeed, the present studies show that the recently identified danger signal, crystalline UA, when added to either dying tumor cells or soluble protein antigen was able to augment antibody immunity. Specifically, it was found that UA increased IgG1-based antibody immunity to both self- and foreign antigens, suggesting that Th2 immunity was the favored response. As previously reported, when UA was used as an adjuvant, the increased immunity generated resulted in enhanced protection against tumor. However, unexpectedly, the antitumor response depended on CD4 T cells but not CD8 T cells.

In the mouse, the predominant Ig produced following the emergence of a Th2-directed immune response is IgG1. In contrast,

the major Ig produced following induction of Th1 immunity is IgG2a. While our study showed little or no increased production of IgG2a, we cannot rule out the possibility that UA influences other antibody subsets (eg, IgG2b, IgG3). In both the dying tumor cell model and the foreign antigen models used in the current study, UA induced significant increases in the IgG1 response, suggesting that the purine is also able to augment Th2 immunity in addition to its reported abilities to augment Th1-based cell-mediated immunity. The observations of increased IL-5 production by ovalbumin-specific CD4 T cells and the increased production of B-cell activators (IL-10 and IL-6) by UA-treated DCs support this conclusion. There are several biologic functions of IgG1 in the mammal that could potentially be beneficial to a cell injury or death response, including complement activation, interference with cell signaling, and opsonization of particles for enhanced phagocytosis.[29] One could envision that such a response may be useful to neutralize viruses that do not express traditional PAMPs. However, it was observed that the augmented antibody response induced by UA had little impact on tumor growth in vivo alone. In contrast, the antibodies seem to be detrimental and counterproductive. Despite that, we cannot rule out the possibility that, in vivo, the antibodies could activate tumor-destruction mechanisms, such as antigen-dependent cellular cytotoxicity, that were offset by the tumor-promoting effects.

It was speculated that the predominant augmentation of IgG1 immunity by UA may have been accompanied by increased numbers of Th2 T-cell responses. Although dying tumor cells elicited a strong increase in tumor antigen–specific Th2 immunity, the addition of UA failed to augment these numbers, suggesting that there were factors other than increased numbers of IL-4–secreting T cells that contributed to the increased IgG response. One possibility is increased elaboration of B-cell activation cytokines (eg, IL-5 and IL-4). Based on the studies with purified TCR transgenic Th cells (ie, D011.1 T cells), IL-4 release was not increased, but rather there was a slight decline in favor of enhanced IL-5 production in response to UA stimulation. While our studies did not reveal the mechanisms behind increased IgG1 immunity, such a cytokine could favor B1 B-cell activation and maturation.[30] B1 B cells are a subset of B cells that specifically responds to IL-5 with increased proliferation and IgG production.[30-32] B1 B cells are associated primarily with the production of autoantibodies targeting self-antigens such as phosphatidylcholine, immunoglobulins (eg, rheumatoid factor), and DNA.[33,34] Although fairly high levels of tumor-binding antibodies were observed in the current study, it is unclear yet as to what antigens are being targeted by the augmented immune response, with the exception that a small fraction bound to rat neu.

Another key finding from our study is that, in both the neu-tg mouse and the TCR-transgenic T-cell models, UA did not result in expansion of cell-mediated immunity (eg, cytotoxic T lymphocytes [CTLs] and IFN-γ) as there was neither an increase in tumor antigen–specific T cells in the dying tumor cell model nor an increase in OT-1 T cells following immunization with ovalbumin. Despite that, the enhanced antitumor activity was completely reversed with the depletion of CD4 T cells, which would have been expected given the important role of CD4 T cells in regulating the antibody responses. In fact, the tumor growth was substantially greater in the CD4-depleted mice compared with untreated mice, suggesting that CD4 T cells have an active role in modulating tumor growth in the absence of prior immunization with irradiated tumor cells. Unlike the effects observed in the CD4-depleted animals, CD8 depletion did not reverse the effects of UA, but rather enhanced the effects. Since it was observed that the inclusion of UA led to increased peripheral Tregs, it was speculated that these specialized regulatory T cells were involved in blocking the expansion of cell-mediated immunity, consistent with their roles in maintaining peripheral tolerance.[16,35,36] However, Treg depletion studies with denileukin diftitox, which we previously showed to be effective in depleting Tregs and elevating cell-mediated immunity, failed to bear this out.[16]

Our inability to see expansion of CD8 T-cell immunity could be explained by the fact that we did not use the same immunization strategies as described in previous studies. In one of the prior studies by Shi and colleagues, it was found that UA when administered with purified, latex bead–bound gp120 antigen led to an increase in the cytotoxic T-cell activity response compared with animals immunized with the antigen alone.[8] The ability of UA to enhance expansion of cytotoxic T cells was shown in another study, by the same group who observed that intraperitoneal pretreatment of RIP-mOVA mice with both allopurinol and uricase reduced in vivo cell division of infused OT-1 T cells, secondarily to UA depletion.[9] There are potential reasons we failed to see enhanced T-cell expansion. First, our study did not use antigens linked to latex beads, the latter of which could alter immune responses. Alternatively, we used concentrations of UA that were lower in many cases. It is possible that UA is a more versatile danger signal than either the current study or past studies suggest with capabilities of supporting both Th1 and Th2 T-cell immune responses, depending on the extent of damage or injury. Lower levels of UA may indicate natural cell senescence in which antibodies could be induced to facilitate phagocytosis by macrophage for reversal of the tissue pathology (ie, healing) and tissue maintenance. Consistent with this reasoning, Martinon et al recently showed that UA crystals also directly activate macrophages.[13] Alternatively, the higher levels as used by Shi and colleagues may reflect massive damage indicative of an infection.

The finding of increased Tregs following the application of UA is also another novel finding. Repeatedly, it has been found that Tregs are elevated in patients with a variety of different types of cancers.[36] Despite these observations, many things remain unclear about the nature of elevated levels of Tregs in patients with cancer, including the factors that signal for Treg expansion. Based on the current study and the prior studies by Shi et al, it could be speculated that danger signals, including UA, that emanate from the dying tumor cells lead to the peripheral increases in Tregs.[8,27] Despite these increases, the clinical significance of elevated peripheral Tregs in cancer patients remains uncertain. What is known is that the tumor burden directly correlates with increased peripheral Tregs in patients with melanoma, and renal and gastric cancers, strongly implicating danger signaling (UA?) from the tumor.[37,38] These peripheral increases in Tregs may result in the often-observed migration of Tregs into the tumor microenvironment, which has been linked to cancer pathogenesis in several cancers such as ovarian cancer.[39]

In conclusion, in the current study we observed that the danger signal UA could, in addition to its previously reported ability to augment CTLs, induce IgG1 responses, suggesting that it can also augment humoral immune responses. Understanding natural mechanisms of danger signaling, apart from exogenous microbial-derived signals (eg, CpGs) may have important implications for vaccines, tumor immunity, and autoimmunity.

Acknowledgments

The authors gratefully acknowledge the assistance of Dr George Vielhauer.

This work was supported by the Mayo Clinic Comprehensive Cancer Center and National Cancer Institute grants K01-CA100764 and R01-CA113861 (K.L.K).

Authorship

Contribution: M.D.B. and W.M.W. performed research and analyzed data; C.J.K., C.L.E., J.K., and E.A.G. performed research; K.R.K. designed research and wrote the paper; M.L.D. provided materials and resources; and K.L.K. designed and performed research, analyzed data, and wrote the paper.

Conflict-of-interest disclosure: The authors declare no competing financial interests.

Correspondence: Keith L. Knutson, Mayo Clinic College of Medicine, 342C Guggenheim, 200 First St SW, Mayo Clinic, Rochester, MN 55905; e-mail: knutson.keith@mayo.edu.

References

1. Janeway CA Jr. The immune system evolved to discriminate infectious nonself from noninfectious self. Immunol Today. 1992;13:11-16.
2. Bianchi ME. DAMPs, PAMPs and alarmins: all we need to know about danger. J Leukoc Biol. 2007; 81:1-5.
3. Uematsu S, Akira S. Toll-like receptors and type I interferons. J Biol Chem. 2007;282:15319-15323.
4. Nava-Parada P, Forni G, Knutson KL, Pease LR. Peptide vaccine administered with a toll-like receptor agonist is effective for the treatment and prevention of spontaneous breast tumors. Cancer Res. 2007;67:1326-1334.
5. Chen CJ, Kono H, Golenbock D, Reed G, Akira S, Rock KL. Identification of a key pathway required for the sterile inflammatory response triggered by dying cells. Nat Med. 2007;13:851-856.
6. Gallucci S, Lolkema M, Matzinger P. Natural adjuvants: endogenous activators of dendritic cells. Nat Med. 1999;5:1249-1255.
7. Rock KL, Hearn A, Chen CJ, Shi Y. Natural endogenous adjuvants. Springer Semin Immunopathol. 2005;26:231-246.
8. Shi Y, Evans JE, Rock KL. Molecular identification of a danger signal that alerts the immune system to dying cells. Nature. 2003;425:516-521.
9. Shi Y, Galusha SA, Rock KL. Cutting edge: elimination of an endogenous adjuvant reduces the activation of CD8 T lymphocytes to transplanted cells and in an autoimmune diabetes model. J Immunol. 2006;176:3905-3908.
10. Idzko M, Hammad H, van Nimwegen M, et al. Extracellular ATP triggers and maintains asthmatic airway inflammation by activating dendritic cells. Nat Med. 2007;13:913-919.
11. Chen CJ, Shi Y, Hearn A, et al. MyD88-dependent IL-1 receptor signaling is essential for gouty inflammation stimulated by monosodium urate crystals. J Clin Invest. 2006;116:2262-2271.
12. Hu DE, Moore AM, Thomsen LL, Brindle KM. Uric acid promotes tumor immune rejection. Cancer Res. 2004;64:5059-5062.
13. Martinon F, Petrilli V, Mayor A, Tardivel A, Tschopp J. Gout-associated uric acid crystals activate the NALP3 inflammasome. Nature. 2006; 440:237-241.
14. von Landenberg P, Scholmerich J. Tissue-associated autoantigens in rheumatoid arthritis: tissue-antigens detected by autoantibodies in synovial fluid and sera of RA patients. Clin Rev Allergy Immunol. 2000;18:59-71.
15. Fernandez Madrid F. Autoantibodies in breast cancer sera: candidate biomarkers and reporters of tumorigenesis. Cancer Lett. 2005;230:187-198.
16. Knutson KL, Dang Y, Lu H, et al. IL-2 immunotoxin therapy modulates tumor-associated regulatory T cells and leads to lasting immune-mediated rejection of breast cancers in neu-transgenic mice. J Immunol. 2006;177:84-91.
17. Knutson KL, Almand B, Dang Y, Disis ML. Neu antigen-negative variants can be generated after neu-specific antibody therapy in neu transgenic mice. Cancer Res. 2004;64:1146-1151.
18. Knutson KL, Disis ML. IL-12 enhances the generation of tumour antigen-specific Th1 CD4 T cells during ex vivo expansion. Clin Exp Immunol. 2004;135:322-329.
19. Knutson KL, Lu H, Stone B, et al. Immunoediting of cancers may lead to epithelial to mesenchymal transition. J Immunol. 2006;177:1526-1533.
20. Knutson KL, Schiffman K, Disis ML. Immunization with a HER-2/neu helper peptide vaccine generates HER-2/neu CD8 T-cell immunity in cancer patients. J Clin Invest. 2001;107:477-484.
21. Knutson KL, Hmama Z, Herrera-Velit P, Rochford R, Reiner NE. Lipoarabinomannan of Mycobacterium tuberculosis promotes protein tyrosine dephosphorylation and inhibition of mitogen-activated protein kinase in human mononuclear phagocytes. Role of the Src homology 2 containing tyrosine phosphatase 1. J Biol Chem. 1998; 273:645-652.
22. Taylor KR, Yamasaki K, Radek KA, et al. Recognition of hyaluronan released in sterile injury involves a unique receptor complex dependent on Toll-like receptor 4, CD44, and MD-2. J Biol Chem. 2007;282:18265-18275.
23. Lotze MT, Tracey KJ. High-mobility group box 1 protein (HMGB1): nuclear weapon in the immune arsenal. Nat Rev Immunol. 2005;5:331-342.
24. Foell D, Wittkowski H, Vogl T, Roth J. S100 proteins expressed in phagocytes: a novel group of damage-associated molecular pattern molecules. J Leukoc Biol. 2007;81:28-37.
25. Foell D, Wittkowski H, Roth J. Mechanisms of disease: a 'DAMP' view of inflammatory arthritis. Nat Clin Pract Rheumatol. 2007;3:382-390.
26. Osterloh A, Breloer M. Heat shock proteins: linking danger and pathogen recognition. Med Microbiol Immunol. 2008;197:1–8.
27. Shi Y, Zheng W, Rock KL. Cell injury releases endogenous adjuvants that stimulate cytotoxic T cell responses. Proc Natl Acad Sci U S A. 2000;97: 14590-14595.
28. Erwig LP, Henson PM. Immunological consequences of apoptotic cell phagocytosis. Am J Pathol. 2007;171:2-8.
29. Hart SP, Smith JR, Dransfield I. Phagocytosis of opsonized apoptotic cells: roles for 'old-fashioned' receptors for antibody and complement. Clin Exp Immunol. 2004;135:181-185.
30. Martin F, Kearney JF. B1 cells: similarities and differences with other B cell subsets. Curr Opin Immunol. 2001;13:195-201.
31. Erickson LD, Foy TM, Waldschmidt TJ. Murine B1 B cells require IL-5 for optimal T cell-dependent activation. J Immunol. 2001;166:1531-1539.
32. Kaneko Y, Hirose S, Abe M, Yagita H, Okumura K, Shirai T. CD40-mediated stimulation of B1 and B2 cells: implication in autoantibody production in murine lupus. Eur J Immunol. 1996;26:3061-3065.
33. Pennell CA, Mercolino TJ, Grdina TA, Arnold LW, Haughton G, Clarke SH. Biased immunoglobulin variable region gene expression by Ly-1 B cells due to clonal selection. Eur J Immunol. 1989;19: 1289-1295.
34. Casali P, Burastero SE, Nakamura M, Inghirami G, Notkins AL. Human lymphocytes making rheumatoid factor and antibody to ssDNA belong to Leu-1+ B-cell subset. Science. 1987;236:77-81.
35. Knutson KL. Strong-arming immune regulation: suppressing regulatory T cell function to treat cancers. Future Oncol. 2006;2:379-389.
36. Knutson KL, Disis ML, Salazar L. CD4 regulatory T cells in human cancer pathogenesis. Cancer Immunol Immunother. 2007;56:271-285.
37. Cesana GC, DeRaffele G, Cohen S, et al. Characterization of CD4+CD25+ regulatory T cells in patients treated with high-dose interleukin-2 for metastatic melanoma or renal cell carcinoma. J Clin Oncol. 2006;24:1169-1177.
38. Kono K, Kawaida H, Takahashi A, et al. CD4(+)CD25high regulatory T cells increase with tumor stage in patients with gastric and esophageal cancers. Cancer Immunol Immunother. 2006;55:1064–1071.
39. Curiel TJ, Coukos G, Zou L, et al. Specific recruitment of regulatory T cells in ovarian carcinoma fosters immune privilege and predicts reduced survival. Nat Med. 2004;10:942-949.